# A DYNAMICAL MODEL FOR HALO NUCLEI AND TWO-NUCLEON TRANSFER REACTIONS


F. Barranco and G. Potel

**Sevilla University**

R.A. Broglia

**Milano University and INFN**

**The Niels Bohr Institute, Copenhagen**

E. Vigezzi

**INFN Milano**


CEA Saclay, 17/11/2011

Table 2

| Data | Value | Refs. |
|---|---|---|
| $S_{2n}$ | $378 \pm 5,\ 369.15 \pm 0.65$ keV | [7,8] |
| $^{11}$Li matter radius | $3.27 \pm 0.24,\ 3.12 \pm 0.16,\ 3.55 \pm 0.10$ fm | [9–11] |
| $^{9}$Li matter radius | $2.30 \pm 0.02$ fm | [10,12] |
| $^{11}$Li charge radius | 2.467(37), 2.423(34), 2.426(34) fm | [13–15] |
| $^{9}$Li charge radius | 2.217(35), 2.185(33) fm | [13,14] |
| $R^2_{\rm ch}(n)$ | $-0.1161 \pm 0.0022$ fm$^{2*}$ | [16] |
| TMD($^{10}$Li) | FWHM $= 56.1 \pm 1.2$ MeV/$c$, shape | [18] |
| Correlation $c_1$ | $-1.03(4)$ | [18] |
| Correlation $c_2$ | 1.41(8) | [18] |
| $\mu(^{11}\mathrm{Li})$ | 3.6673(25), 3.6712(3) n.m. | [19,22] |
| $\mu(^{9}\mathrm{Li})$ | 3.43678(6) n.m. | [20] |
| $Q_9$ | $-30.6(2)$ mb | [20] |
| $Q_{11}$ | $-35.0(49),\ -31.5(45),\ -33.3(5)$ mb | [19,21,22] |
| $Q_{11}/Q_9$ | $1.088 \pm 0.015$ | [22] |
| $\sigma 264_{-2n}$ | 242(8), 280(30) mb | [23,24] |
| $\sigma 264_{-1n}$ | 144(20), 170(20) mb | [23,24] |
| $\sigma 790_R$ | 1040(60), 1056(30), 1060(10) mb | [9,25,26] |
| $\sigma 790_{-2n}$ | 213(21), 220(10) mb | [25,26] |

* A small and positive $R^2_{\rm ch}(n) = 0.012$ fm$^2$ has been obtained in [17] with new model of the nucleon quark structure.

# *To what extent is this picture correct?*

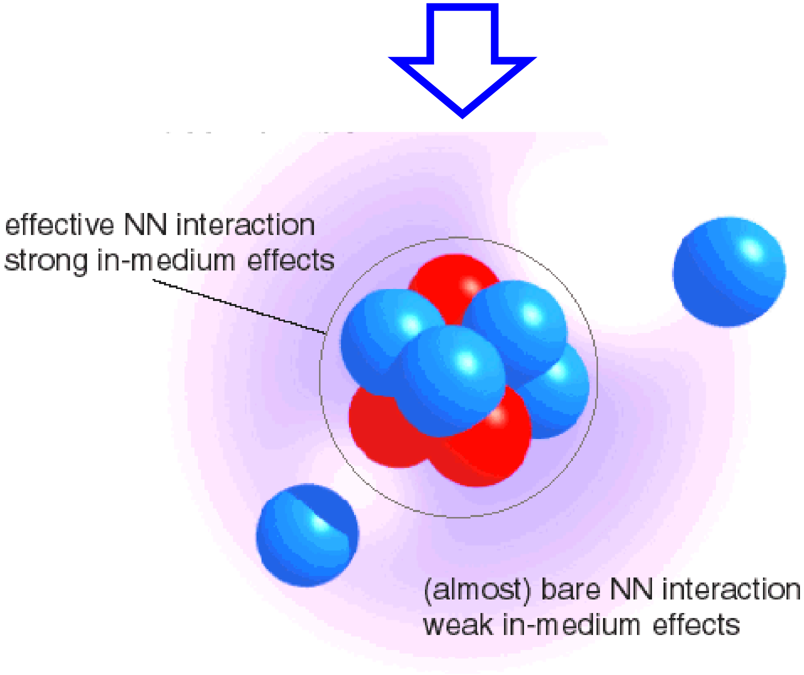


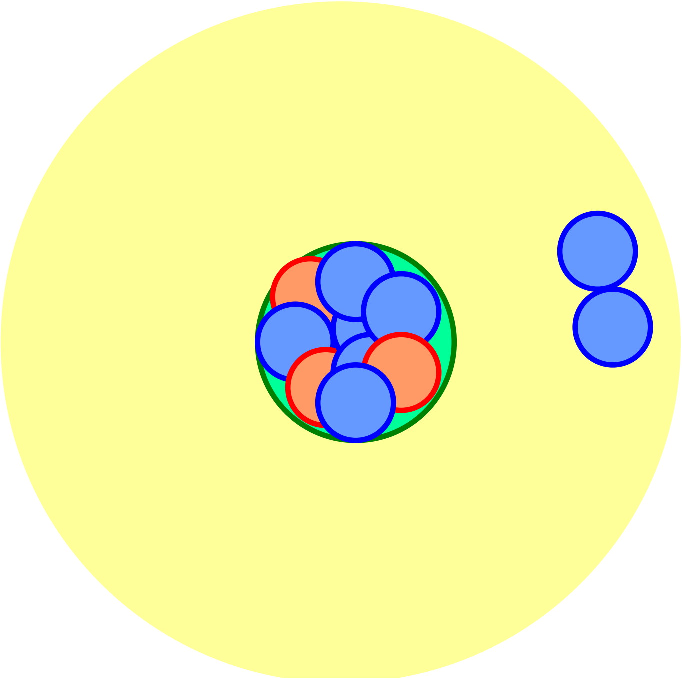

Talk by K. Hagino DCEN 2011

# Suppression of Core Polarization in Halo Nuclei

T. T. S. Kuo,[1] F. Krmpotić,[2] and Y. Tzeng[3]
[1]*Department of Physics, SUNY-Stony Brook, Stony Brook, New York 11794*
[2]*Departamento de Fisica, Facultad de Ciencias Exactas, Universidad Nacional de La Plata, C. C. 67, 1900 La Plata, Argentina*
[3]*Institute of Physics, Academia Sinica, Nankang, Taipei, Taiwan*
(Received 18 June 1996; revised manuscript received 8 October 1996)

Halo nuclei are studied using a $G$-matrix interaction derived from the Paris and Bonn potentials and employing a two-frequency shell model approach. It is found that the core-polarization effect is dramatically suppressed in such nuclei. Consequently, the effective interaction for halo nucleons is almost entirely given by the bare $G$ matrix alone, which presently can be evaluated with a high degree of accuracy. The experimental pairing energies between the two halo neutrons in $^6$He and $^{11}$Li nuclei are satisfactorily reproduced by our calculation. It is suggested that the fundamental nucleon-nucleon interaction can be probed in a clearer and more direct way in halo nuclei than in ordinary nuclei.

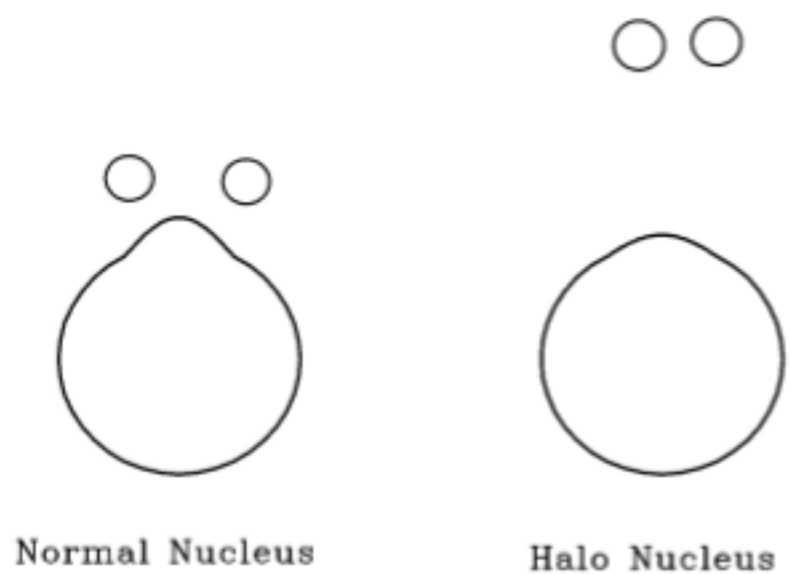

# Three-body model with density-dependent delta force

G.F. Bertsch and H. Esbensen,
*Ann. of Phys. 209('91)327*
H. Esbensen, G.F. Bertsch, K. Hencken,
*Phys. Rev. C56('99)3054*

$^{11}$Li, $^{6}$He

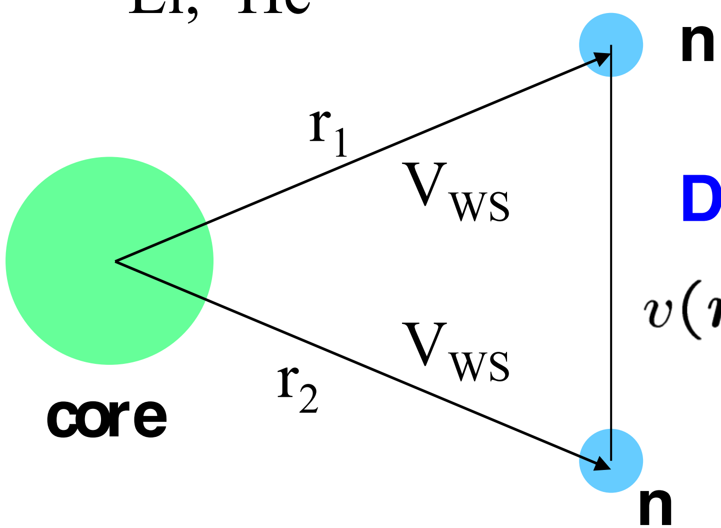


**Density-dependent delta-force**

$$v(\boldsymbol{r}_1, \boldsymbol{r}_2) = v_0(1 + \alpha\rho(r)) \times \delta(\boldsymbol{r}_1 - \boldsymbol{r}_2)$$

$$\boxed{H = \frac{\boldsymbol{p}_1^2}{2m} + \frac{\boldsymbol{p}_2^2}{2m} + V_{nC}(r_1) + V_{nC}(r_2) + V_{nn} + \frac{(\boldsymbol{p}_1 + \boldsymbol{p}_2)^2}{2A_c m}}$$

$$H = \frac{\boldsymbol{p}_1^2}{2m} + \frac{\boldsymbol{p}_2^2}{2m} + V_{nC}(r_1) + V_{nC}(r_2) + V_{nn} + \frac{(\boldsymbol{p}_1 + \boldsymbol{p}_2)^2}{2A_c m}$$

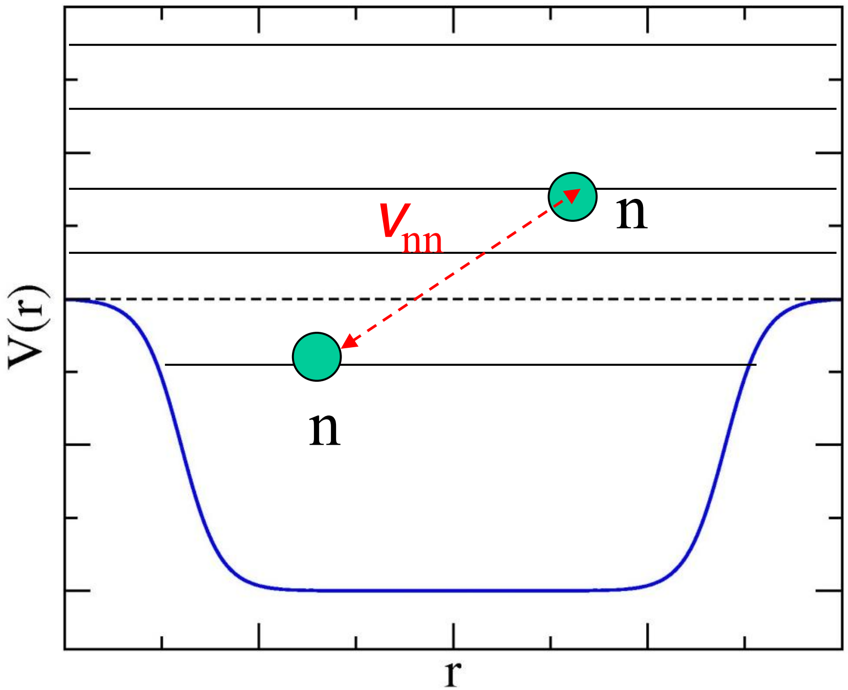


continuum states:
discretized in a large box

$$V_{nn}(\boldsymbol{r}_1, \boldsymbol{r}_2) = \delta(\boldsymbol{r}_1 - \boldsymbol{r}_2)\left(v_0 + \frac{v_\rho}{1 + \exp[(r_1 - R_\rho)/a_\rho]}\right)$$

- ✓ contact interaction
- ✓ $v_0$: free n-n
- ✓ density dependent term: medium many-body effects

$$H = \frac{\boldsymbol{p}_1^2}{2m} + \frac{\boldsymbol{p}_2^2}{2m} + V_{nC}(r_1) + V_{nC}(r_2) + V_{nn} + \frac{(\boldsymbol{p}_1 + \boldsymbol{p}_2)^2}{2A_c m}$$

$$\boxed{\Psi_{gs}(\boldsymbol{r}, \boldsymbol{r}') = \mathcal{A} \sum_{nn'lj} \alpha_{nn'lj} \Psi^{(2)}_{nn'lj}(\boldsymbol{r}, \boldsymbol{r}')}$$

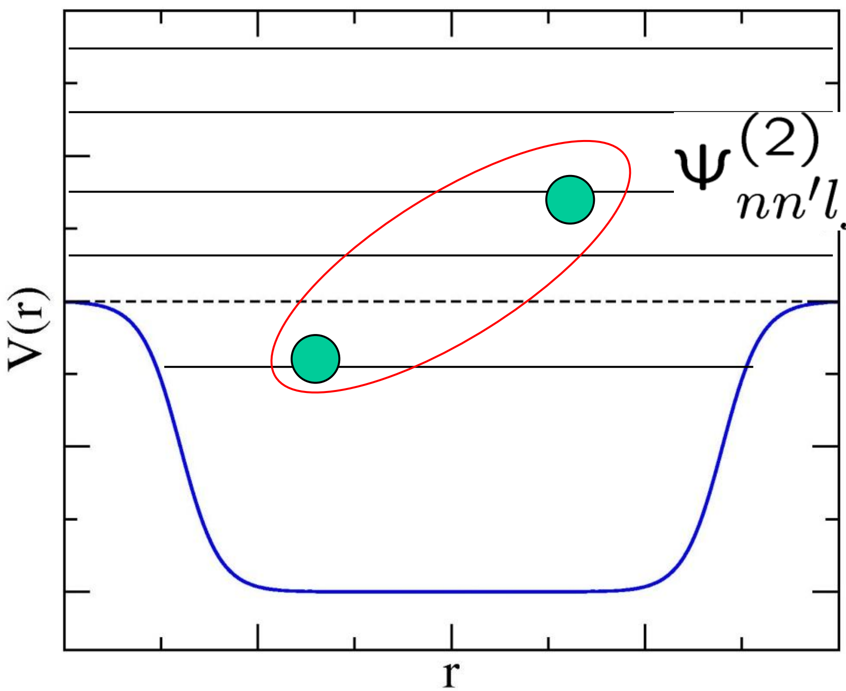


$\Psi^{(2)}_{nn'lj}(\boldsymbol{r}, \boldsymbol{r}')$

uncorrelated basis

⇓

diagonalization of Hamiltonian matrix

Good agreement with Faddeev calculations

TABLE I. Ground state properties of $^{11}$Li obtained with the shallow neutron-core potential (4.1). All of our calculations employ a radial box of 40 fm; the cutoff in the two-particle spectrum is 15 MeV, except in line 6. Line 7 is the no-recoil limit corresponding to line 5.

| Line | Comments | $a_{nn}$ (fm) | $S_{2n}$ (keV) | $\langle r^2_{c,2n} \rangle$ (fm$^2$) | $\langle r^2_{n,n} \rangle$ (fm$^2$) | $(s_{1/2})^2$ (%) |
|---|---|---|---|---|---|---|
| 1 | HHM [10] | −18.5 | 300 | 25.0 | 60.8 | 98.4 |
| 2 | Faddeev [11] | −18.5 | 318 | 28.1 | 62.4 | 95.1 |
| 3 | $v_\rho=0$ | −18.5 | 569 | 20.3 | 49.0 | 92.1 |
| 4 | $v_\rho=0$ | −9.81 | 318 | 26.0 | 65.3 | 93.5 |
| 5 | $v_\rho\neq 0$ | −15.0 | 318 | 28.3 | 67.1 | 92.4 |
| 6 | $v_\rho\neq 0$, $E_{cut}$=25 MeV | −15.0 | 318 | 27.6 | 62.9 | 91.1 |
| 7 | line 5, no recoil | −15.0 | 318 | 25.3 | 67.9 | 94.4 |

H. Esbensen, G.F. Bertsch, K. Hencken, Phys. Rev. C 56 (1997) 3054

Relax some of the assumptions of Bertsch and Esbensen:

Inert core

Different potentials for s- and p- waves

Zero range interaction, with ad hoc density dependence

Low-lying collective modes of the core taken into account

Standard mean field potential

Bare N-N interaction (Argonne)

H. Esbensen, G.F. Bertsch, K. Hencken, Phys. Rev. C 56 (1997) 3054

**$^{10}$Li, $^{11}$Li** F. Barranco et al. EPJ A11 (2001) 385
**$^{11}$Be, $^{12}$Be** G. Gori et al. PRC 69 (2004) 041302(R)

Admixture of $d_{5/2}$ x $2^+$ configuration in the $1/2^+$ g.s. of $^{11}$Be is about 20%

Calculated ground state

$$|1/2+\rangle = \sqrt{0.87}\,|s_{1/2}\rangle + \sqrt{0.13}\,|d_{5/2} \otimes 2+\rangle$$

Exp.:

J.S. Winfield et al., Nucl.Phys. **A683** (2001) 48

$$|1/2+\rangle = \sqrt{0.84}\,|s_{1/2}\rangle + \sqrt{0.16}\,|d_{5/2} \otimes 2+\rangle$$

$^{11}$Be(p,d)$^{10}$Be in inverse kinematic detecting both the ground state and the 2+ excited state of $^{10}$Be.

9Be(11Be,10Be+ $\gamma$) X

T. Aumann et al.
PRL 84(2000)35

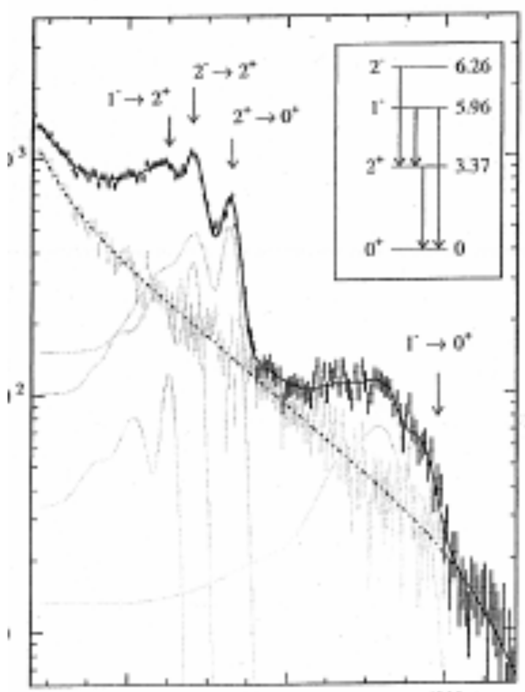


p(11Be,10Be)d

S. Fortier et al.
Phys. Lett.B461(1999)22

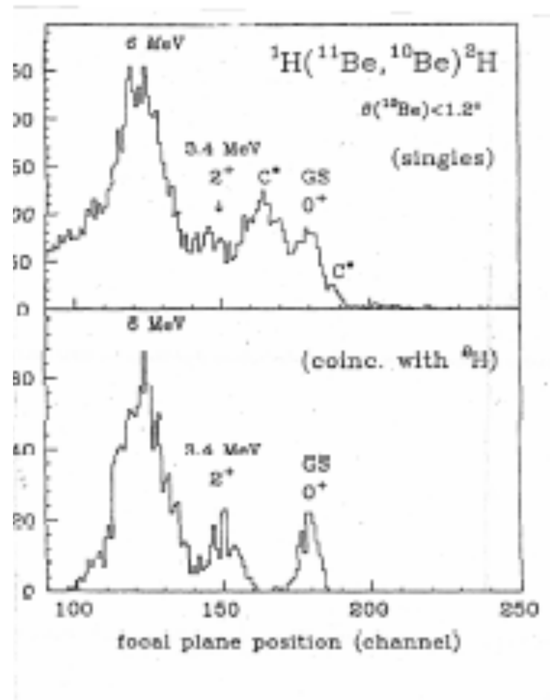

# Measurement of the Two-Halo Neutron Transfer Reaction $^{1}\mathrm{H}(^{11}\mathrm{Li}, {}^{9}\mathrm{Li})^{3}\mathrm{H}$ at $3A$ MeV

I. Tanihata,* M. Alcorta,† D. Bandyopadhyay, R. Bieri, L. Buchmann, B. Davids, N. Galinski, D. Howell, W. Mills, S. Mythili, R. Openshaw, E. Padilla-Rodal, G. Ruprecht, G. Sheffer, A. C. Shotter, M. Trinczek, and P. Walden

*TRIUMF, 4004 Wesbrook Mall, Vancouver, BC, V6T 2A3, Canada*

H. Savajols, T. Roger, M. Caamano, W. Mittig,‡ and P. Roussel-Chomaz

*GANIL, Bd Henri Becquerel, BP 55027, 14076 Caen Cedex 05, France*

R. Kanungo and A. Gallant

*Saint Mary's University, 923 Robie St., Halifax, Nova Scotia B3H 3C3, Canada*

M. Notani and G. Savard

*ANL, 9700 S. Cass Ave., Argonne, Illinois 60439, USA*

I. J. Thompson

*LLNL, L-414, P.O. Box 808, Livermore, California 94551, USA*

(Received 22 January 2008; published 14 May 2008)

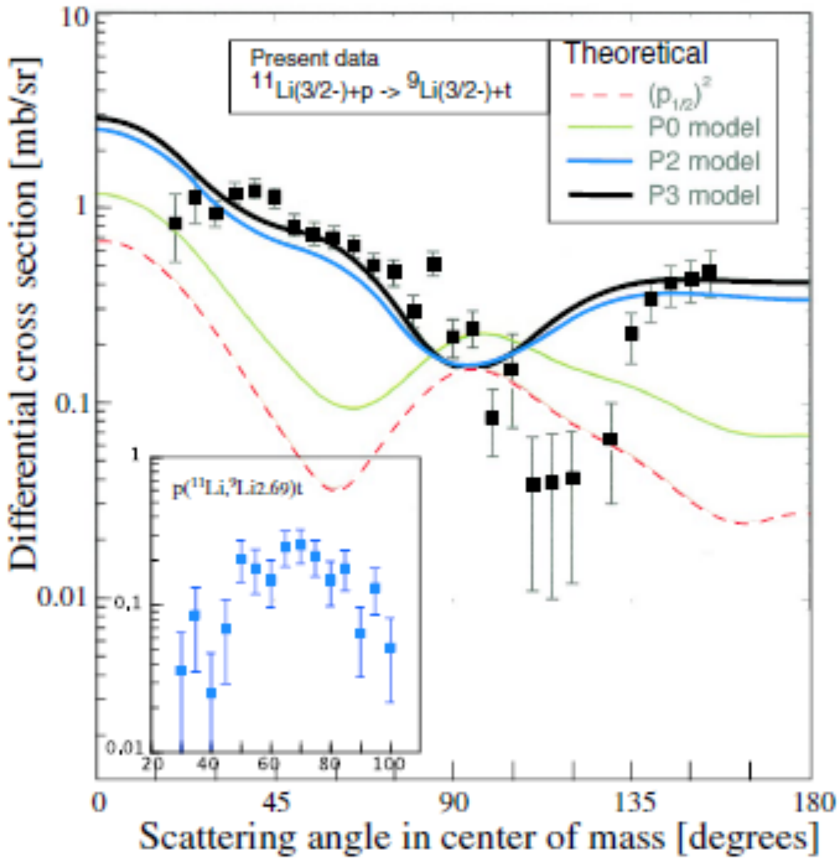


The cross section for transitions to the first excited state (Ex = 2.69 MeV) is shown also in Fig. 3. If this state were populated by a direct transfer, it would indicate that a $1^+$ or $2^+$ halo component is present in the ground state of $^{11}$Li($\frac{3}{2}^-$), because the spin-parity of the $^9$Li first excited state is $\frac{1}{2}^-$. This is new information that has not yet been observed in any of previous investigations. A compound

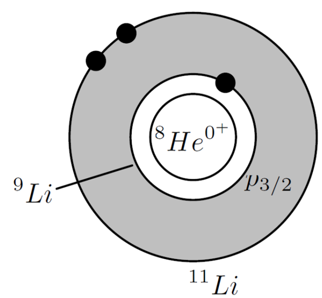


Schematic depiction of $^{11}$Li

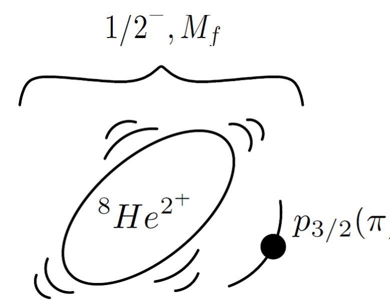


First excited state of $^9$Li

# Structure of $^8$He extracted from direct reactions on proton target

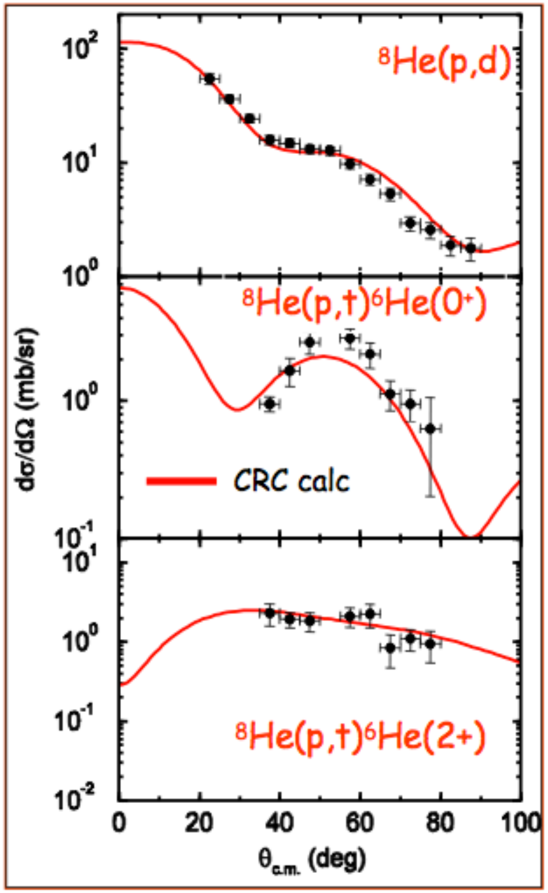


SPIRAL $^8$He +p @ 15.7A.MeV

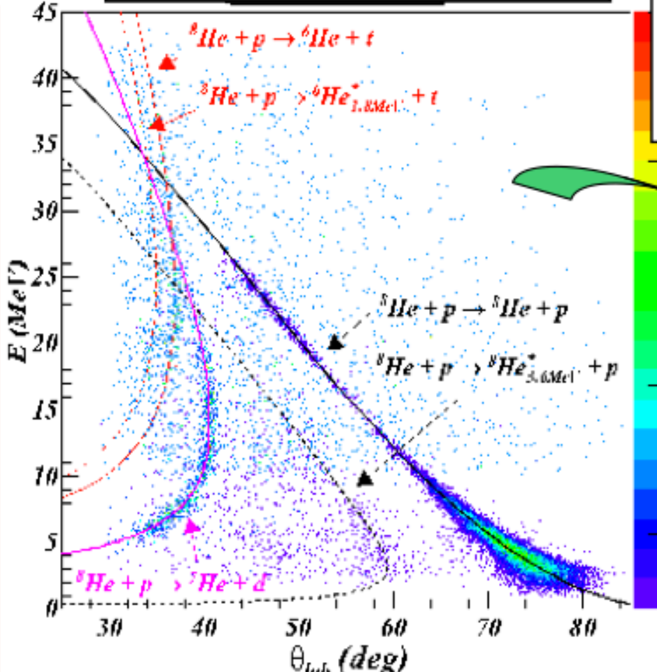


Coupled-channel calc.:
N. Keeley (SPhN)

F. Skaza PhD SPhN
F. Skaza, N. Keeley, VL *et al.*, PLB **619**. 82 ('05)
N. Keeley *et al.*, PLB **646**,222('07)

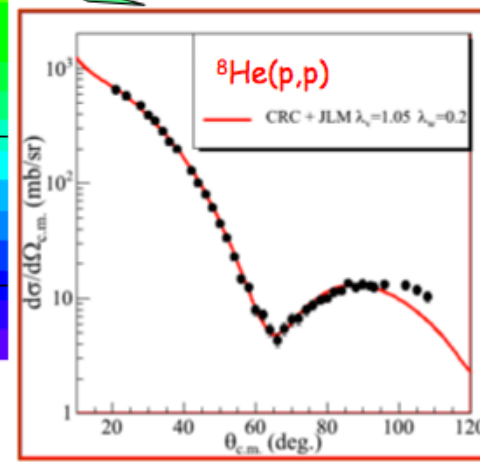


*Structure of ground state & search for unbound excited states*

→ spectroscopy of light charged particles p,d,t (MUST)
→ measurements of resonances in $^8$He NPA 788c, 260 ('07)
→ angular distributions ; analysis in **coupled reaction channels**
PLB **619**. 82 ('05) ; **646**, 222 ('07)

## *Application to* $^{11}\mathrm{Be} + ^{12}\mathrm{C}$ Halo nucleus breakup

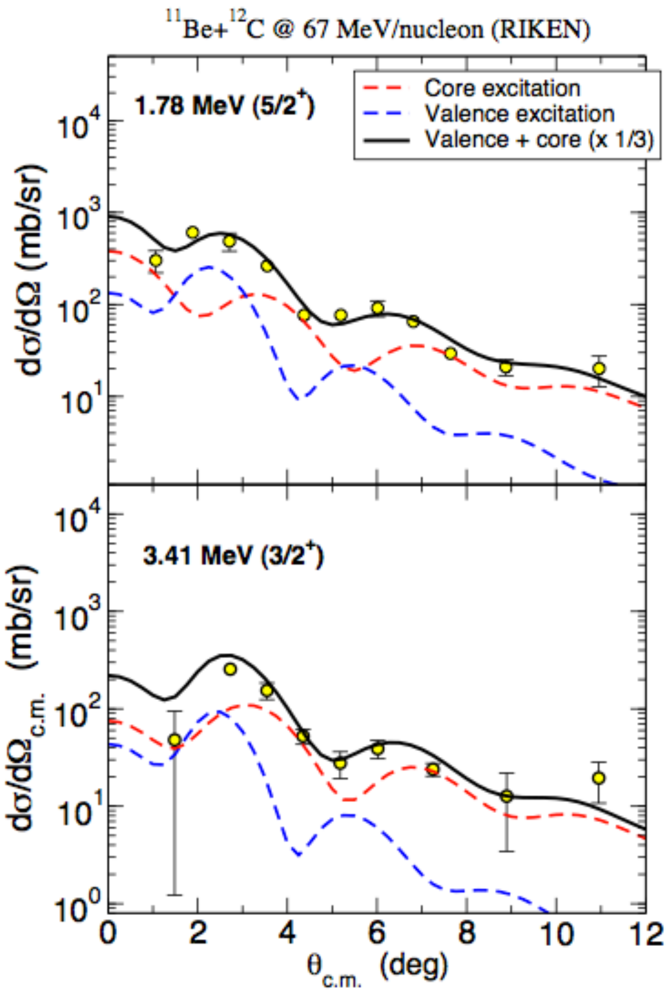


- Neither the valence or core excitation describe the shape of the data
- Coherent superposition valence+core describes very well the shape.
- Magnitude overestimated by a factor of $\sim 3$!

A.M. Moro, DCEN2011

# Parity inversion in N=7 isotones

Experimental systematics

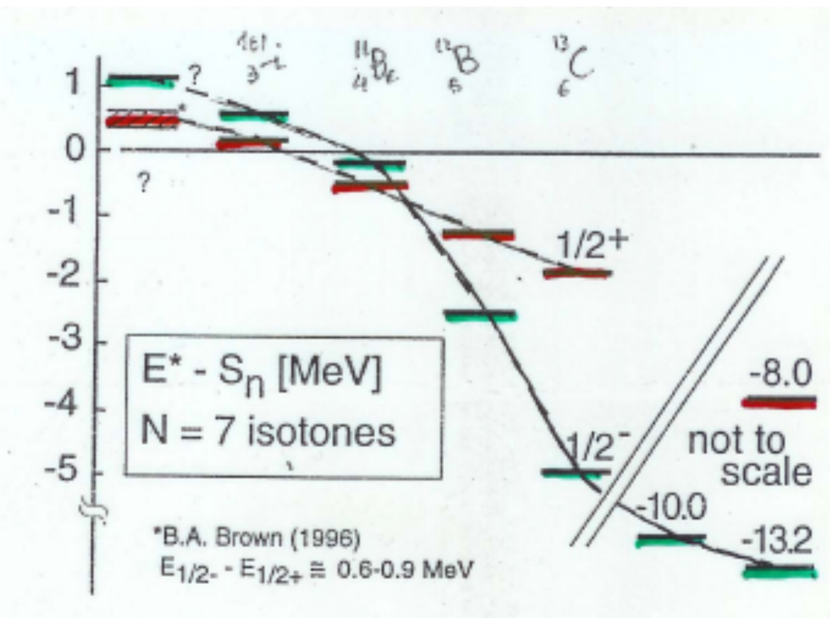


Mean-field results

(Sagawa,Brown,Esbensen PLB 309(93)1)

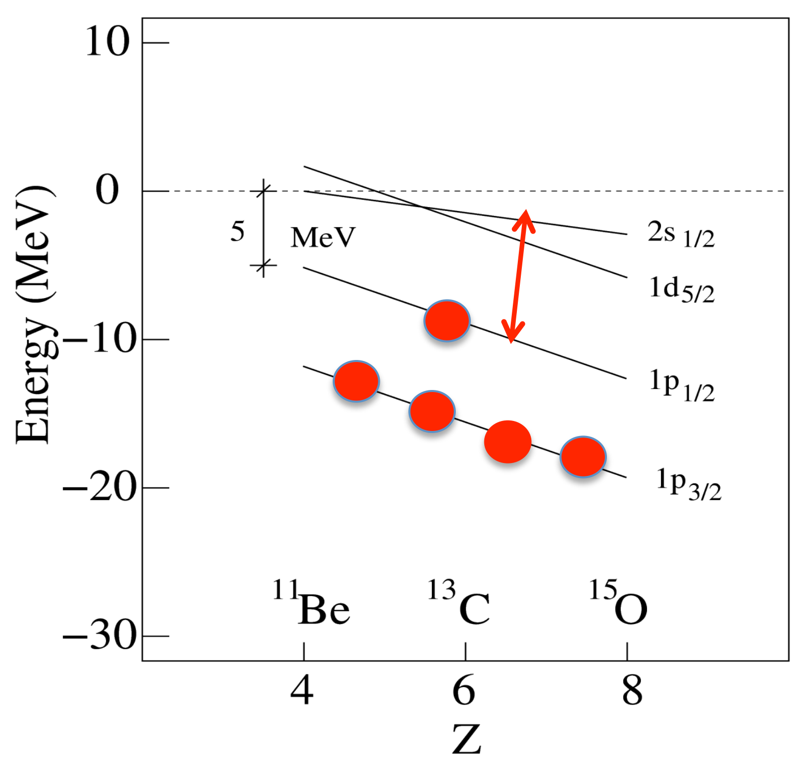

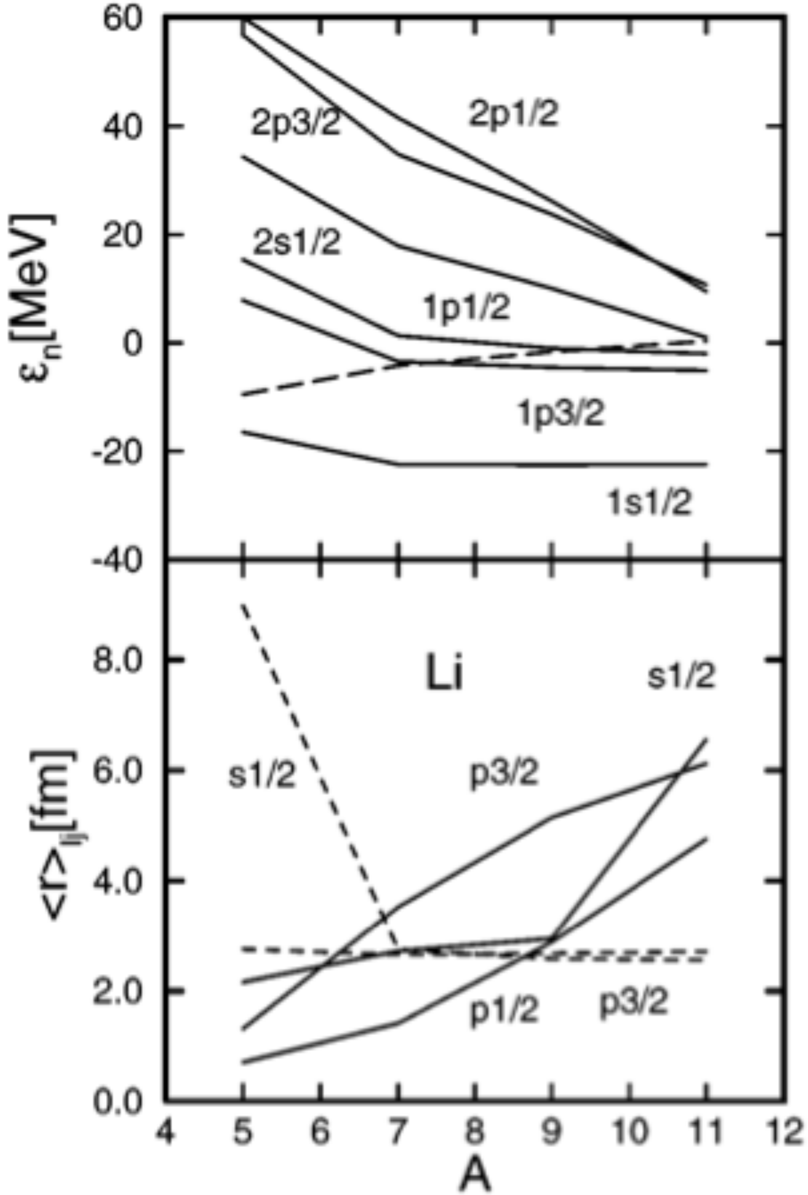


J. Meng and P. Ring, PRL 77(1998)3963

However, we can break up the complicated motion into two independent simple motions: motion of the centre of mass and motion about the centre of mass. The centre of mass moves exactly as if it were an independent body of mass $m_1+m_2$, so it is one of the non-interacting fictitious bodies here. The other fictitious body is a body of mass $m_1 m_2/(m_1+m_2)$—the so-called 'reduced mass'—which moves independently relative to the centre of mass. Thus the system acts as if it were composed of two non-interacting fictitious bodies: the 'centre of mass body' and the 'reduced mass body'. (See appendix $\mathscr{A}$, eqs. ($\mathscr{A}$.11)→($\mathscr{A}$.14) for details.)

### 0.2 Quasi particles and quasi horses

The above two-body example is easy enough to understand, but finding the weakly interacting fictitious bodies in a set of *many* strongly interacting real bodies is a bit harder. We consider first the fictitious bodies called 'quasi particles'. These arise from the fact that when a real particle moves through the system, it pushes or pulls on its neighbours and thus becomes surrounded by a 'cloud' of agitated particles similar to the dust cloud kicked up by a galloping horse in a western. The real particle plus its cloud is the quasi particle (Fig. 0.4).

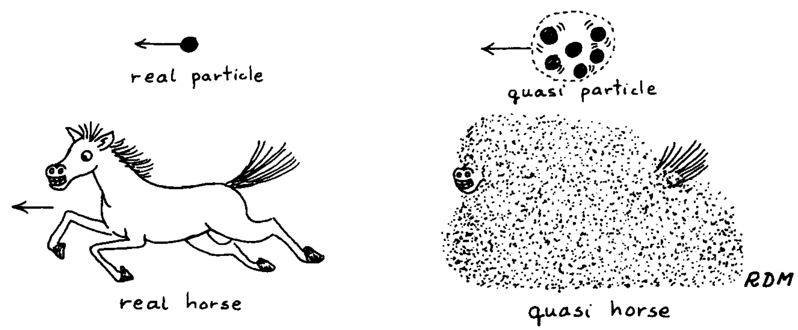


Fig. 0.4 *Quasi Particle Concept*

Just as the dust cloud hides the horse, the particle cloud 'shields' or 'screens' the real particles so that quasi particles interact only weakly with one another. The presence of the cloud also makes the properties of the quasi particle different from that of the real particle—it may have an '*effective mass*' different from the real mass, and a '*lifetime*'. These properties of quasi particles are directly observable experimentally.

It should be remarked that the quasi particle is in an excited energy level of the many-body system. Hence it is referred to as an '*elementary excitation*' of the system. (See appendix $\mathscr{A}$, §$\mathscr{A}$.2.) We now consider some examples of quasi particles.

# SELF ENERGY RENORMALIZATION OF SINGLE-PARTICLE STATES: CLOSED SHELL

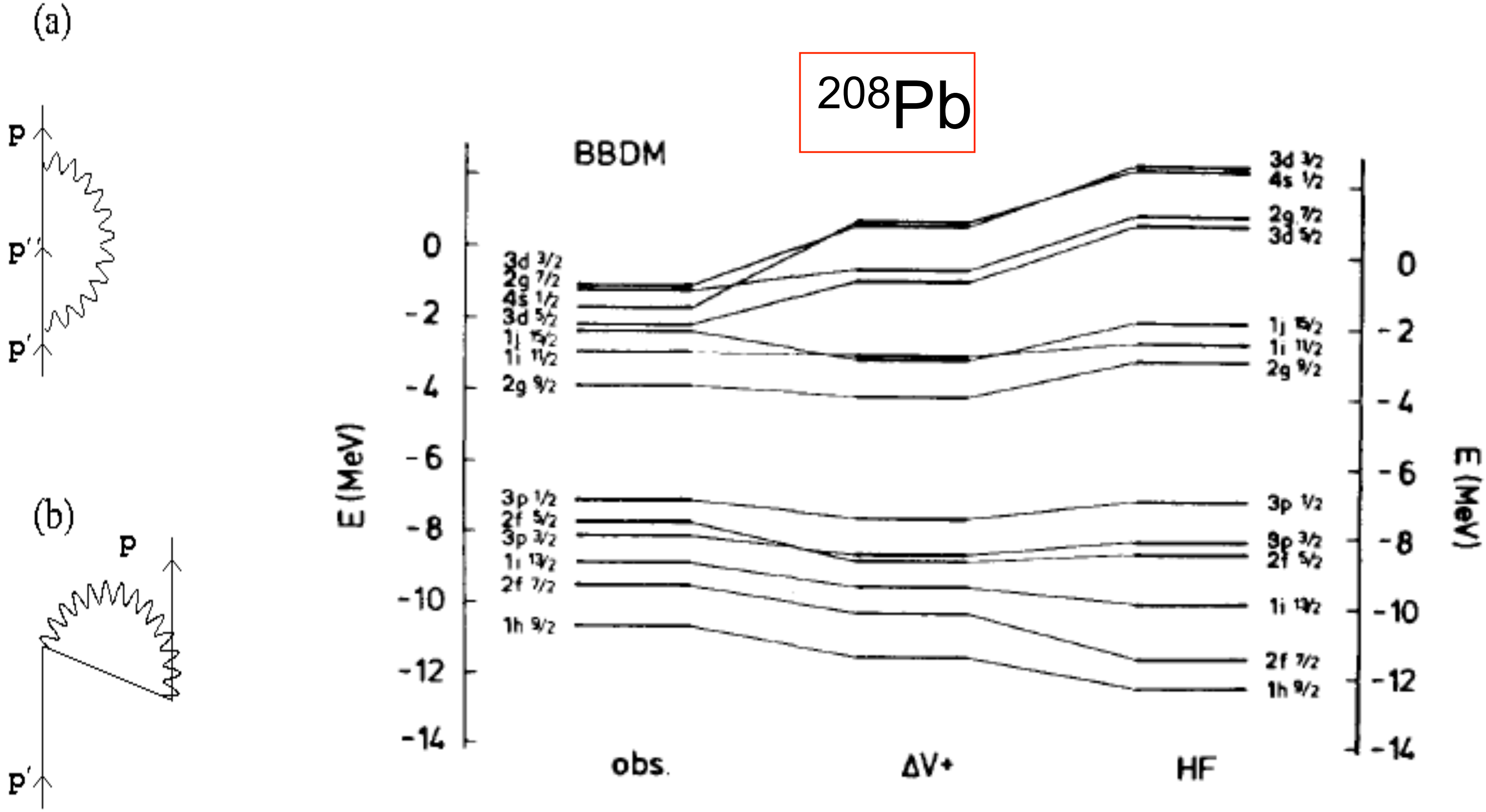


C. Mahaux, P.F. Bortignon, R.A. Broglia, C.H. Dasso and Mahaux, Phys. Rep.(1985)1

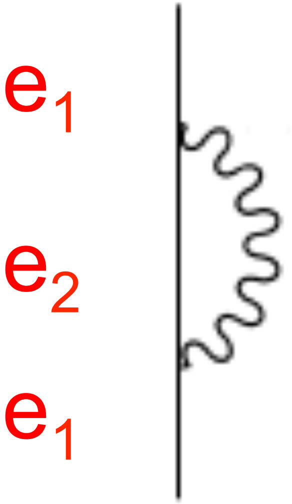


$$= \frac{V^2}{e_1 - (e_2 + \hbar\omega_\lambda)} \approx -\frac{V^2}{\hbar\omega_\lambda}$$

$$m_\omega \approx \left(1 + \frac{2N(0)V^2}{\hbar\omega_\lambda}\right) m$$

$$\boxed{\begin{aligned} m_\omega &\approx 1.5m \\ \hbar\omega_\lambda &\approx 1\text{MeV} \\ N(0) &\approx 3\text{MeV}^{-1} \end{aligned}} \rightarrow \boxed{V^2 \approx 0.1 \quad \text{MeV}^2}$$

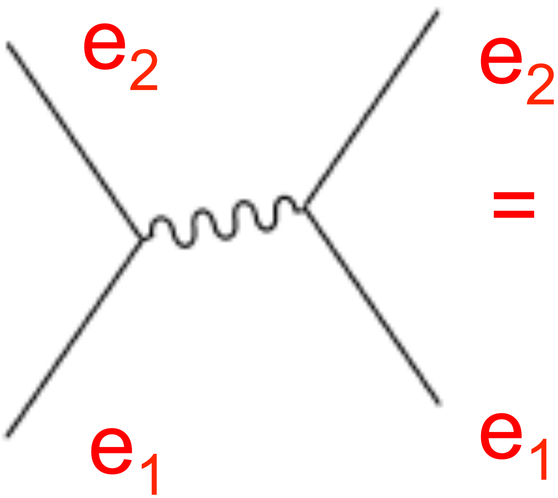


$$= \frac{V^2}{2e_1 - (e_1 + e_2 + \hbar\omega_\lambda)} = \frac{V^2}{e_1 - (e_2 + \hbar\omega_\lambda)} \approx -\frac{V^2}{\hbar\omega_\lambda}$$

$$\boxed{V_{ind} \approx -0.2\text{MeV}}$$

$^{11}$Be

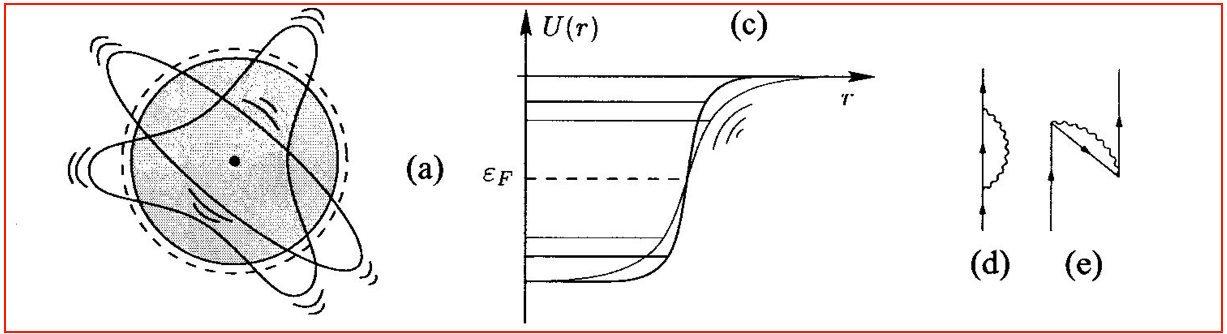


H. Sagawa et al., PLB 309 (1993)1

Eshift = - 2.5 MeV

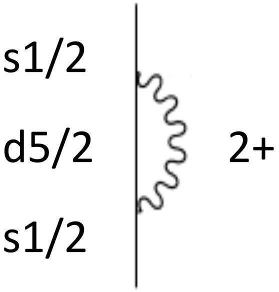


Self-energy

+

Eshift = + 2.5 MeV

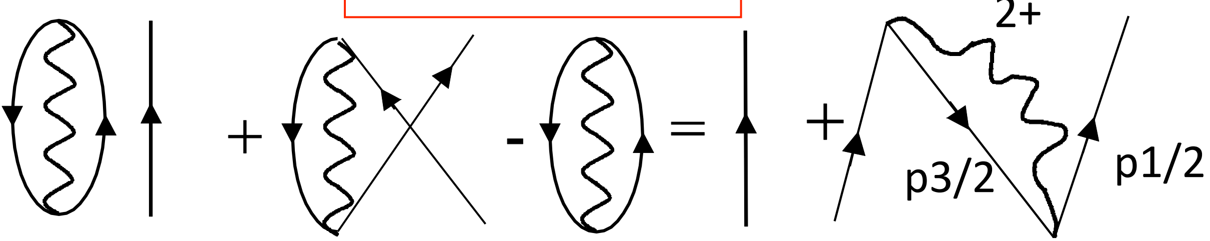


Pauli blocking of core ground state correlations

↓

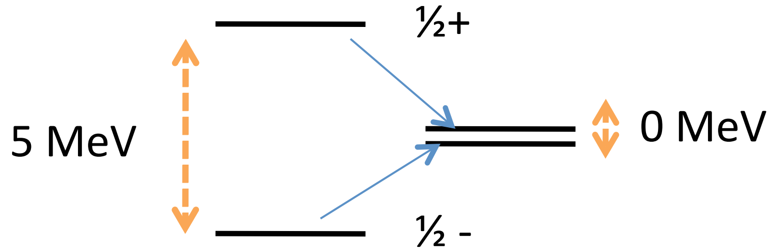


Level inversion

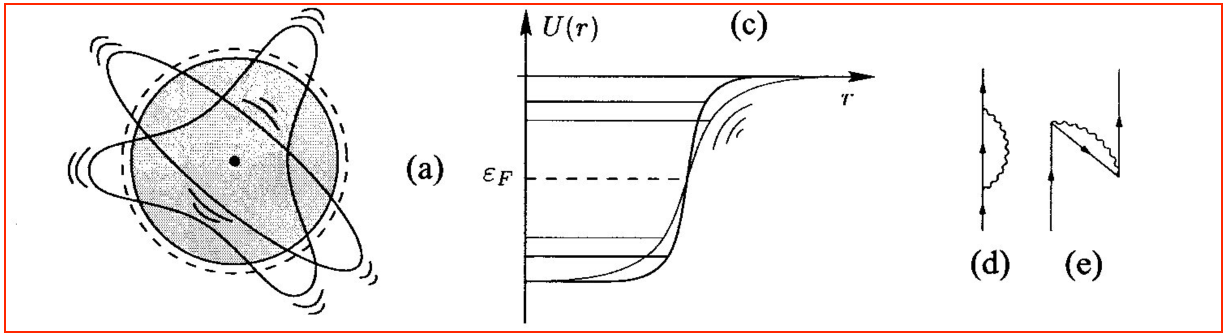


Mean field potential

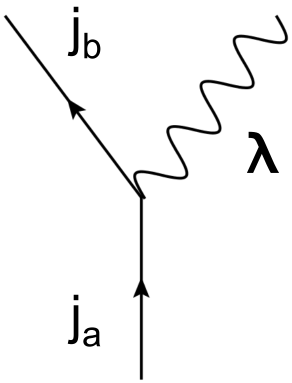


$$= \frac{1}{\sqrt{4\pi}} \langle j_a \lambda | j_b \rangle \beta_\lambda \left\langle j_a \left| \frac{\partial U}{\partial r} \right| j_b \right\rangle = h(a, b\lambda)$$

From B(EL) experimental value
in the core nucleus

# Effective, energy-dependent matrix (Bloch-Horowitz)

$^{11}$Be

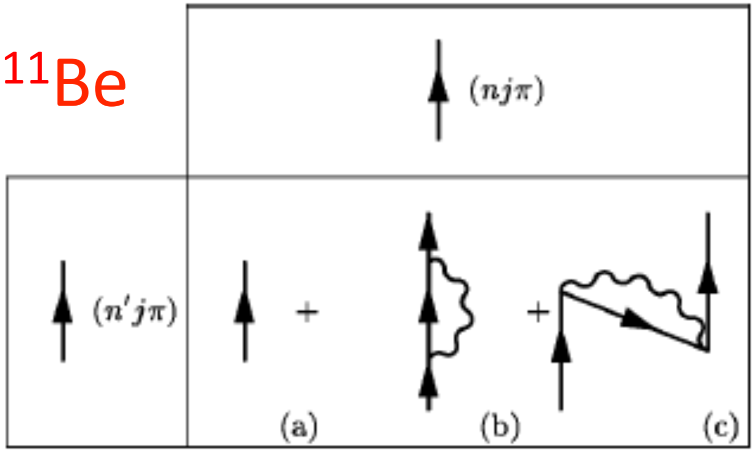


## Main ingredients of our calculation

**Fermionic degrees of freedom**:

• s1/2, p1/2, d5/2 Wood-Saxon levels up to 150 MeV (discretized continuum) from a standard (Bohr-Mottelson) Woods-Saxon potential

**Bosonic degrees of freedom**:

• 2+ and 3- QRPA solutions with energy up to 50 MeV; residual interaction: multipole-multipole separable with the coupling constant tuned to reproduce E(2+)=3.36 MeV and $0.6<\beta_2<0.7$

# A dynamical description of two-neutron halos

**$^{11}$Li**

F. Barranco et al. EPJ A11 (2001) 385

**$^{12}$Be**

G. Gori et al. PRC 69 (2004) 041302(R)

Energy-dependent matrix

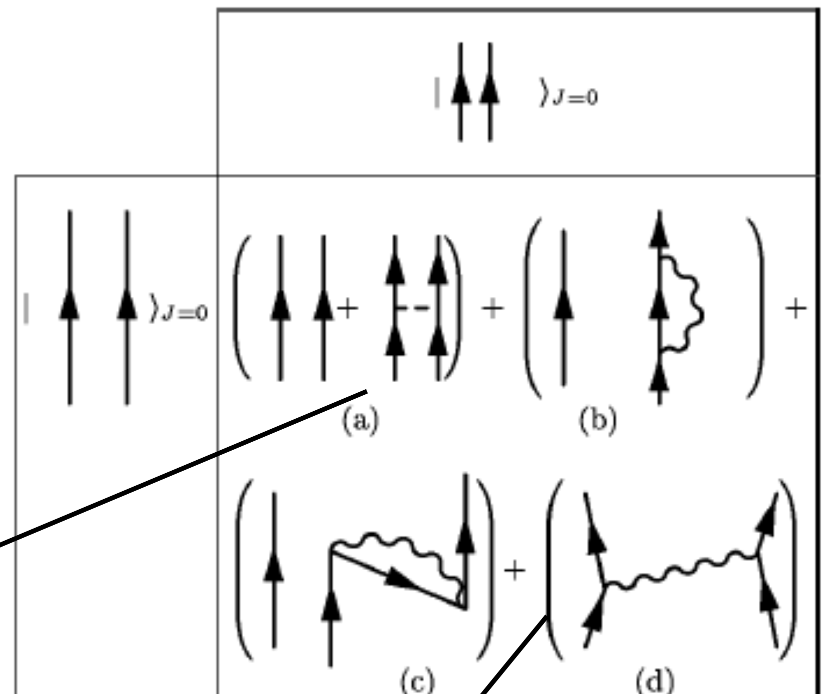


Bare interaction

Induced interaction

Theoretical calculation for $^{10}$Li and $^{11}$Li

Low-lying dipole strength

s-p mixing

Phenomenological input:
properties of collective models

Predictions:
binding energy,
spectroscopic factors

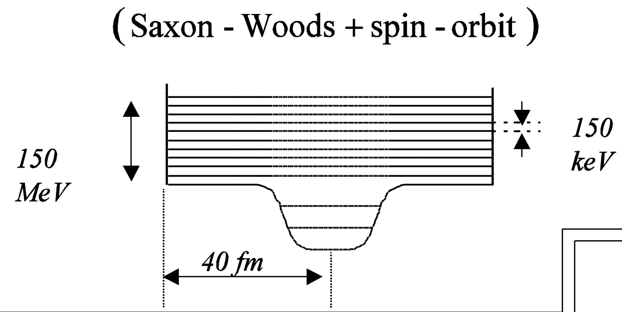


Vibrations

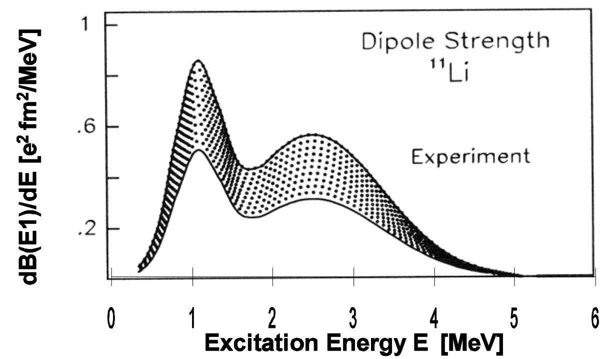


$B(E2)\uparrow = [5.2 \pm 0.6]10^{-3} e^2 b^2 \quad (^{10}Be)$

Bare interaction

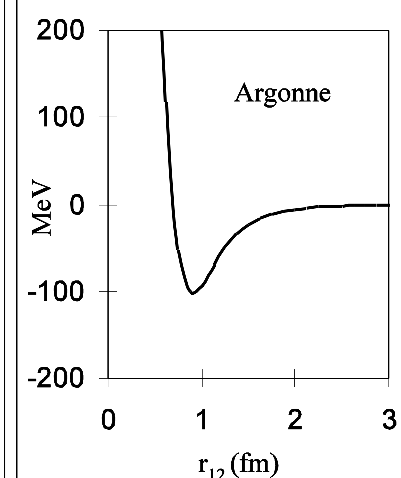


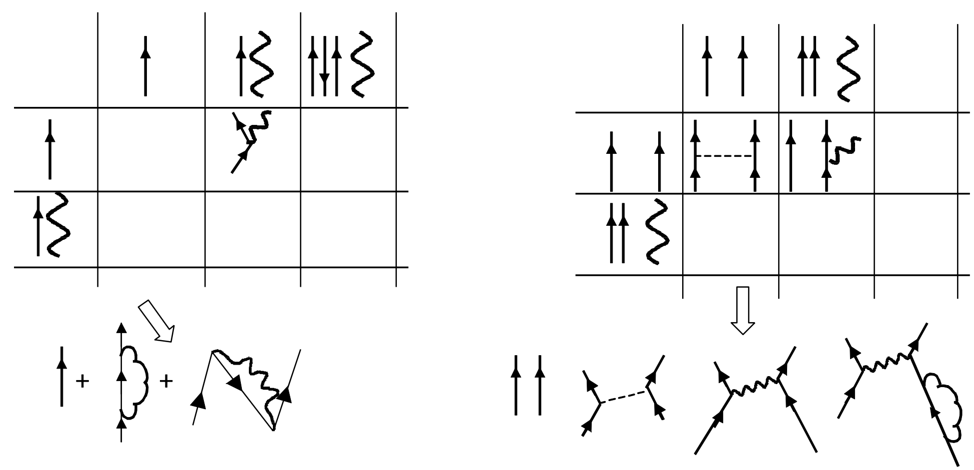

**Table 2.** RPA wave function of the collective low-lying quadrupole phonon in $^{11}$Li, of energy $E_{2^+} = 5.05$ MeV, and leading to the most important contribution to the induced interaction in fig. 1, II. All the listed amplitudes refer to neutron transitions, except for the last column. We have adopted the self-consistent value ($\chi_2 = 0.013\,\mathrm{MeV}^{-1}$ ) for the coupling constant. The resulting value for the deformation parameter is $\beta_2 = 0.5$.

| | $1p_{3/2}^{-1}1p_{1/2}$ | $2s_{1/2}^{-1}5d_{3/2}$ | $1p_{1/2}^{-1}6p_{3/2}$ | $2s_{1/2}^{-1}3d_{5/2}$ | $2s_{1/2}^{-1}5d_{5/2}$ | $1p_{3/2}^{-1}1p_{1/2}$ ($\pi$) |
|---|---|---|---|---|---|---|
| $X_{\mathrm{ph}}$ | 0.824 | 0.404 | 0.151 | 0.125 | 0.126 | 0.16 |
| $Y_{\mathrm{ph}}$ | 0.119 | 0.011 | −0.002 | −0.049 | −0.011 | 0.07 |

B(E1) calculated with separable force; coupling constant tuned to reproduce experimental strength;
part of the strength comes from admixture of GDR

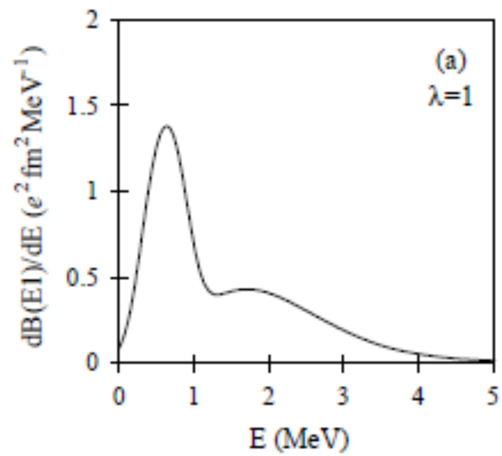


**Table 3.** RPA wave function of the strongest low-lying dipole vibration of $^{11}$Li, ($E_{1^-} = 0.75$ MeV), and contributing most importantly to the pairing induced interaction (fig. 1, II). All the listed amplitudes refer to neutron transitions. We have used the value $\chi_1 = 0.0043$ MeV$^{-1}$ for the isovector coupling constant in order to get a good agreement with the experimental findings. To be noted that this value coincides within 25% close to the selfconsistent value of 0.0032 MeV$^{-1}$. The resulting strength function (cf. fig. 2(a)) integrated up to 4 MeV gives 7% of the Thomas-Reiche-Kuhn energy weighted sum rule, to be compared to the experimental value of 8% [38].

| | $1p_{1/2}^{-1}2s_{1/2}$ | $1p_{1/2}^{-1}3s_{1/2}$ | $1p_{1/2}^{-1}4s_{1/2}$ | $1p_{1/2}^{-1}1d_{3/2}$ | $1p_{3/2}^{-1}5d_{5/2}$ | $1p_{3/2}^{-1}6d_{5/2}$ | $1p_{3/2}^{-1}7d_{5/2}$ |
|---|---|---|---|---|---|---|---|
| $X_{\mathrm{ph}}$ | 0.847 | −0.335 | 0.244 | 0.165 | 0.197 | 0.201 | 0.157 |
| $Y_{\mathrm{ph}}$ | 0.088 | 0.060 | 0.088 | 0.008 | 0.165 | 0.173 | 0.138 |

# Results for $^{10}$Li and $^{11}$Li

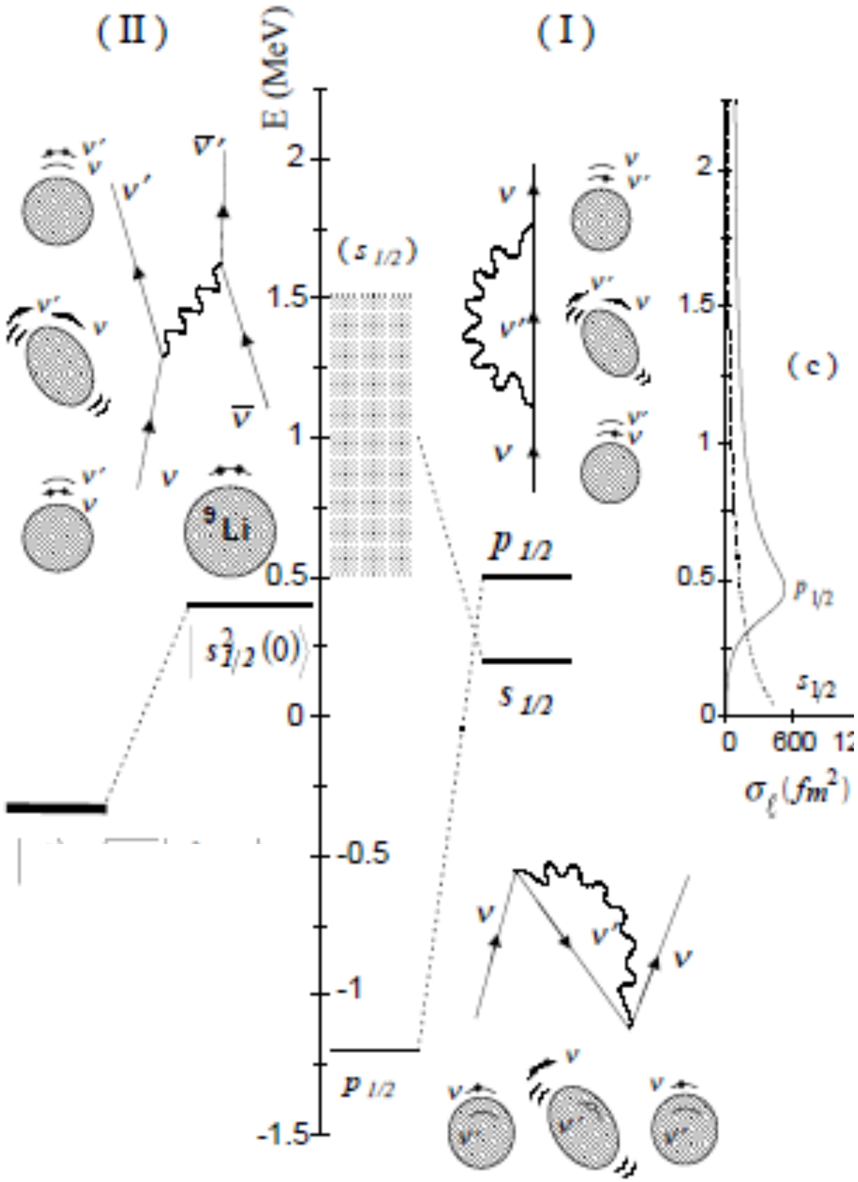


| | | Exp. | Theory | |
|---|---|---|---|---|
| | | | particle-vibration +Argonne | mean field |
| $^{10}_{3}$Li$_7$ (not bound) | s | 0.1-0.2 MeV | 0.2 MeV (virtual) | ~ 1 MeV (virtual) |
| | p | 0.5-0.6 MeV | 0.5 MeV (res.) | -1.2 MeV (bound) |
| $^{11}_{3}$Li$_8$ (bound) | $S_{2n}$ | 0.369 MeV | 0.33 MeV | 2.4 MeV |
| | s$^2$,p$^2$ | 50% , 50% | 41% , 59% | 0% , 100% |
| | $\langle r^2\rangle^{1/2}$ | 3.55±0.1 fm | 3.9 fm | |
| | $\Delta p_\perp$ | 48±10 MeV/c | 55 MeV/c | |

[11Li correlated wave function]

$$|\tilde{0}\rangle = |0\rangle + 0.7|(ps)_{1^-} \otimes 1^-;0\rangle + 0.1|(sd)_{2^+} \otimes 2^+;0\rangle$$

$$|0\rangle = 0.45|s^2_{1/2}(0)\rangle + 0.55|p^2_{1/2}(0)\rangle + 0.04|d^2_{5/2}(0)\rangle$$

# Correlated halo wavefunction

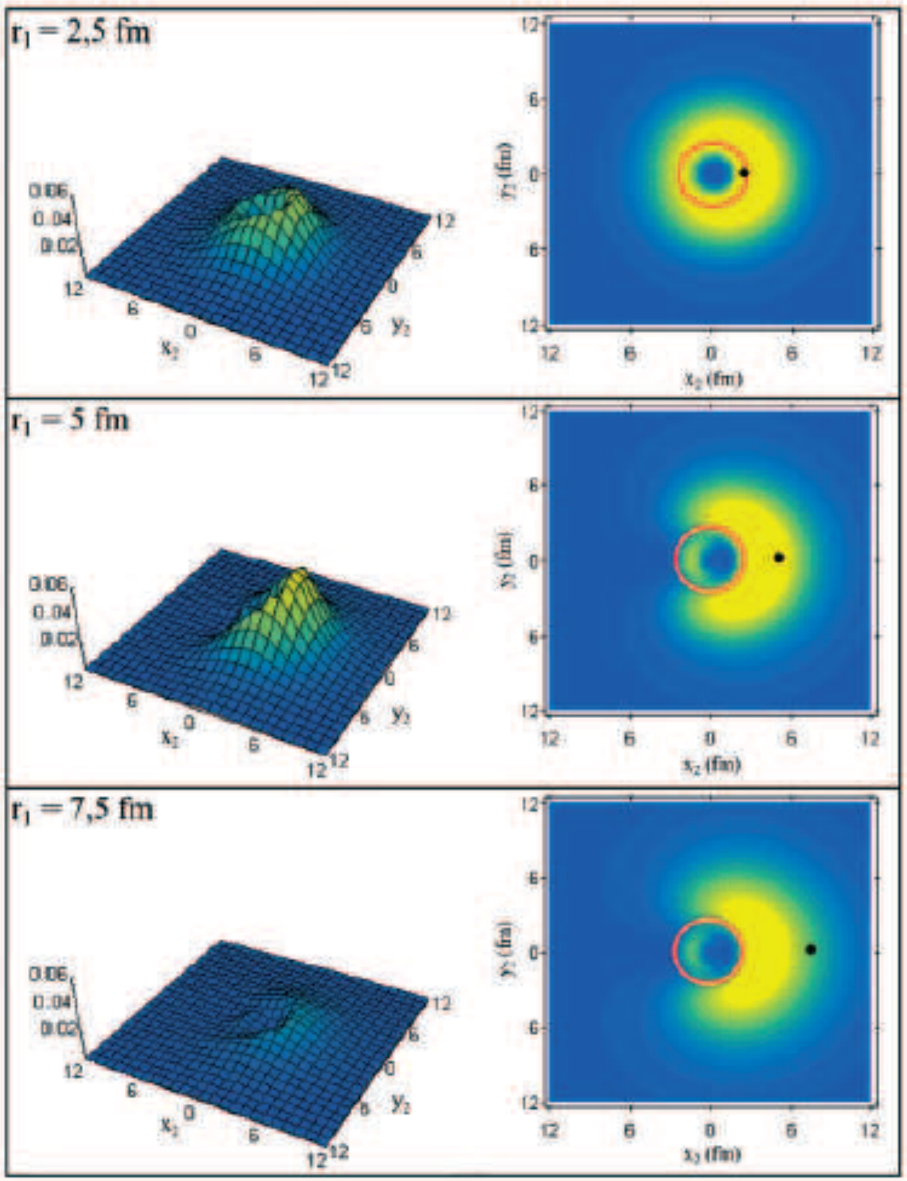


# Uncorrelated

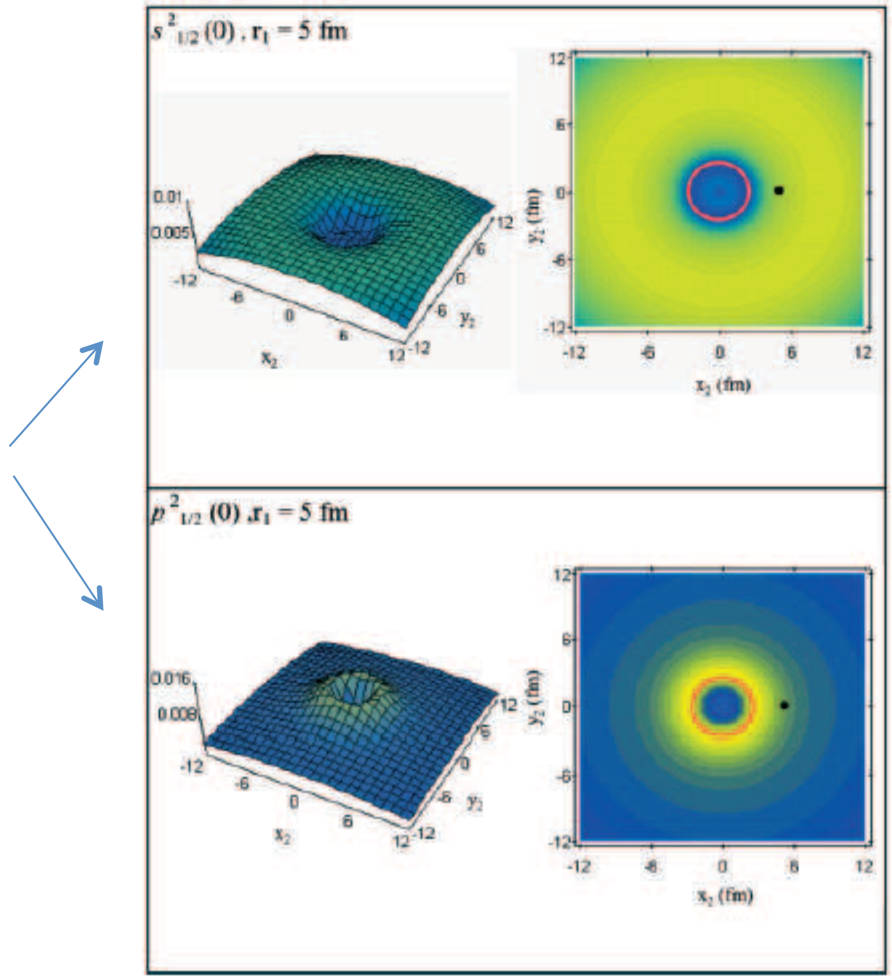

# $^{11}$Li correlated wave function

The halo wavefunction is made out of components which are superposition of single-particle wavefunctions in the discretized continuum, leading to a bound state:

$$|0\rangle = 0.45|s^2_{1/2}(0)\rangle + 0.55|p^2_{1/2}(0)\rangle + 0.04|d^2_{5/2}(0)\rangle$$

A part of the wavefunction is explicitly coupled to 1- and 2+ vibrations:

$$|\tilde{0}\rangle = |0\rangle + 0.7|(ps)_{1^-} \otimes 1^-; 0\rangle + 0.1|(sd)_{2^+} \otimes 2^+; 0\rangle$$

Results for $^{11}Be$, $^{12}Be$
Good agreement between theory and experiment concerning energies and spectroscopic factors

New result for S[1/2+]: $0.28^{+0.03}_{-0.07}$

Kanungo et al.
PLB 682 (2010) 39

Spectroscopic factors from (12Be,11Be+γ) reaction to ½⁺ and ½- final states:
S[1/2-]= 0.37±0.10 S[1/2+]= 0.42±0.10

| | | Expt. | Theory: Particle vibration | Theory: Mean field |
|---|---|---|---|---|
| $^{11}_{4}Be_7$ | $E_{s_{1/2}}$ | −0.504 MeV | −0.48 MeV | ~0.14 MeV |
| | $E_{p_{1/2}}$ | −0.18 MeV | −0.27 MeV | −3.12 MeV |
| | $E_{d_{5/2}}$ | 1.28 MeV | ~0 MeV | ~2.4 MeV |
| | $S[1/2^+]$ | 0.65−0.80 [19] | 0.87 | 1 |
| | | 0.73±0.06 [20] | | |
| | | 0.77 [21] | | |
| | $S[1/2^-]$ | 0.63±0.15 [20] | 0.96 | 1 |
| | | 0.96 [21] | | 1 |
| | $S[5/2^+]$ | | 0.72 | 1 |
| $^{12}_{4}Be_8$ | $S_{2n}$ | −3.673 MeV | −3.58 MeV | −6.24 MeV |
| | $s^2, p^2, d^2$ | | 23%, 29%, 48% | 0%, 100%, 0% |
| | $S[1/2^+]$ | 0.42±0.10 [7] | 0.31 | 0 |
| | $S[1/2^-]$ | 0.37±0.10 [7] | 0.57 | 2 |

A. Navin et al.,
PRL 85(2000)266

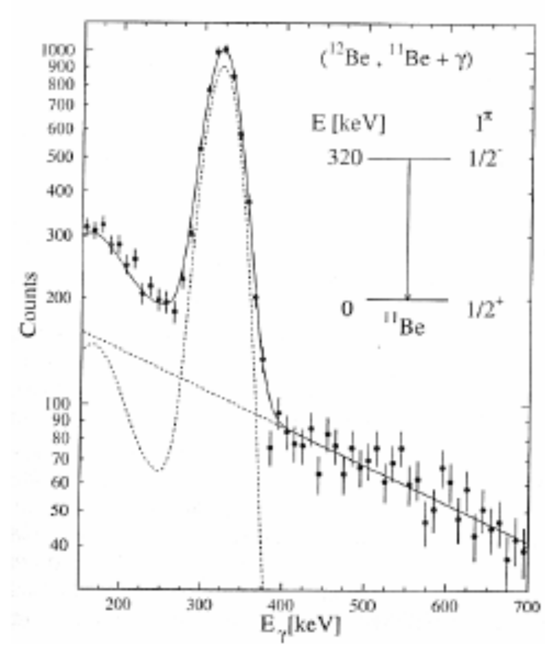

# Probing $^{11}$Li halo-neutrons correlations via (p,t) reaction

PRL **100**, 192502 (2008) PHYSICAL REVIEW LETTERS week ending 16 MAY 200

**Measurement of the Two-Halo Neutron Transfer Reaction $^{1}$H($^{11}$Li, $^{9}$Li)$^{3}$H at 3*A* MeV**

I. Tanihata,* M. Alcorta,† D. Bandyopadhyay, R. Bieri, L. Buchmann, B. Davids, N. Galinski, D. Howell, W. Mills, S. Mythili, R. Openshaw, E. Padilla-Rodal, G. Ruprecht, G. Sheffer, A.C. Shotter, M. Trinczek, and P. Walden

*TRIUMF, 4004 Wesbrook Mall, Vancouver, BC, V6T 2A3, Canada*

H. Savajols, T. Roger, M. Caamano, W. Mittig,‡ and P. Roussel-Chomaz

*GANIL, Bd Henri Becquerel, BP 55027, 14076 Caen Cedex 05, France*

R. Kanungo and A. Gallant

*Saint Mary's University, 923 Robie St., Halifax, Nova Scotia B3H 3C3, Canada*

M. Notani and G. Savard

*ANL, 9700 S. Cass Ave., Argonne, Illinois 60439, USA*

I. J. Thompson

*LLNL, L-414, P.O. Box 808, Livermore, California 94551, USA*

(Received 22 January 2008; published 14 May 2008)

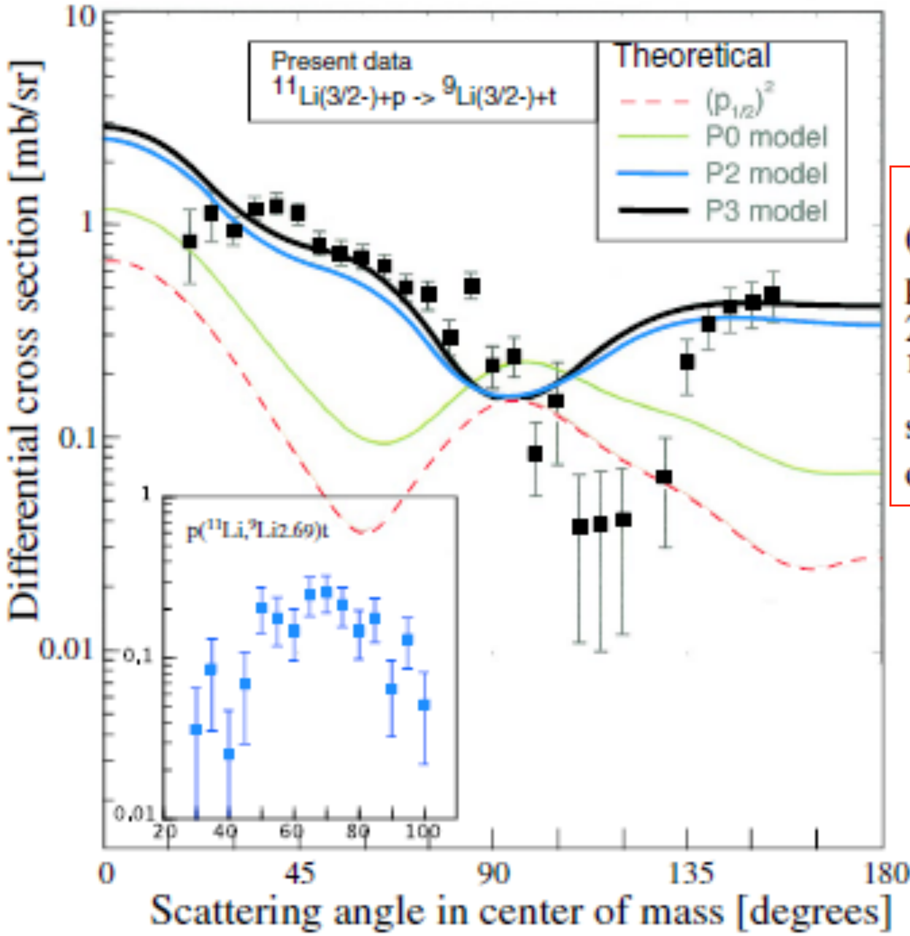


The cross section for transitions to the first excited state (Ex = 2.69 MeV) is shown also in Fig. 3. If this state were populated by a direct transfer, it would indicate that a $1^+$ or $2^+$ halo component is present in the ground state of $^{11}$Li($\frac{3}{2}^-$), because the spin-parity of the $^{9}$Li first excited state is $\frac{1}{2}^-$. This is new information that has not yet been observed in any of previous investigations. A compound

TABLE I. Optical potential parameters used for the present calculations.

| | $V$ MeV | $r_V$ fm | $a_V$ fm | $W$ MeV | $W_D$ MeV | $r_W$ fm | $a_W$ fm | $V_{so}$ MeV | $r_{so}$ fm | $a_{so}$ fm |
|---|---|---|---|---|---|---|---|---|---|---|
| $p+{}^{11}$Li [10] | 54.06 | 1.17 | 0.75 | 2.37 | 16.87 | 1.32 | 0.82 | 6.2 | 1.01 | 0.75 |
| $d+{}^{10}$Li [11] | 85.8 | 1.17 | 0.76 | 1.117 | 11.863 | 1.325 | 0.731 | 0 | | |
| $t+{}^{9}$Li [12] | 1.42 | 1.16 | 0.78 | 28.2 | 0 | 1.88 | 0.61 | 0 | | |

# Calculation of absolute two-nucleon transfer cross section by finite-range DWBA calculation

## simultaneous and successive contributions

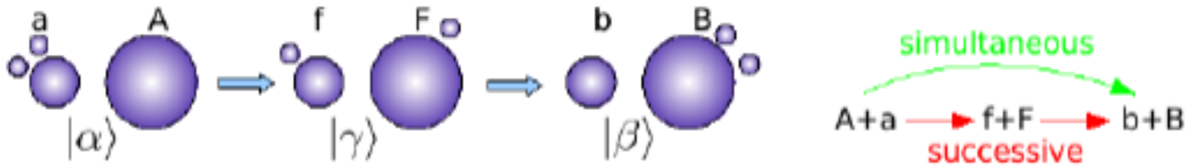


the initial and final channel wave functions are

$$|\alpha\rangle = \phi_a(\xi_b, \mathbf{r}_1, \mathbf{r}_2)\phi_A(\xi_A)\chi_{aA}(\mathbf{r}_{aA})$$
$$|\beta\rangle = \phi_b(\xi_b)\phi_B(\xi_A, \mathbf{r}_1, \mathbf{r}_2)\chi_{bB}(\mathbf{r}_{bB})$$

very schematically, the first order (*simultaneous*) contribution is

$$T^{(1)} = \langle\beta|V|\alpha\rangle,$$

while the second order contribution can be separated in a *successive* and a *non-orthogonality* term

$$T^{(2)} = T^{(2)}_{succ} + T^{(2)}_{NO}$$
$$= \sum_{\gamma}\langle\beta|V|\gamma\rangle G\langle\gamma|V|\alpha\rangle - \sum_{\gamma}\langle\beta|\gamma\rangle\langle\gamma|V|\alpha\rangle.$$

B.F. Bayman and J. Chen, Phys. Rev. C 26 (1982) 150
M. Igarashi, K. Kubo and K. Yagi, Phys. Rep. 199 (1991) 1
G. Potel et al., arXiv: 0906.4298

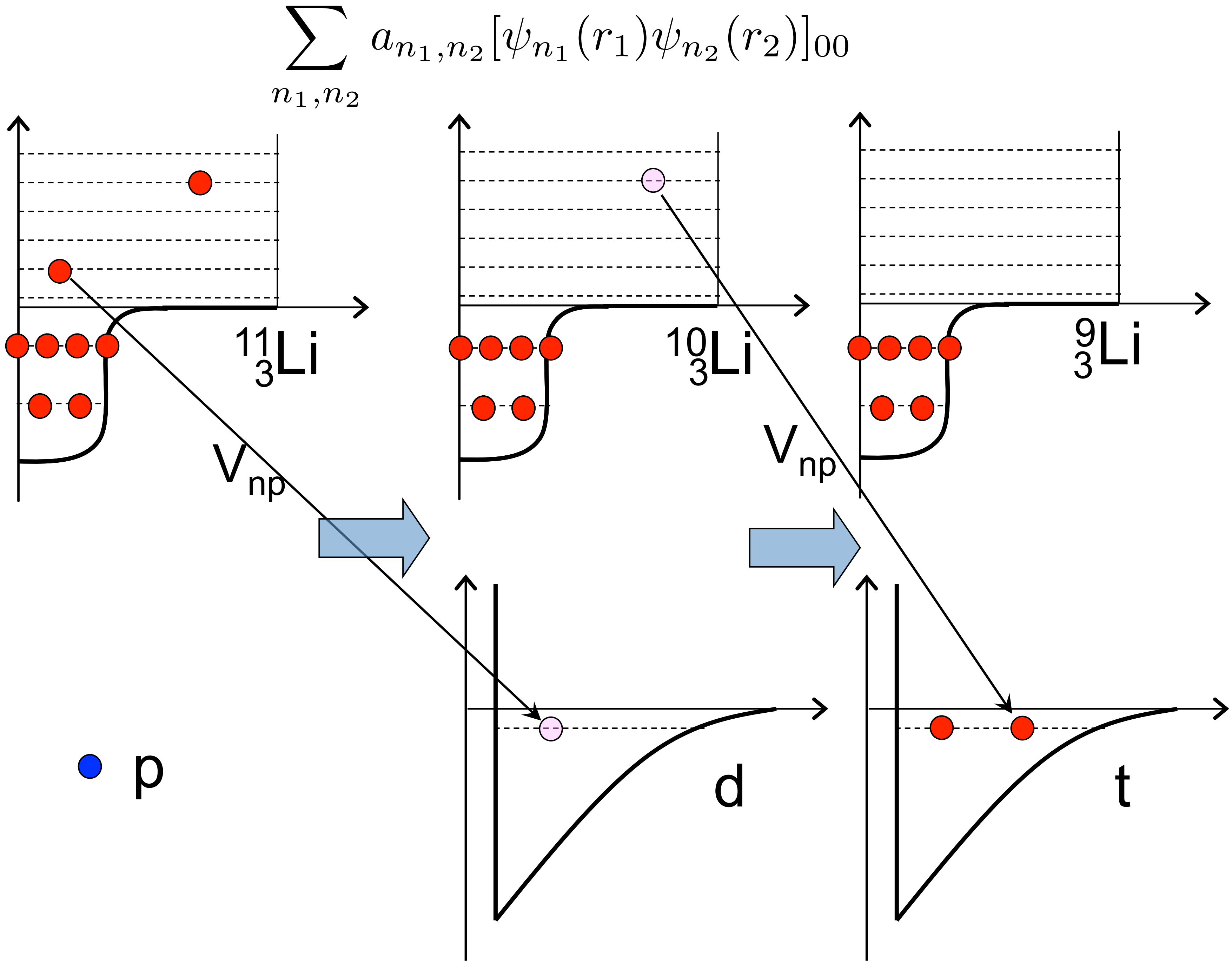
$\sum_{n_1,n_2} a_{n_1,n_2}[\psi_{n_1}(r_1)\psi_{n_2}(r_2)]_{00}$
$^{11}_{3}$Li
$^{10}_{3}$Li
$^{9}_{3}$Li
$V_{np}$
$V_{np}$
d
t
p

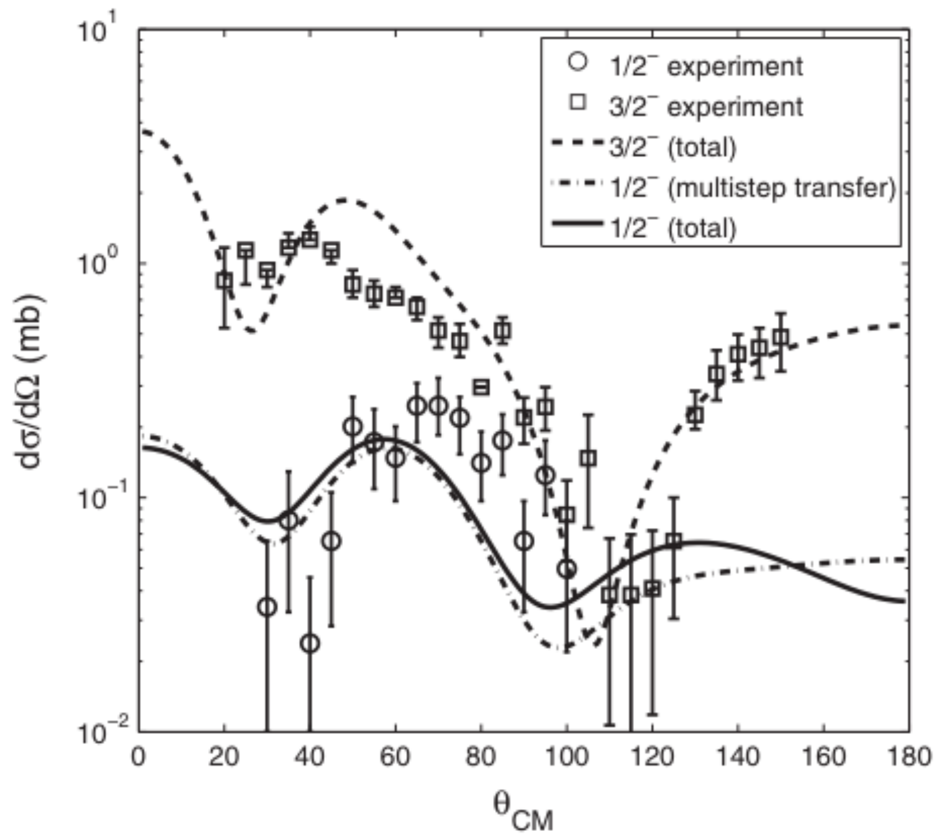


| | $\sigma(^{11}\mathrm{Li(gs)} \to {}^{9}\mathrm{Li\ (i)})$ (mb) | | |
|---|---|---|---|
| i | $\Delta L$ | Theory | Experiment |
| gs ($3/2^-$) | 0 | 6.1 | $5.7 \pm 0.9$ |
| 2.69 MeV ($1/2^-$) | 2 | 0.5 | $1.0 \pm 0.36$ |

G. Potel et al., PRL 105 (2010) 172502

Decomposition into successive and simultaneous contributions

3/2- ground state

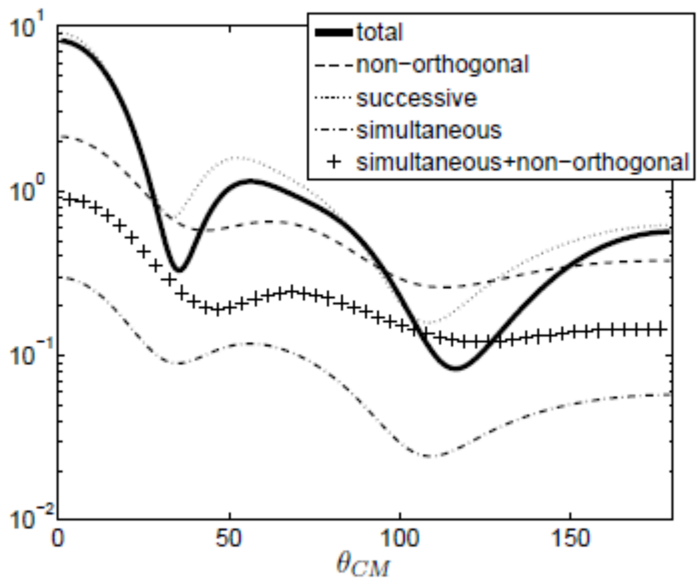


1/2- excited state

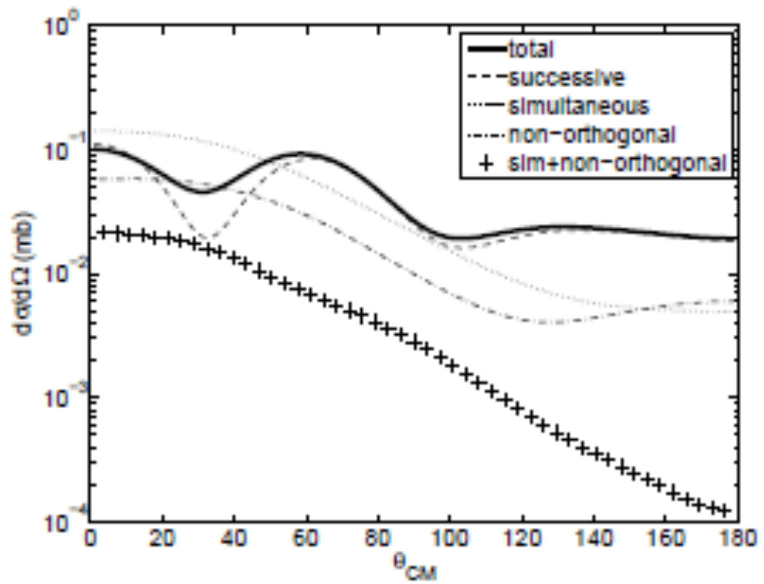

# Convergence of the calculation

With box radius

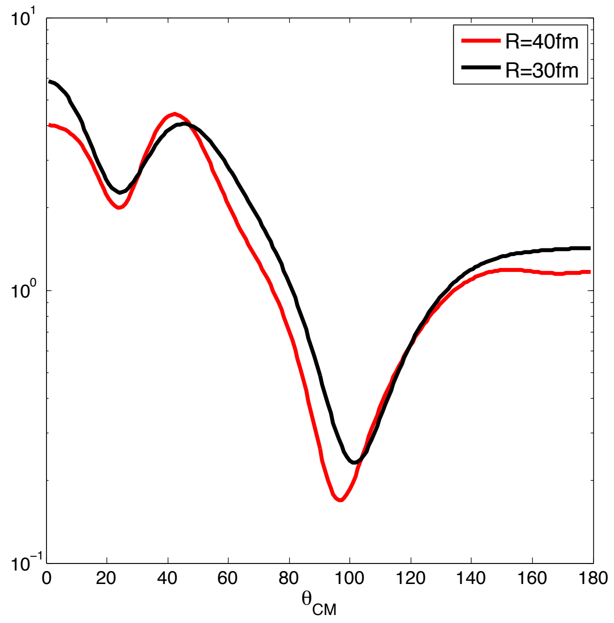


With number of intermediate states

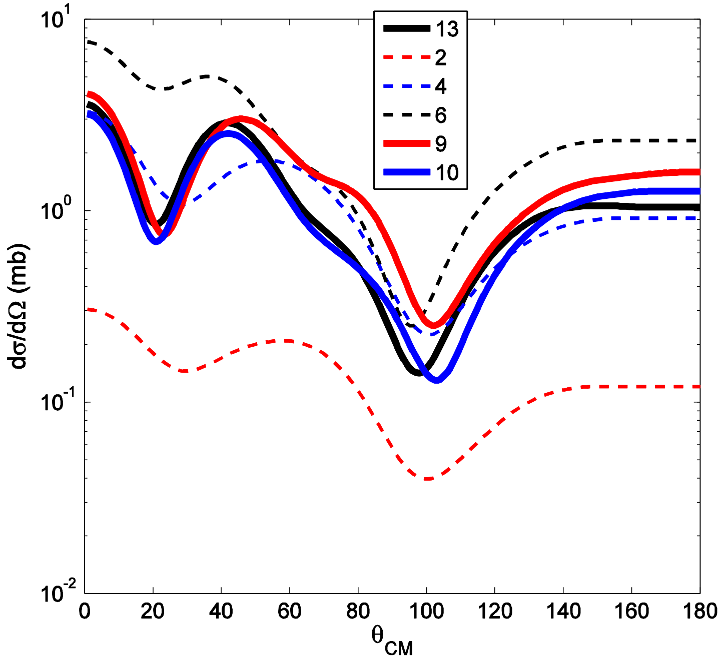

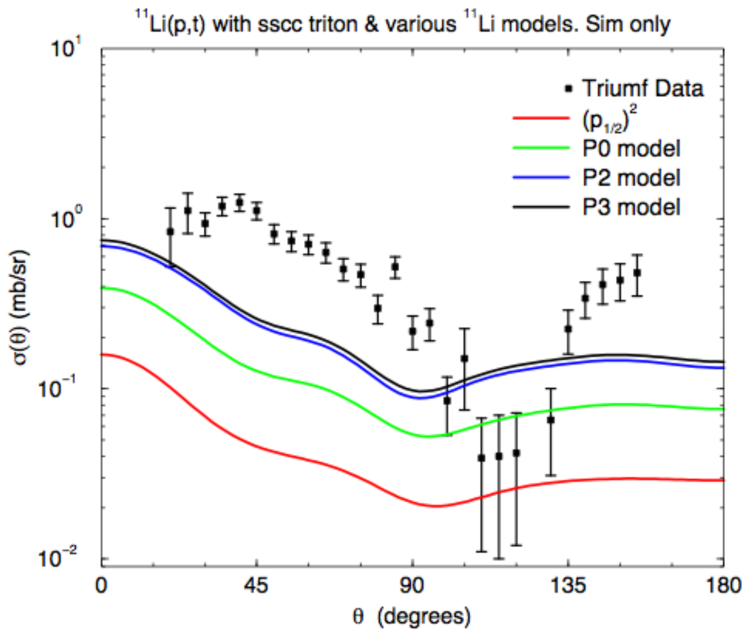


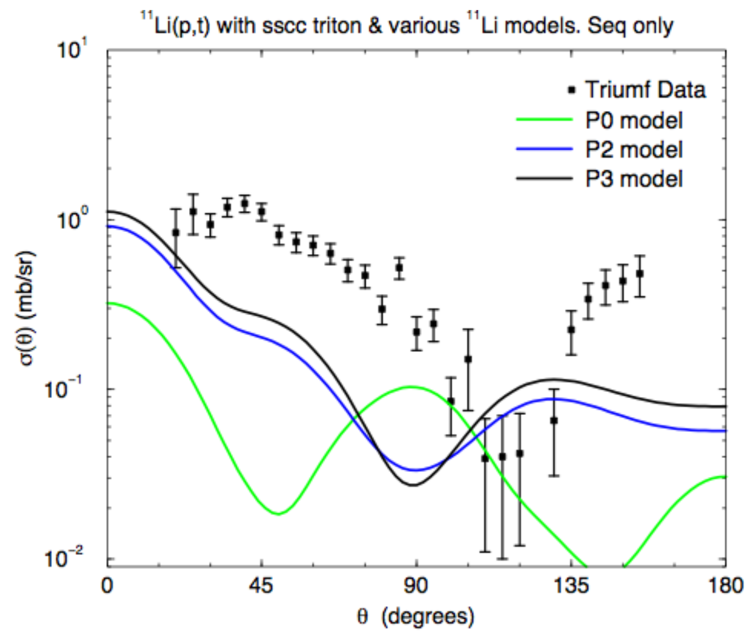


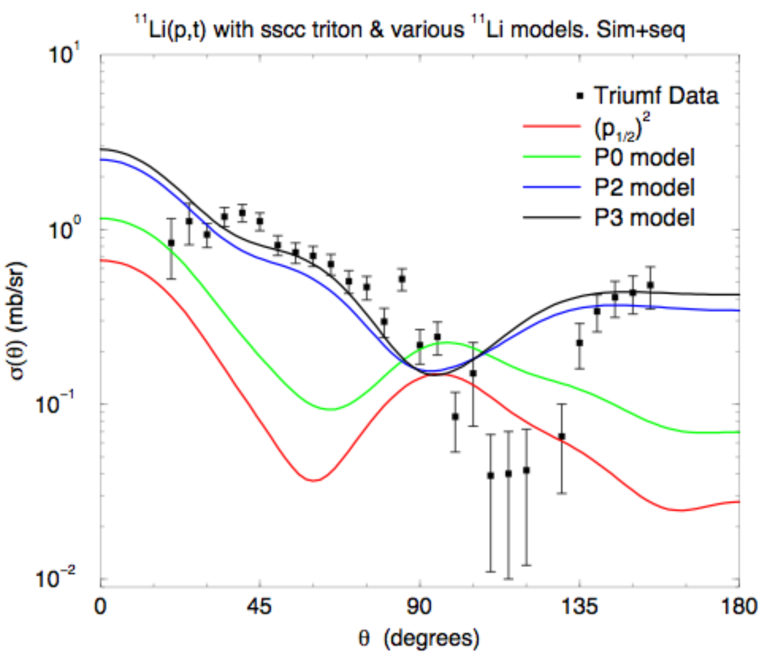


I. Thompson, http://www.int.washington.edu/talks/WorkShops/int_11_48W/

# Channels $c$ leading to the first $1/2^-$ excited state of $^9$Li

$c = 1$: Transfer of the two halo neutrons
$c = 2$: Transfer of a $p_{1/2}$ halo neutron and a $p_{3/2}$ core neutron
$c = 3$: Transfer to the ground state + inelastic excitation

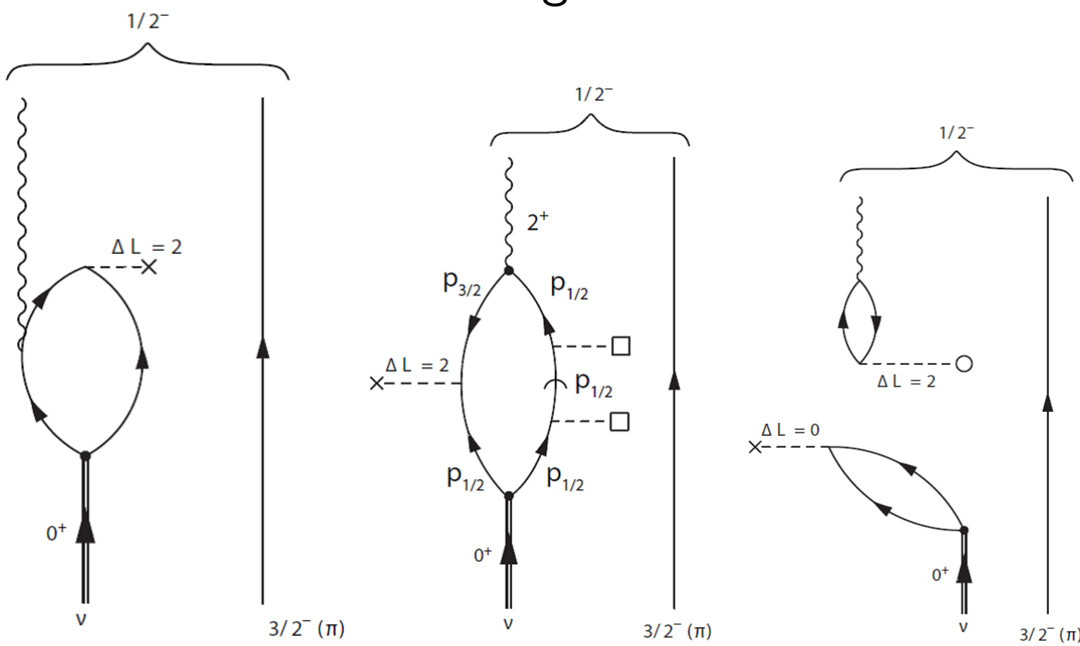


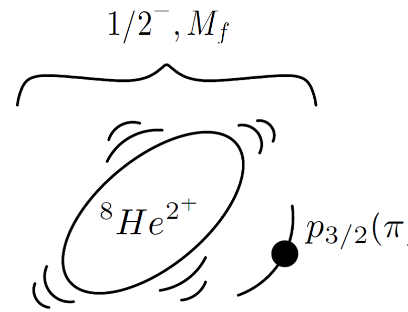


$P^{(1)} = 1.3 \times 10^{-3}$

$P^{(2)} = 4.6 \times 10^{-5}$
$P^{(3)} = 2.6 \times 10^{-6}$

$\sigma_c = \frac{\pi}{k^2} \sum_l (2l+1)|S_l^{(c)}|^2$, $P^{(c)} = \sum_l |S_l^{(c)}|^2$ $(c = 1, 2, 3)$.
Small probabilities $\Rightarrow$ use of second order perturbation theory.

# Two-step effects : how important are they?

| Reaction | $\sigma$(mb) | Notation |
|---|---|---|
| $^{1}H+^{11}Li \rightarrow {}^{1}H+^{11}Li$ | 452 | $\sigma_{el}$ |
| $^{1}H+^{11}Li\rightarrow {}^{3}H+^{9}Li(gs)$ | 8.0 | $\sigma_{2n}$ |
| $^{1}H+^{11}Li\rightarrow {}^{3}H+^{9}Li(1/2^{-}; 2.69\ MeV)$ | 0.79 | $\sigma_{2n}^{1/2^{-}}$ |
| $^{3}H+^{9}Li(gs) \rightarrow {}^{3}H+^{9}Li(1/2^{-}; 2.69 MeV)$ | 35 | $\sigma_{inel}$ |

Excitation of ½- state following transfer

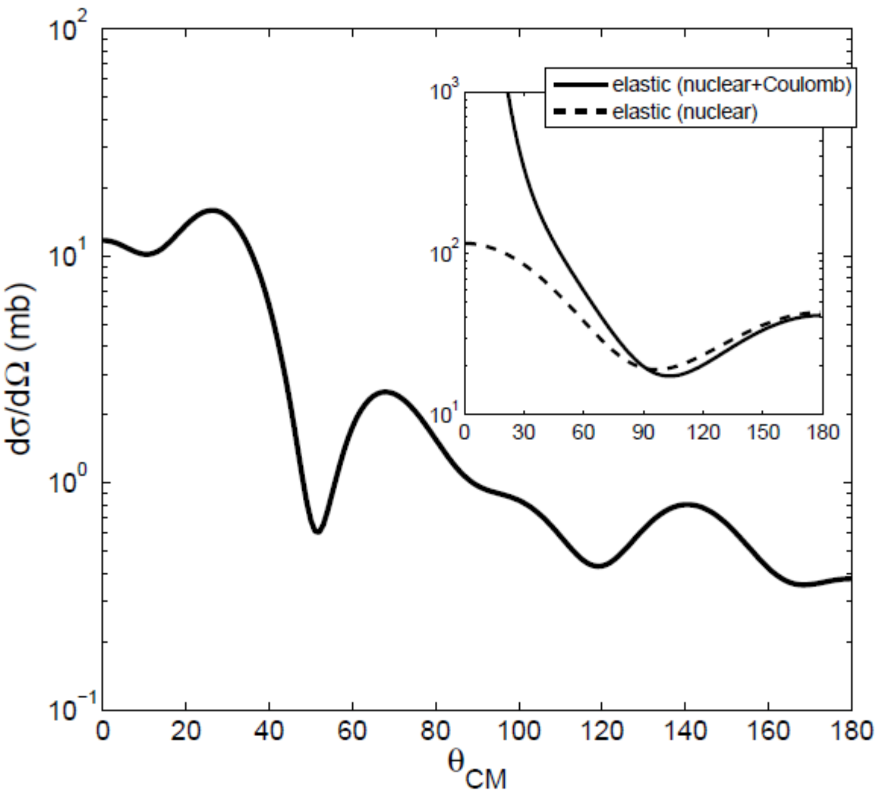


E. Vigezzi et al.,
J. Phys. G Conf. Ser. 312 (2011) 092061

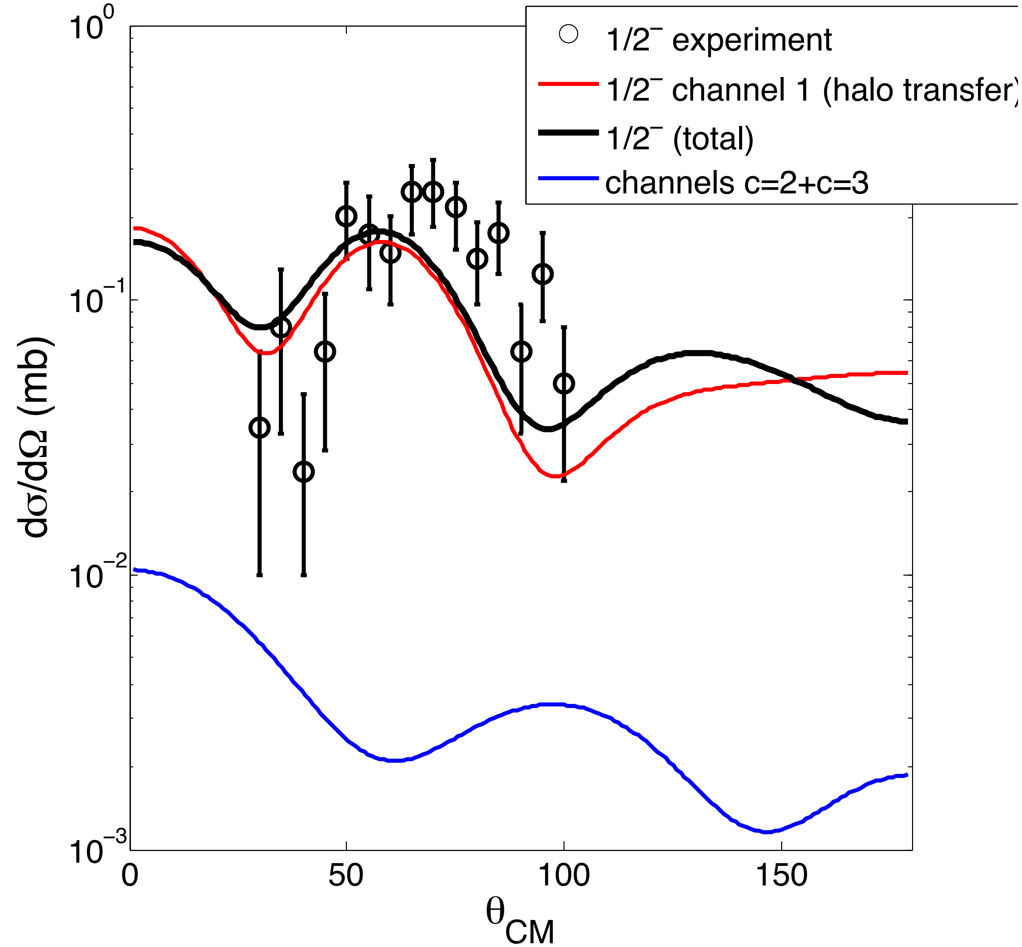

1/2⁻ experiment
1/2⁻ channel 1 (halo transfer)
1/2⁻ (total)
channels c=2+c=3
dσ/dΩ (mb)
θ_CM
10^0
10^-1
10^-2
10^-3
0
50
100
150

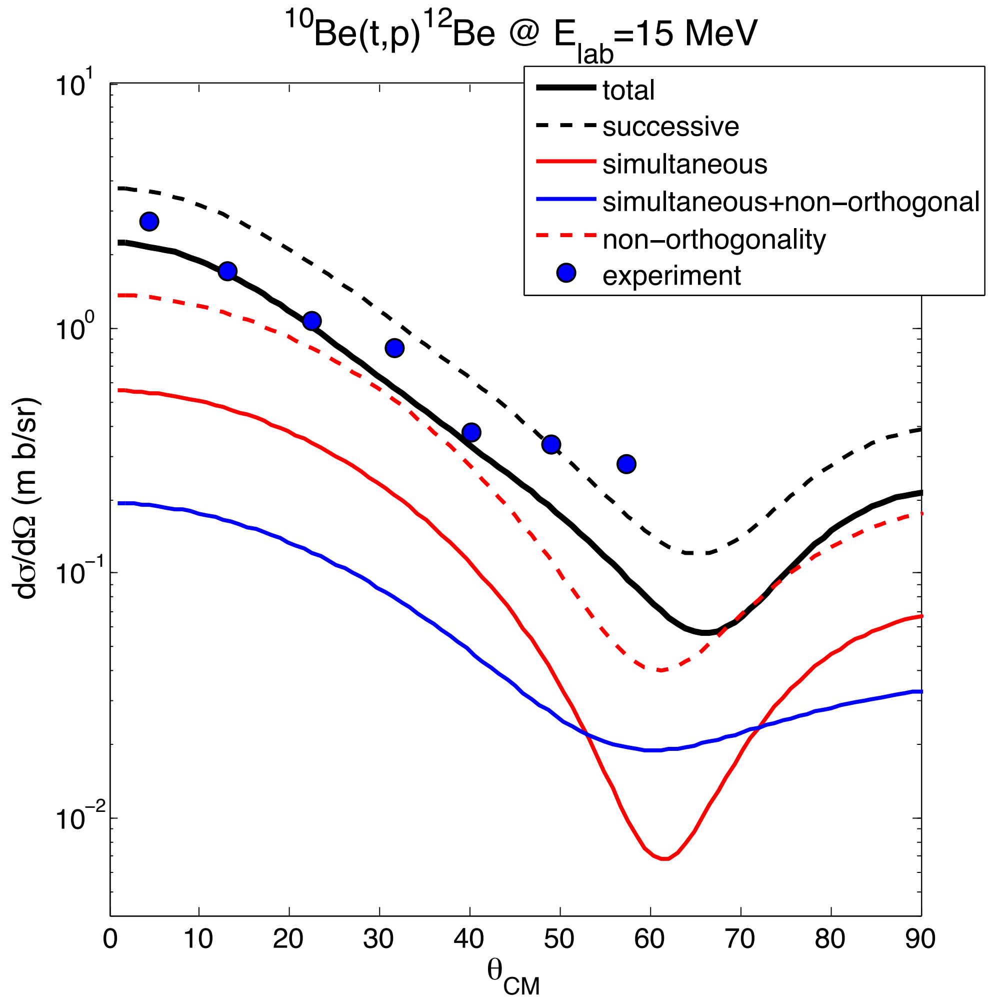


Data:
H.T. Fortune, G.B. Liu, D.E. Alburger,
Phys. Rev C50 (1994) 1355

CONCLUSION:

According to a dynamical model of the halo nucleus 11Li,
a key role is played by the coupling of the valence nucleons
with the vibrations of the system.
The structure model has been tested with a detailed reaction
calculation, comparing with data obtained in a recent (t,p) experiment.
Theoretical and experimental cross section are in reasonable agreement.

Many open issues, among them:

Optical potentials

The role of the tensor force

# Parity inversion in N=7 isotones

Experimental systematics

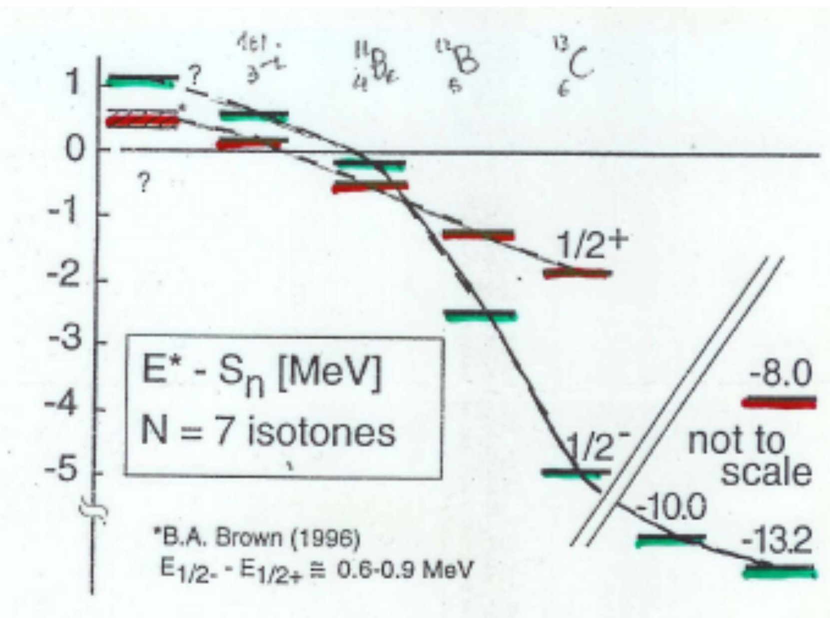


Mean-field results

(Sagawa,Brown,Esbensen PLB 309(93)1)

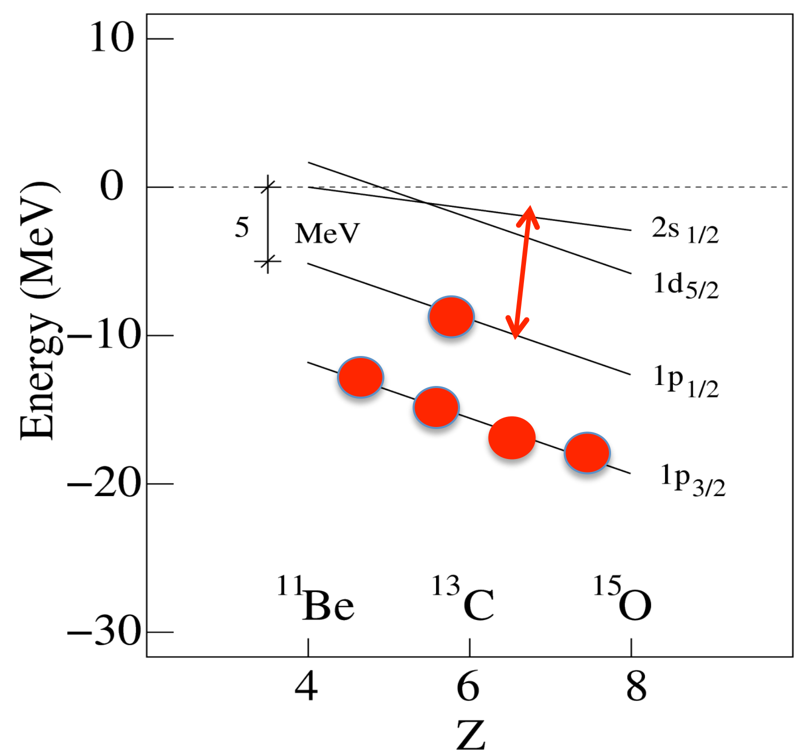

# Comparison with the model by Ikeda, Myo et al.

K. Ikeda et al,
Lect. Notes in Physics 818 (2010)

and essentially all the theoretical works of 11Li had to accept that the 1s1/2 single particle state is brought down to the 0p1/2 state without knowing its reason …

The theoretical challenge on the halo structure is therefore summarized as follows. There are many indications that the $s$-wave component is very large in the ground state wave function. Hence, we have to find a mechanism to bring down the $s_{1/2}$ orbit with the amount to wash out the $N = 8$ magic structure.

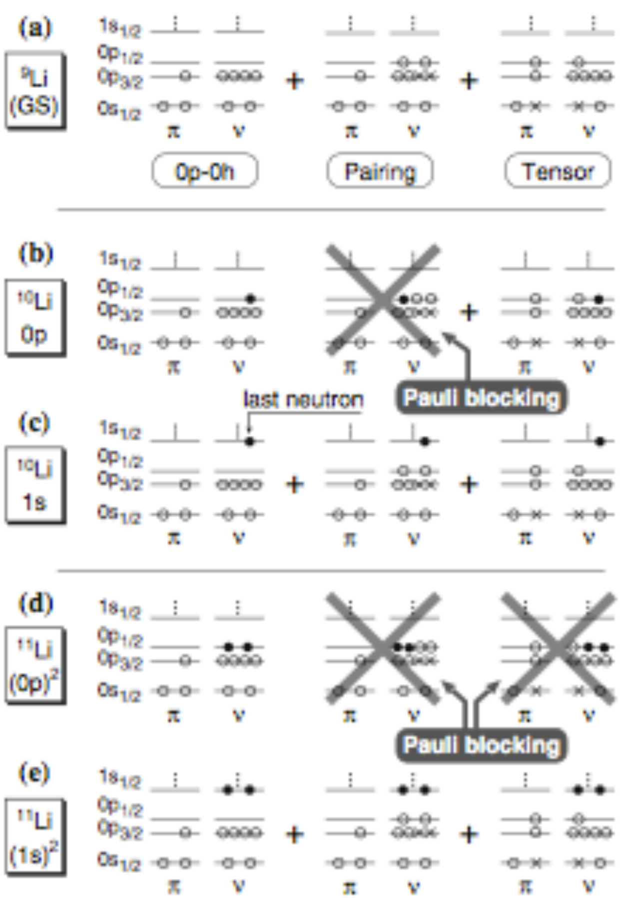


$$
\begin{aligned}
|{}^9Li\rangle = {} & C_1|(s_{1/2})^2_\pi(s_{1/2})^2_\nu(p_{3/2})_\pi(p_{3/2})^4_\nu\rangle_{J=3/2} \\
& + C_2|(s_{1/2})^2_\pi(s_{1/2})^2_\nu(p_{3/2})_\pi(p_{3/2})^2_{\nu J=0}(p_{1/2})^2_{\nu J=0}\rangle_{J=3/2} \\
& + C_3|[(s_{1/2})_\pi(s_{1/2})_\nu]_{J=1}(p_{3/2})_\pi(p_{3/2})^4_\nu[(p_{1/2})_\pi(p_{1/2})_\nu]_{J=1}\rangle_{J=3/2} \\
& + \cdots
\end{aligned}
$$

$p_{1/2}$ orbit is pushed up by pairing correlations and tensor force. Only 3/2- configurations are included: coupling to core vibrations (1/2-) is not considered. Binding energy is given as input. 50%($s^2$)-50%($p^2$) wavefunction is obtained

## Analysis of elastic $^{8}He(p,p)$ within optical model framework

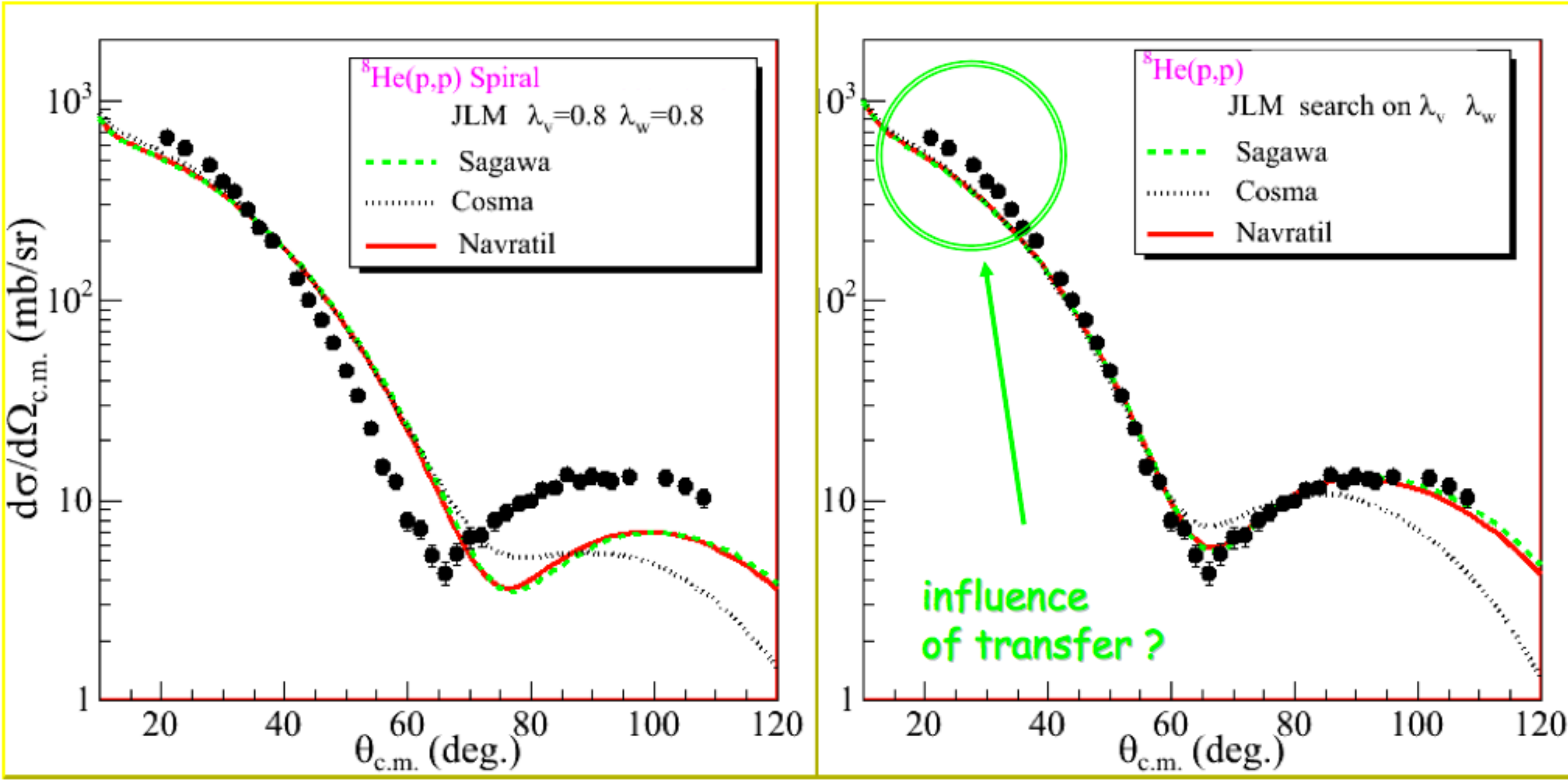


$$U_{JLM}(^{8}He+p) = \lambda_V V + i\,\lambda_W W$$

| | $\lambda_v$ | $\lambda_w$ |
|---|---|---|
| COSMA | 1.04 | 1.16 |
| SAGAWA | 1.13 | 1.07 |
| Navrátil | 1.11 | 1.06 |

Repulsive surface terme generated by the coupling
→ Complex Virtual Coupling Potential PCV

At low energy not only the reduction of $V_r$
change of the shape of the complex potential due to the coupling

**Coupled reaction channel (CRC) calculations needed:**
*Cf $^8$He+p Analysis → N. Keeley, SPhN [now: univ of Varsaw]*
F. Skaza *et al.*, PLB **619**. 82 ('05) ; PRC **73**, 044301 ('06)
N. Keeley *et al.*, PLB **646**, 222('07)

E405s -GANIL-MUST
$^8$He +p @ 15.6 MeV/n

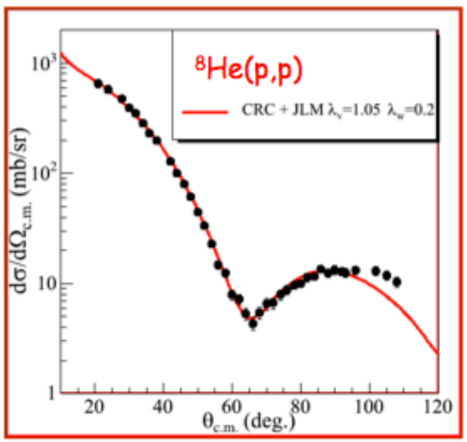


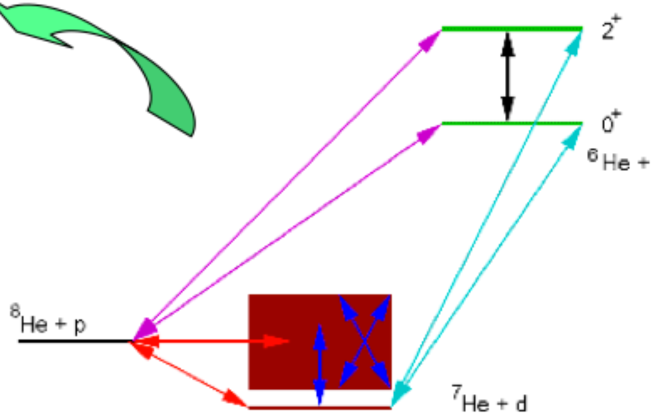


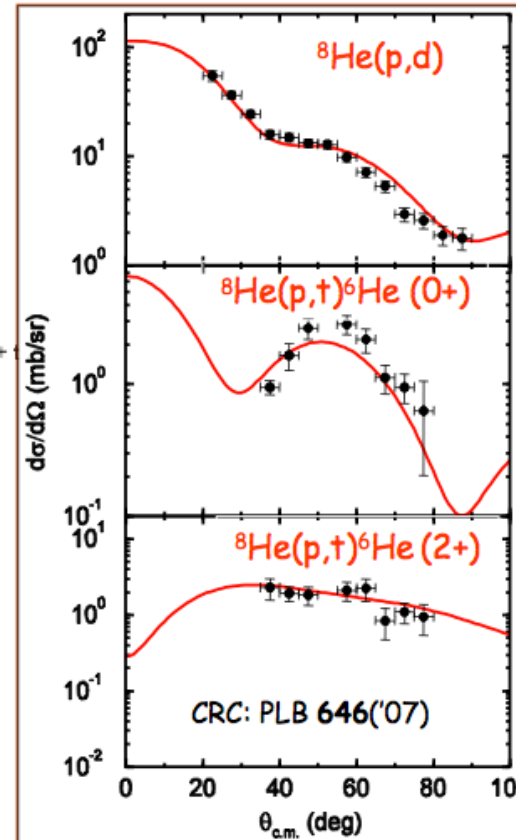


Spectroscopic factors $C^2S$ from $(d\sigma/d\Omega)_{theo}$ % $(d\sigma/d\Omega)_{exp}$

The transferred angular momentum $L_t$ indicates $J^\pi$

PREVIOUS INTERPRETATION → Data $^8He(p,t)$ @ 61.3 A.MeV - RIKEN
A.A.Korsheninnikov et al, PRL **90**, 082501 ('03)
DWBA analysis : $[^8He/^6He(0+)] = [^8He/^6He(2+)] = 1$
(only (p,t) no elastic data)

CRC ANALYSIS INTERPRETATION OF SPIRAL DATA → N. Keeley et al. : PLB **646**, 222('07)

$^8He(p,d)^7He$ $C^2S = 3.4 \pm 1.3$

complete set:
(p,p), (p,d) and (p,t)
@ 15.6 MeV/n

and re-analysis
of RIKEN data

(p,t) → wave function $^8He$ % $^6He$
$[^8He/^6He(0+)] = 1$ ;
$[^8He/^6He(2+)] = 0.014$
Mixing: $(p3/2)^4$ and $(p3/2)^2$ $(p1/2)^2$

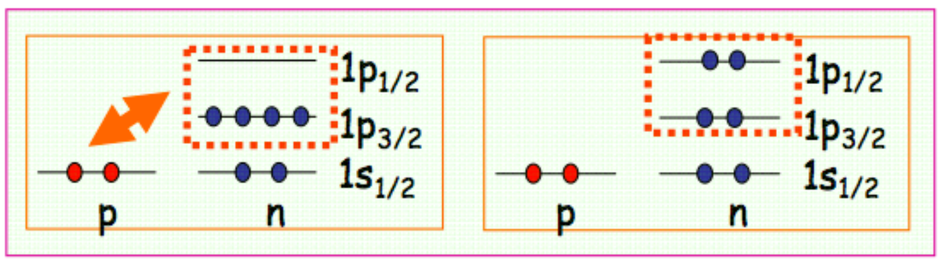


Consistent with the results from quasi-elastic scattering of $^8He$ at GSI,
LV Chulkov et al, NP*A759*, 43('05) $[^8He/^6He(0+)]$ : $1.3 \pm 0.1$
And recent theoretical calculations: Hagino, Takahashi, Sagawa PRC **77**, 054317 ('08)
Neutron configurations % $^8He$ (gs.) : $(1p_{3/2})^4$ : 34.9 % ; $[(1p_{3/2})^2(p_{1/2})^2]$ : 23.7 %

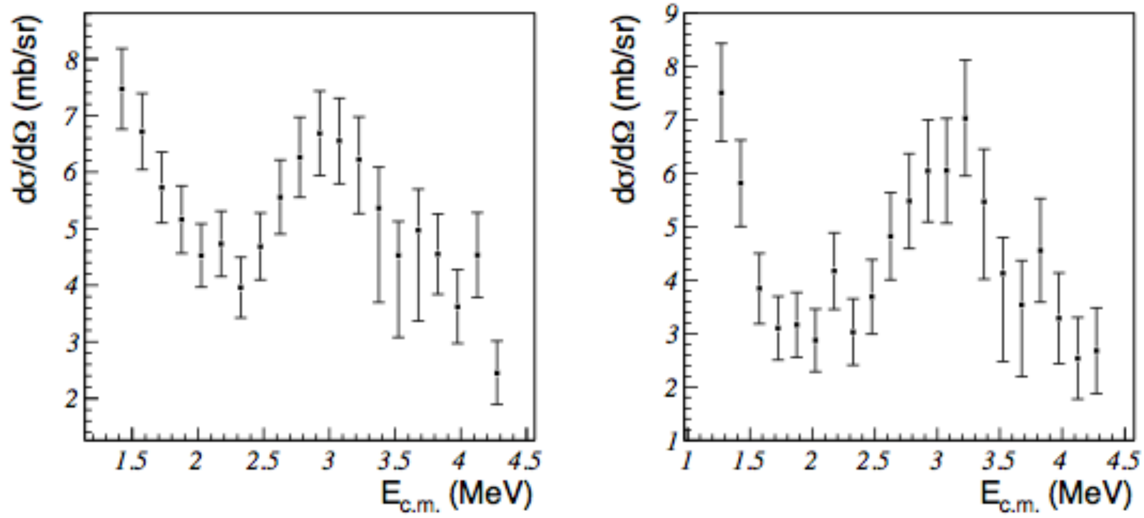


FIG. 3.17 *Fonctions d'excitation pour la réaction* $^{1}H(^{11}Li,p)^{11}Li$ *(G.S.) à 150° c.m. (à gauche) et à 175° c.m. (à droite).*

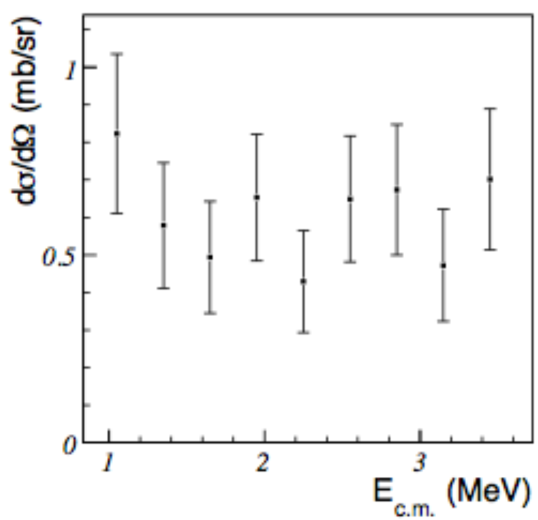


T. Roger, Ph.D Thesis

FIG. 3.18 – *Fonction d'excitation pour la réaction* $^{1}H(^{11}Li,t)^{9}Li$ *(G.S.) à 175° c.m.*

# CRC Calculations (I.J. Thompson)

## Simultaneous 2n-transfer

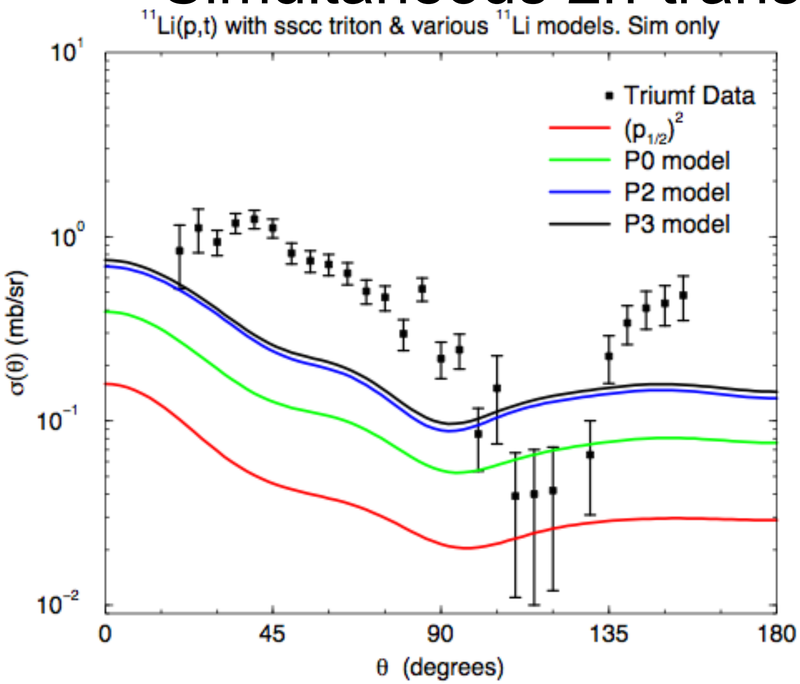


## Sequential 2n-transfer

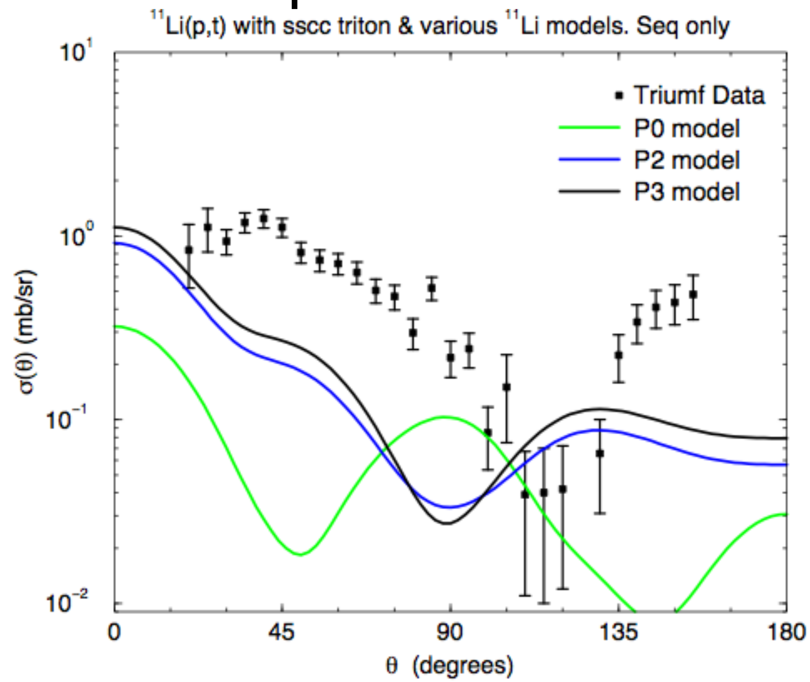


**Magnitude varies**

- shows $s^2$ strengths in the $^{11}$Li w.f.

**Shapes vary**

- Shows interference between s- and p-wave parts of $^{10}$Li.

Note: this interference will diminish if a complete set of $^{10}$Li states included at same energies.

(May reappear when energies in $^{10}$Li* included properly)

# Results

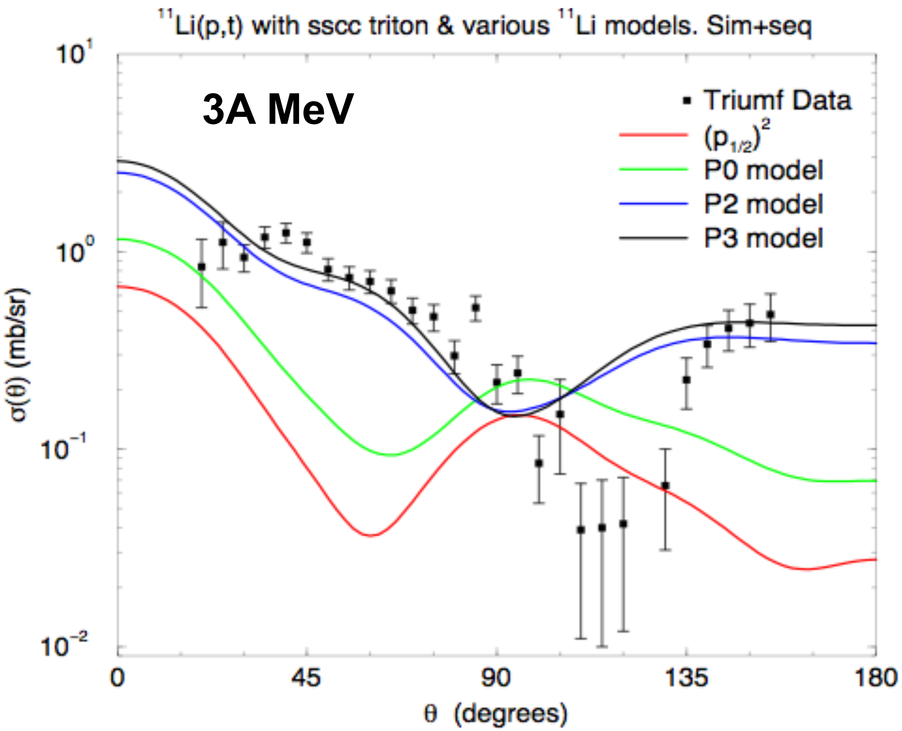


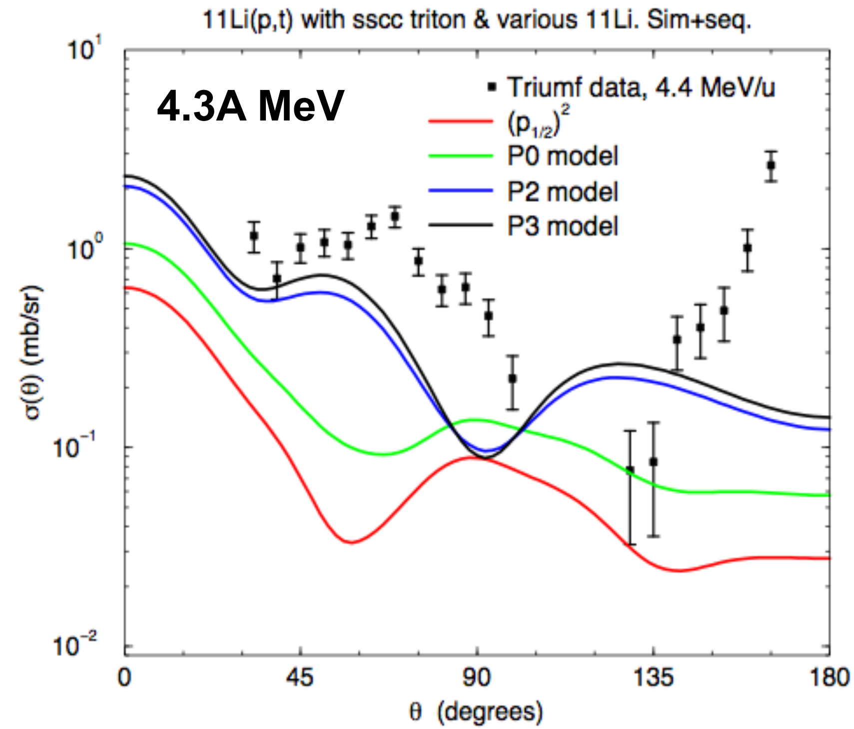


I. Tanihata *et al*. (Phys. Rev. Lett. **100**, 192502 (2008))

➔ P2 and P3 ~ reproduce the amplitudes

➔ ... but minimum missed by ~20°

➔ Not easy to come to a conclusion yet!!

# Perspectives

➔Use a more realistic optical potential :

→ Try to reproduce elastic scattering data

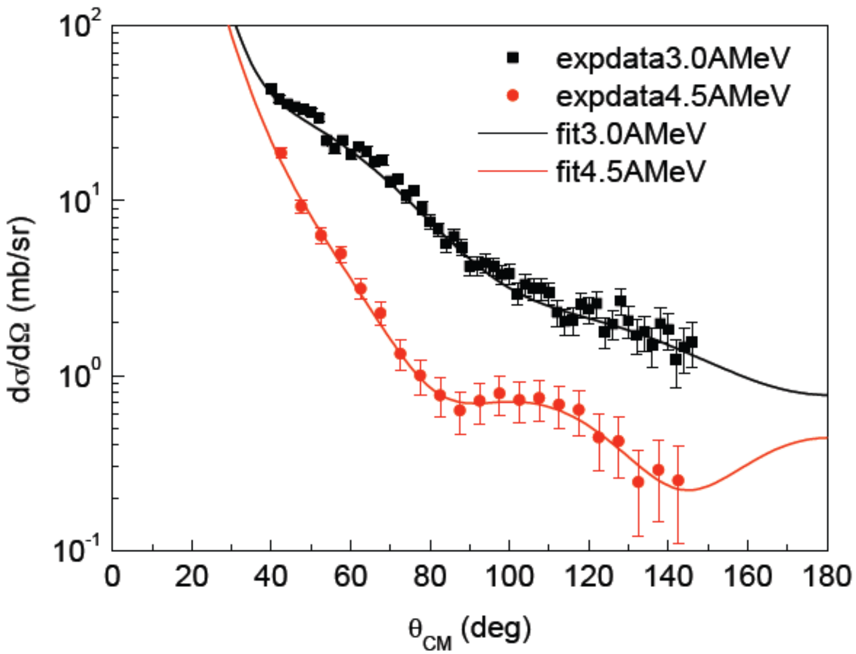


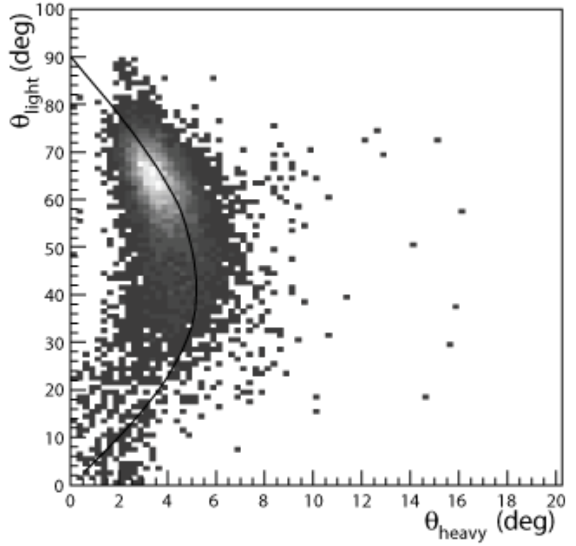


CH89 potential :

→ $W_S > 0$ !!

→ large radius

JLM potential

→ 3 parameters (normalisation V, W & data)

→ Re-Normalisation of data necessary!!!

➔ More realistic calculations i.e. include coupling to 1n transfer channel ( like $^{1}H(^{8}He,^{6}He)t$ : N.Keeley *et al*. (Phys. Lett. B **646**, 222 (2007)) )

# Perspectives

➔ Do the experiment at higher energy (get rid of compound nucleus effects)

No compound nucleus effect for (p,t) … but strong resonance populated by (p,p)!!

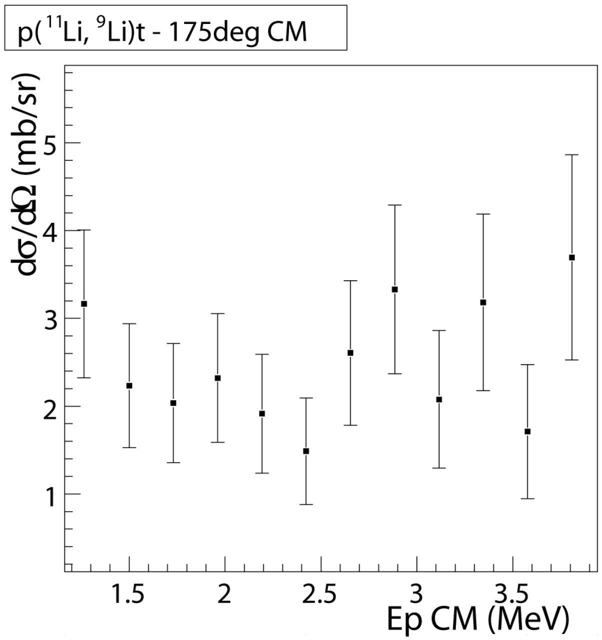


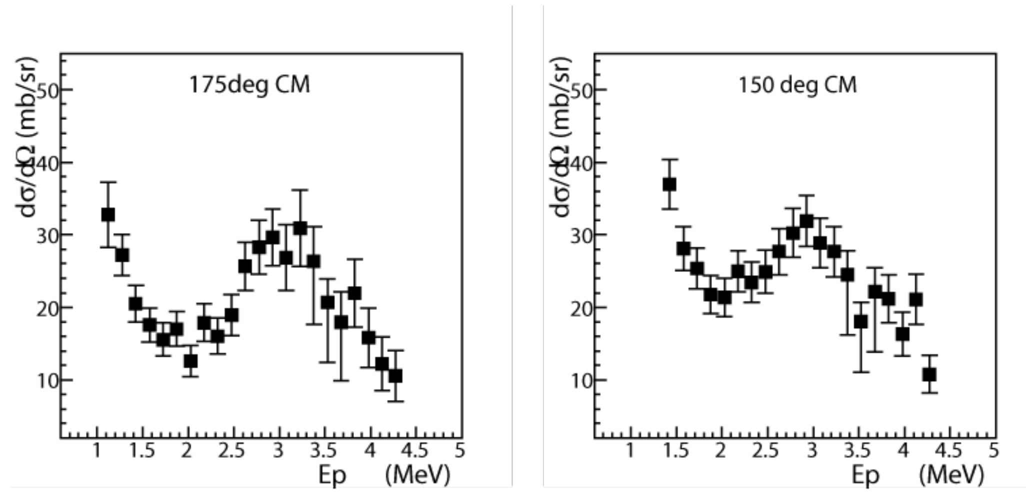


(→ IAS of $^{12}$Li(G.S.)!!)

➔ 20A MeV $^{11}$Li beam possible at RCNP (Osaka) ?

### *3.1. Q–values*

The different reaction channels which can populate the two states observed in the $^{1}\mathrm{H}\,(^{11}\mathrm{Li}, {}^{9}\mathrm{Li})\,{}^{3}\mathrm{H}$ reaction directly, or in terms of multistep processes are:

(i) two–particle transfer, which receives contributions from successive, simultaneous and non–orthogonality channels [5, 16, 17], processes which are associated with the following $Q$–values

  (a) $^{11}\mathrm{Li}(p,t)^{9}\mathrm{Li}(gs)\;;\quad Q = 8.2\ \mathrm{MeV}\,,$

  (b) $^{11}\mathrm{Li}(p,t)^{9}\mathrm{Li}^{*}(2.69\ \mathrm{MeV})\;;\quad Q = 5.5\ \mathrm{MeV}\,,$

(ii) Breakup channels

  (a) two particle breakup, both neutrons in the $s_{1/2}$ resonance of $^{10}$Li (most probable event)
  $^{11}\mathrm{Li}(p,p')^{9}\mathrm{Li} + 2n(\mathrm{cont.})\;;\quad Q \approx -0.5\ \mathrm{MeV}\,,$

  (b) one particle breakup
  $^{11}\mathrm{Li}(p,p')^{9}\mathrm{Li} + n(\mathrm{halo}) + n(\mathrm{cont.})\;;\quad Q \approx -0.5\ \mathrm{MeV}\,,$

(iii) One–particle transfer

  (a) $^{11}\mathrm{Li}(p,d)^{10}\mathrm{Li}\;;\quad Q \approx 1.9\ \mathrm{MeV}$
  Such a process, considered as an on–the–energy–shell process, can populate the observed final states in keeping with the fact that once a neutron is picked-up from $^{11}$Li, the other leaves the system almost at once. It can also populate the final states in an off–the–energy shell process, i.e. successive transfer.

  (b) $^{10}\mathrm{Li}(d,t)^{9}\mathrm{Li}(gs)\;;\quad Q = 6.3\ \mathrm{MeV}\,,$
  and
  $^{10}\mathrm{Li}(d,t)^{9}\mathrm{Li}(2.69\ \mathrm{MeV})\;;\quad Q = 3.6\ \mathrm{MeV}\,.$

(iv) Inelastic scattering

  (a) entrance channel
  $^{11}\mathrm{Li}(p,p')^{11}\mathrm{Li}^{*}(1^{-};\ E \approx 0.5\ \mathrm{MeV})\;;\quad Q \approx -0.5\ \mathrm{MeV}\,.$
  Of course, this process is in competition with the break up process, in keeping with the fact that $^{11}$Li, being so weakly bound ($S_{2n} \approx 380$ keV), displays no bound excited state

  (b) exit channel
  $^{9}\mathrm{Li}(t,t')^{9}\mathrm{Li}^{*}(2.69\ \mathrm{MeV})\;;\quad Q = -2.69\ \mathrm{MeV}\,.$
  This process can populate the final excited state, as a two–step process involving transfer to the ground state of $^{9}$Li (i.e. process (i)(a) above, $Q = 8.2$ MeV) and then exit channel inelastic scattering.

All the above $Q$–values are to be reported to the bombarding conditions, that is,

$$\text{Center of mass energy/nucleon} = 2.75\ \mathrm{MeV}\ ,$$
$$\text{Coulomb barrier} \approx 0.6\ \mathrm{MeV}\ .$$

# SELF ENERGY RENORMALIZATION OF SINGLE-PARTICLE STATES: CLOSED SHELL

(a)

(b)

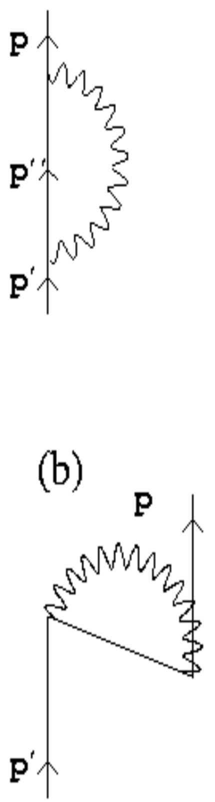


$^{208}$Pb

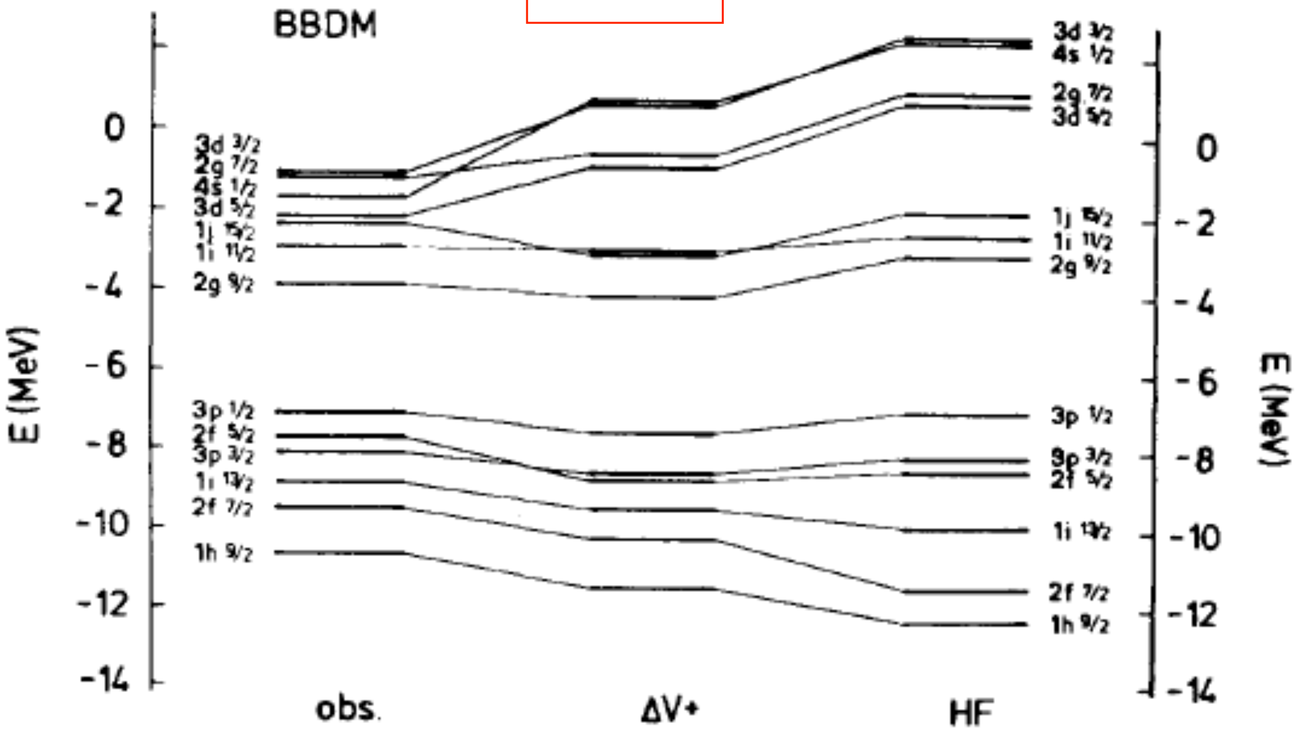


C. Mahaux, P.F. Bortignon, R.A. Broglia, C.H. Dasso and Mahaux, Phys. Rep.(1985)1

# $^{12}$Be

**Fermionic degrees of freedom:**

• two particle states coupled to zero angular momentum on s1/2, p1/2, d5/2 Woods-Saxon levels up to 150 MeV

**Bosonic degrees of freedom:**

•1-, 2+ and 3- QRPA solutions up to 50 MeV, associated to a multipole-multipole separable interaction with coupling constant tuned to reproduce E(1-)=2.7 MeV and B(E1)=0.052 e$^2$fm$^2$ E(2+)=2.1 MeV and $0.6<\beta_2<0.7$

Spectroscopic factors: overlap between $^{11}$Be and $^{12}$Be

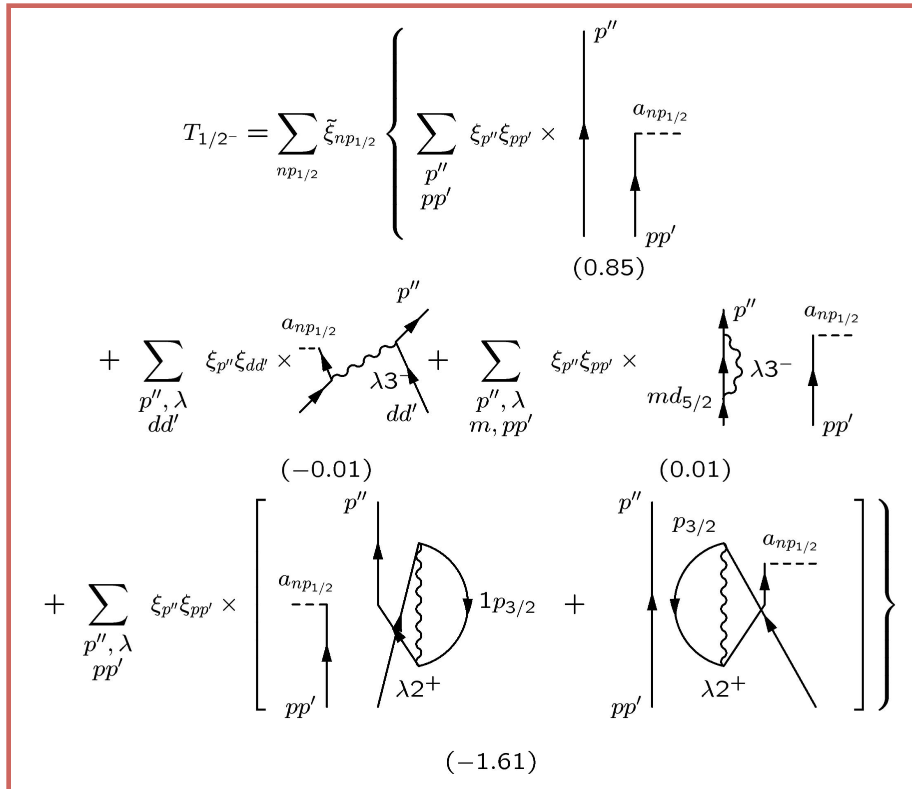

Theoretical calculation for $^{11}$Li

Low-lying dipole strength

s-p mixing

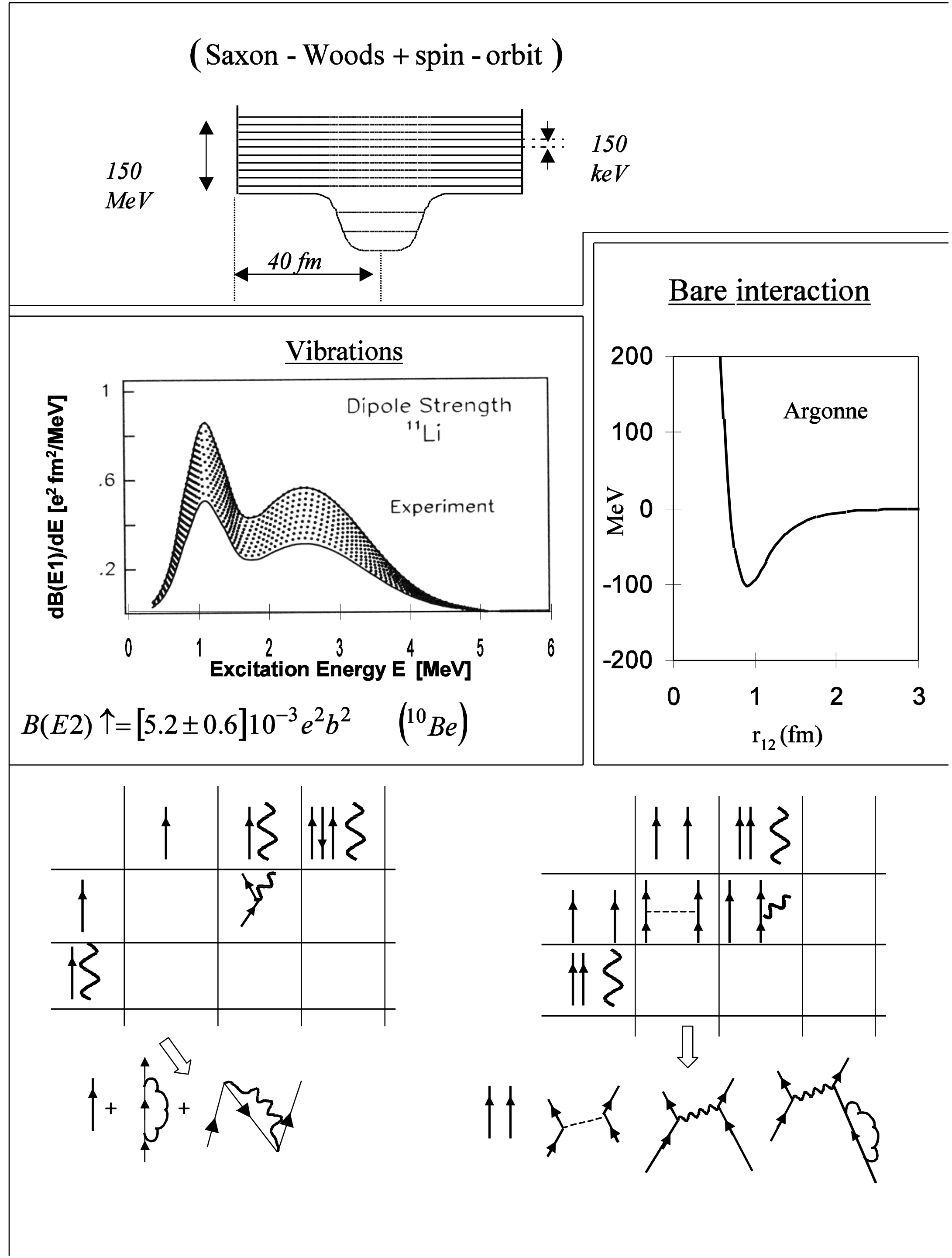

**Table 2.** RPA wave function of the collective low-lying quadrupole phonon in $^{11}$Li, of energy $E_{2^+} = 5.05$ MeV, and leading to the most important contribution to the induced interaction in fig. 1, II. All the listed amplitudes refer to neutron transitions, except for the last column. We have adopted the self-consistent value ($\chi_2 = 0.013\,\mathrm{MeV}^{-1}$ ) for the coupling constant. The resulting value for the deformation parameter is $\beta_2 = 0.5$.

| | $1p_{3/2}^{-1}1p_{1/2}$ | $2s_{1/2}^{-1}5d_{3/2}$ | $1p_{1/2}^{-1}6p_{3/2}$ | $2s_{1/2}^{-1}3d_{5/2}$ | $2s_{1/2}^{-1}5d_{5/2}$ | $1p_{3/2}^{-1}1p_{1/2}$ ($\pi$) |
|---|---|---|---|---|---|---|
| $X_{\mathrm{ph}}$ | 0.824 | 0.404 | 0.151 | 0.125 | 0.126 | 0.16 |
| $Y_{\mathrm{ph}}$ | 0.119 | 0.011 | −0.002 | −0.049 | −0.011 | 0.07 |

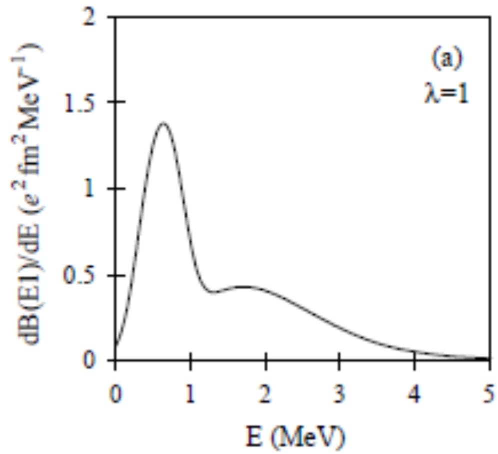


**Table 3.** RPA wave function of the strongest low-lying dipole vibration of $^{11}$Li, ($E_{1^-} = 0.75$ MeV), and contributing most importantly to the pairing induced interaction (fig. 1, II). All the listed amplitudes refer to neutron transitions. We have used the value $\chi_1 = 0.0043$ MeV$^{-1}$ for the isovector coupling constant in order to get a good agreement with the experimental findings. To be noted that this value coincides within 25% close to the selfconsistent value of 0.0032 MeV$^{-1}$. The resulting strength function (cf. fig. 2(a)) integrated up to 4 MeV gives 7% of the Thomas-Reiche-Kuhn energy weighted sum rule, to be compared to the experimental value of 8% [38].

| | $1p_{1/2}^{-1}2s_{1/2}$ | $1p_{1/2}^{-1}3s_{1/2}$ | $1p_{1/2}^{-1}4s_{1/2}$ | $1p_{1/2}^{-1}1d_{3/2}$ | $1p_{3/2}^{-1}5d_{5/2}$ | $1p_{3/2}^{-1}6d_{5/2}$ | $1p_{3/2}^{-1}7d_{5/2}$ |
|---|---|---|---|---|---|---|---|
| $X_{\mathrm{ph}}$ | 0.847 | −0.335 | 0.244 | 0.165 | 0.197 | 0.201 | 0.157 |
| $Y_{\mathrm{ph}}$ | 0.088 | 0.060 | 0.088 | 0.008 | 0.165 | 0.173 | 0.138 |

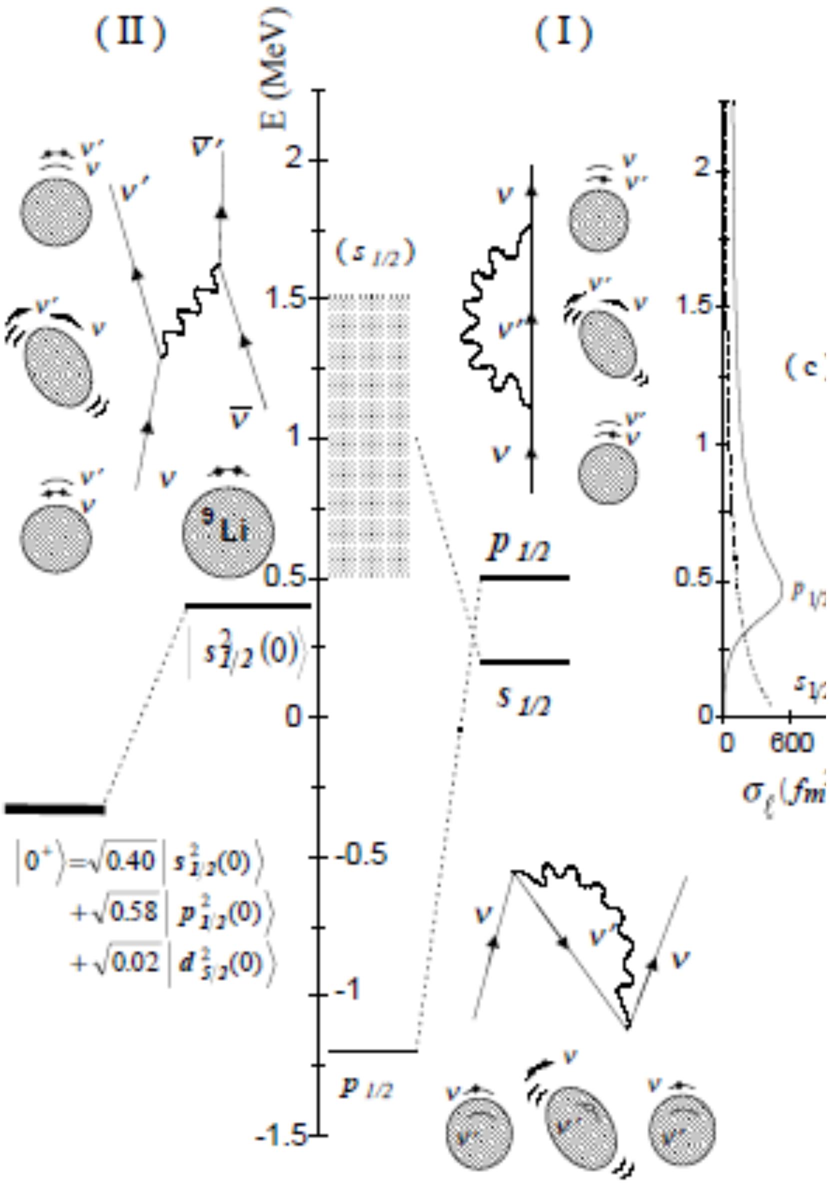


| | | Exp. | Theory | |
|---|---|---|---|---|
| | | | particle-vibration +Argonne | mean field |
| $^{10}_{3}\mathrm{Li}_7$ (not bound) | s | 0.1-0.2 MeV | 0.2 MeV (virtual) | $\sim$ 1 MeV (virtual) |
| | p | 0.5-0.6 MeV | 0.5 MeV (res.) | -1.2 MeV (bound) |
| $^{11}_{3}\mathrm{Li}_8$ (bound) | $S_{2n}$ | 0.369 MeV | 0.33 MeV | 2.4 MeV |
| | $s^2$,$p^2$ | 50% , 50% | 41% , 59% | 0% , 100% |
| | $\langle r^2\rangle^{1/2}$ | 3.55±0.1 fm | 3.9 fm | |
| | $\Delta p_\perp$ | 48±10 MeV/c | 55 MeV/c | |

# Correlated halo wavefunction

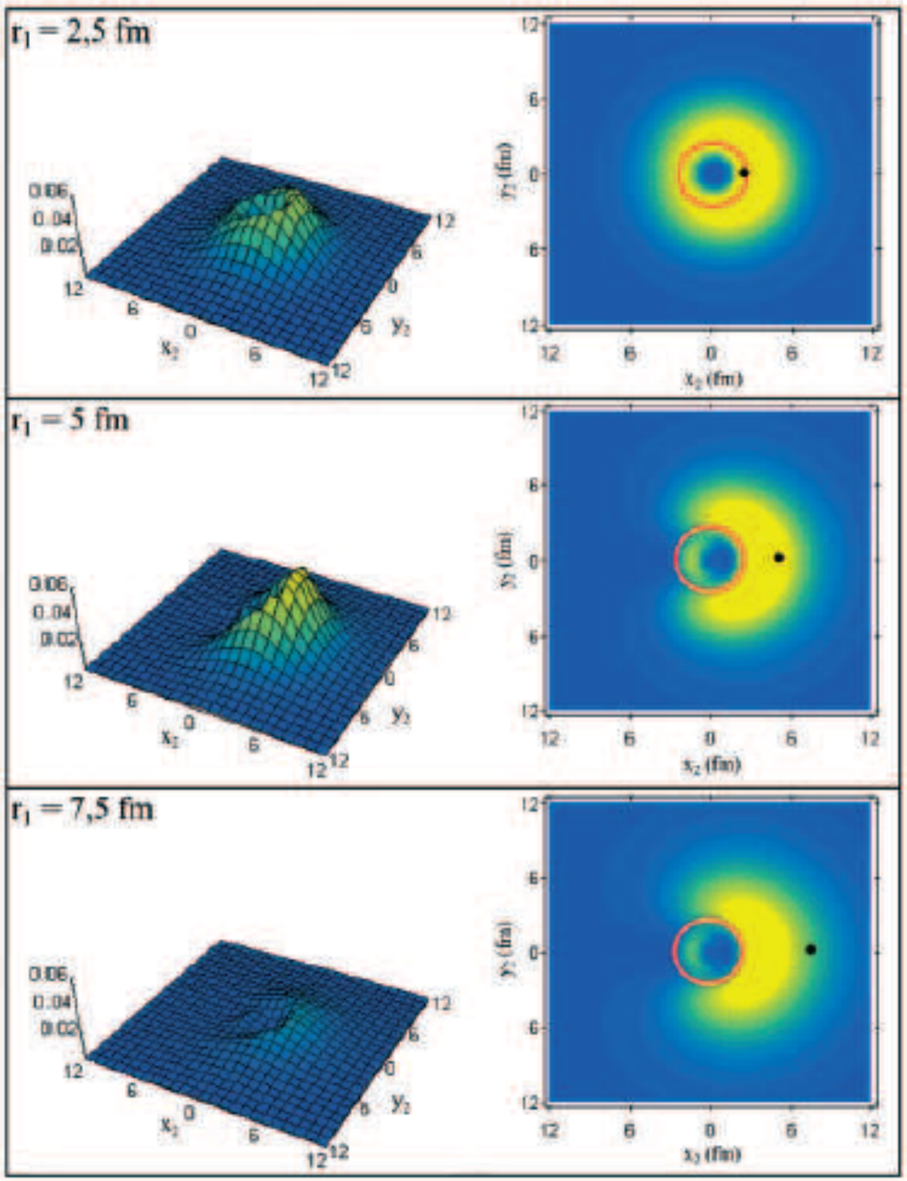


## Uncorrelated

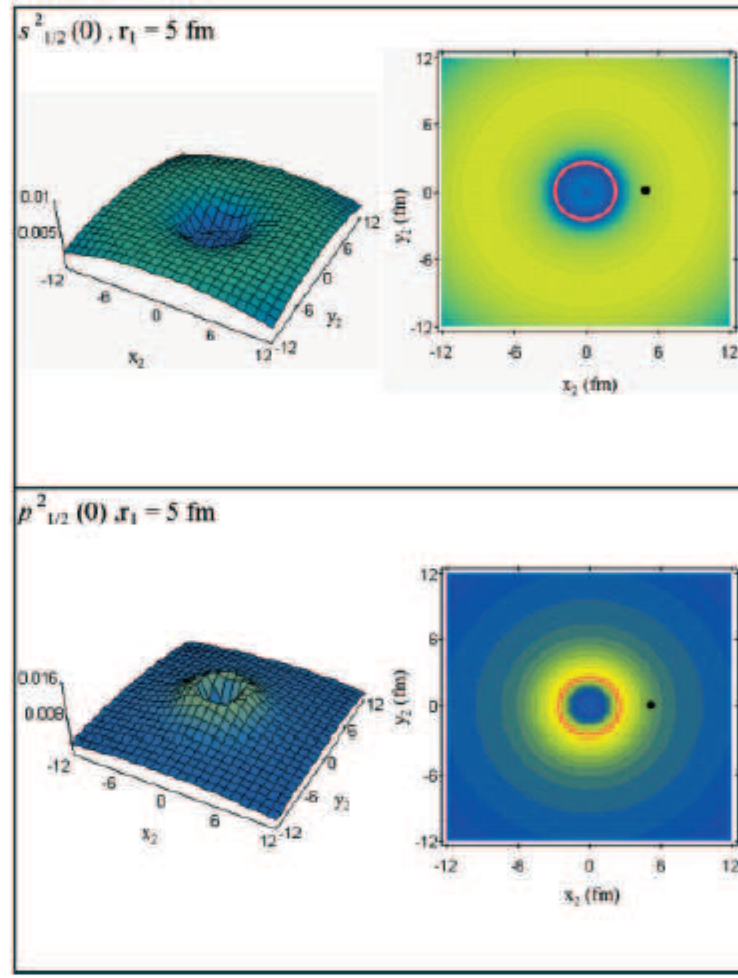

# Comparison with the model by Bertsch and Esbensen

OUR MODEL

Ann. Phys.209(1991)327
PRC56(1997)3054

## Single-particle potential

Standard Bohr-Mottelson

Depth adjusted to experimental $p_{1/2}$ single particle energy

## 2-body interaction

Bare Argonne interaction+ particle-vibration coupling with phenomenological parameters (low-lying vibrations)

Strength fitted to $S_{2n}$ in $^{12}Be$

$$v_{\rm eff}(\mathbf{r}_1,\mathbf{r}_2)=\delta(\mathbf{r}_1-\mathbf{r}_2)\left(v_0+v_\rho\left(\frac{\rho_c((\mathbf{r}_1+\mathbf{r}_2)/2)}{\rho_0}\right)^P\right).$$

## Results

Good reproduction of binding energies in $^{12}Be$ and $^{11}Li$
50% $(s_{1/2})^2$

Good reproduction of binding energy
Low $(s_{1/2})^2$ admixture unless
two different s.p. potentials are used

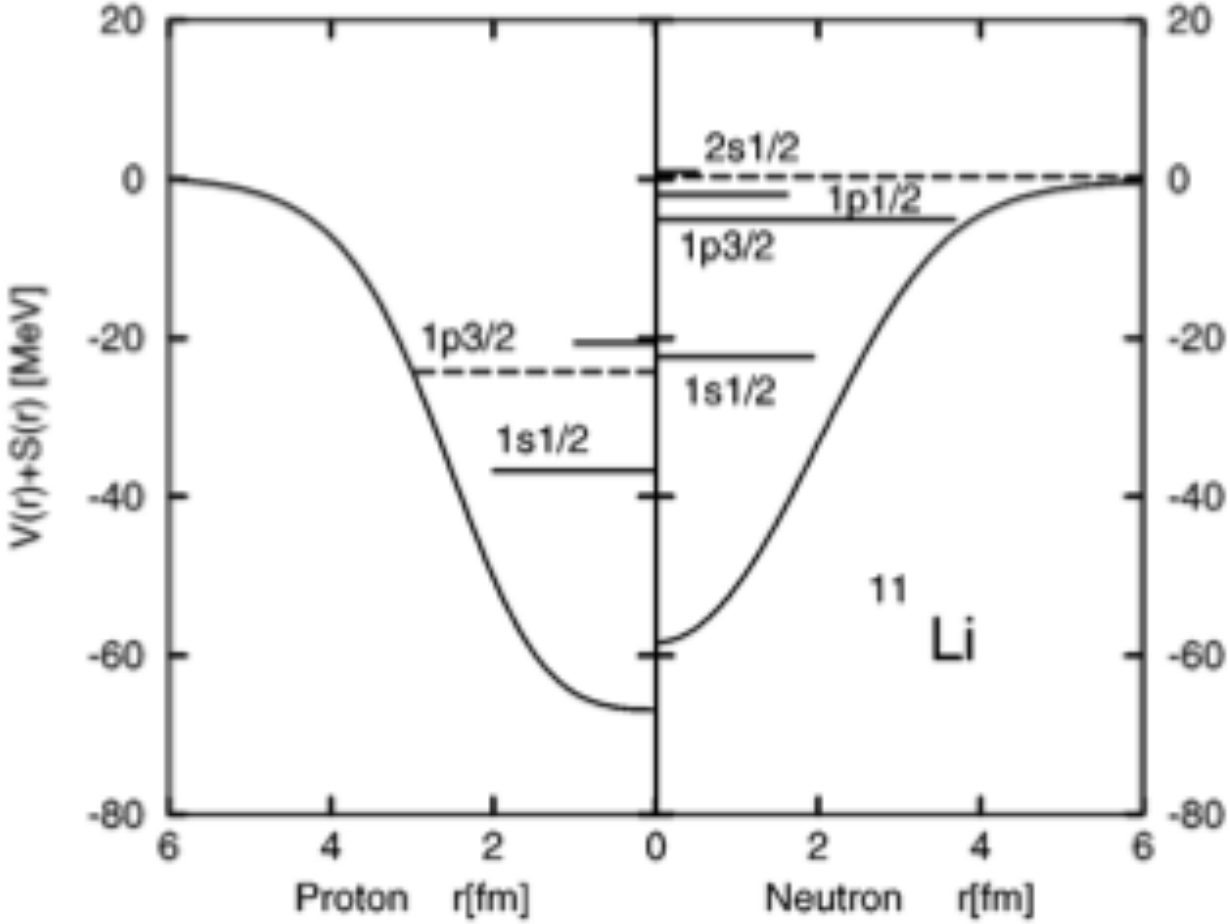


J. Meng and P. Ring,
PRL 77(1998)3963

# Vibrational vs. deformed core

Shell-model calculations [21] indicate that $^{10}$Be is not a perfect rotor: the calculated quadrupole moment of the lowest $2^+$ state is only 34% of the value predicted from the $\beta_2$ value, assuming a static deformation. We have

H. Esbensen, B.A. Brown, H. Sagawa, PRC 51 (1995) 1274

How to probe the particle-phonon coupling?
Test the microscopic correlated wavefunction with phonon admixture

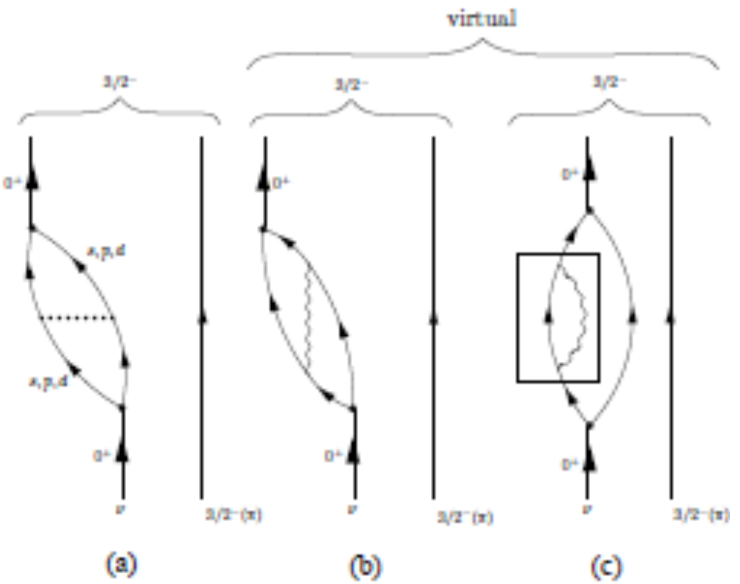


$$|\tilde{0}\rangle = |0\rangle + 0.7|(ps)_{1^-} \otimes 1^-; 0\rangle + 0.1|(sd)_{2^+} \otimes 2^+; 0\rangle$$

$$|0\rangle = 0.45|s^2_{1/2}(0)\rangle + 0.55|p^2_{1/2}(0)\rangle + 0.04|d^2_{5/2}(0)\rangle$$

**Two-neutron transfer to**

ground state

exc. state

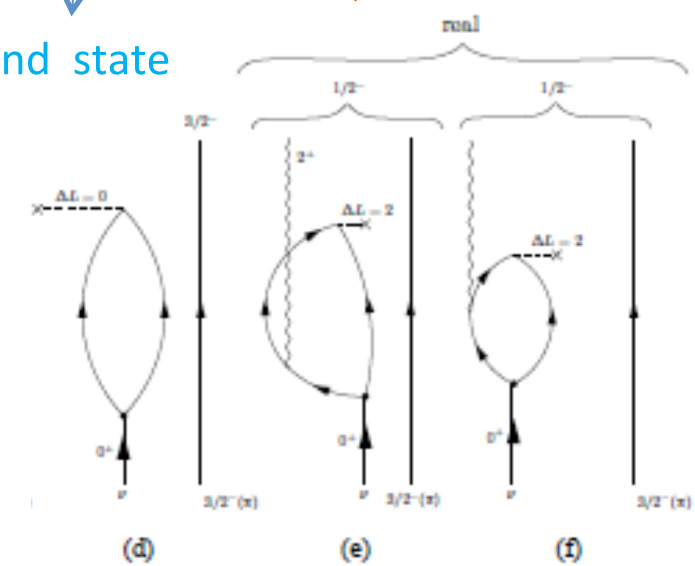


We will try to draw information about the halo structure of $^{11}$Li from the reactions $^1$H($^{11}$Li,$^9$Li)$^3$H and $^1$H($^{11}$Li,$^9$Li*(2.69 MeV))$^3$H (I. Tanihata *et al.*, Phys. Rev. Lett. **100**, 192502 (2008))

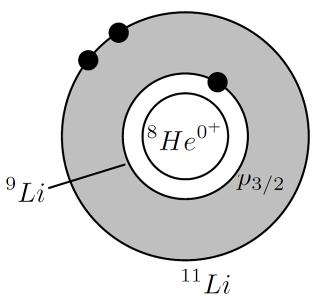


Schematic depiction of $^{11}$Li

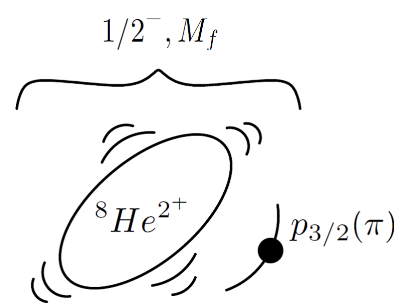


First excited state of $^9$Li

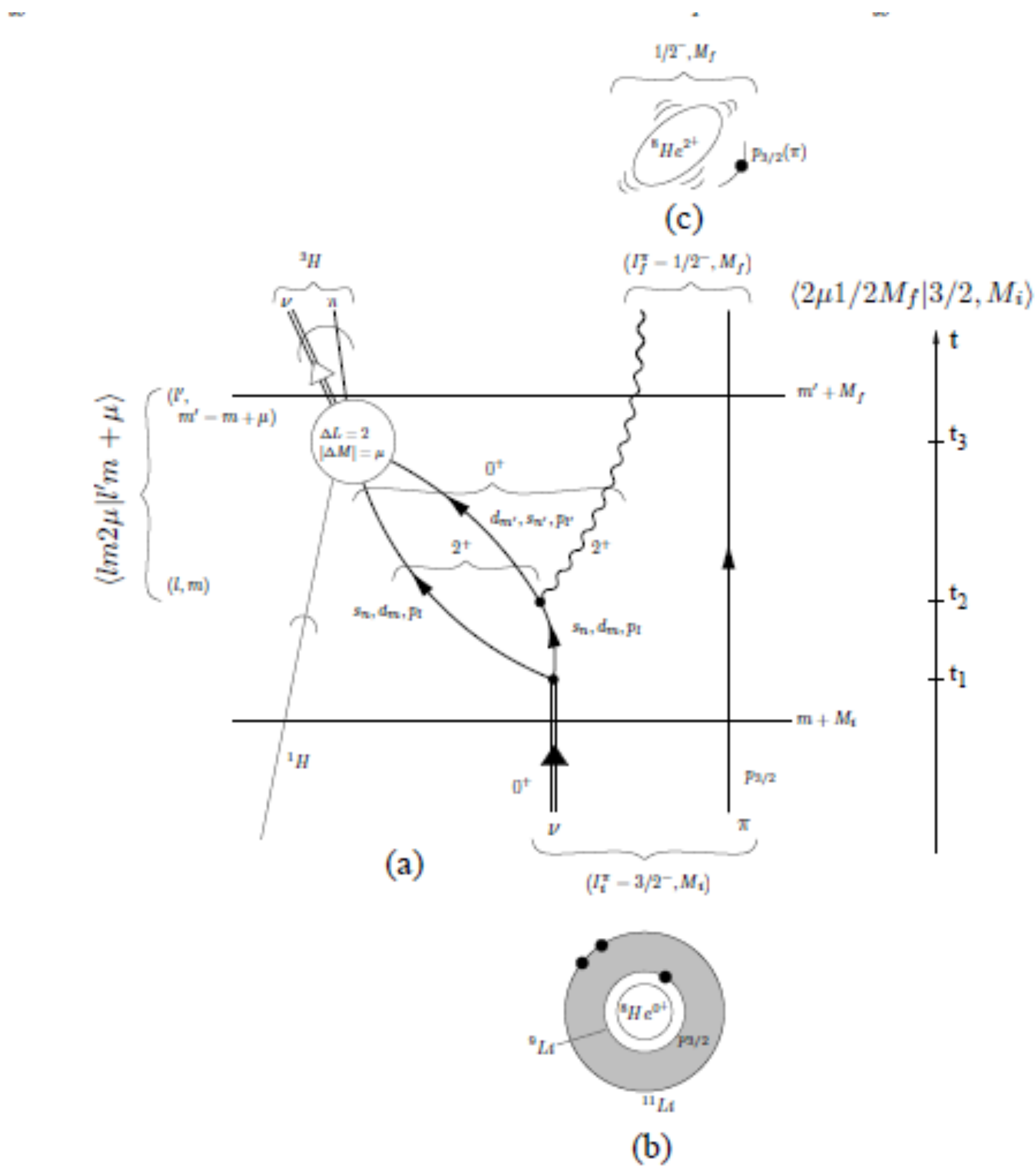

1/2⁻, $M_f$
$^8He^{2+}$
$p_{3/2}(\pi)$
(c)
$^3H$
$(I_f^\pi = 1/2^-, M_f)$
$\langle 2\mu 1/2 M_f | 3/2, M_i \rangle$
t
$\langle lm2\mu | l'm + \mu \rangle$
$(l', m' = m + \mu)$
$m' + M_f$
$t_3$
$\Delta L = 2$
$|\Delta M| = \mu$
$0^+$
$d_{m'}, s_{n'}, p_{l'}$
$2^+$
$2^+$
$(l, m)$
$t_2$
$s_n, d_m, p_l$
$s_n, d_m, p_l$
$t_1$
$m + M_i$
$^1H$
$0^+$
$p_{3/2}$
$\nu$
$\pi$
(a)
$(I_i^\pi = 3/2^-, M_i)$
$^8He^{0+}$
$^9Li$
$p_{3/2}$
$^{11}Li$
(b)

# Probing $^{11}$Li halo-neutrons correlations via (p,t) reaction

PRL **100**, 192502 (2008) PHYSICAL REVIEW LETTERS week ending 16 MAY 200

## Measurement of the Two-Halo Neutron Transfer Reaction $^{1}$H($^{11}$Li, $^{9}$Li)$^{3}$H at 3*A* MeV

I. Tanihata,* M. Alcorta,† D. Bandyopadhyay, R. Bieri, L. Buchmann, B. Davids, N. Galinski, D. Howell, W. Mills, S. Mythili, R. Openshaw, E. Padilla-Rodal, G. Ruprecht, G. Sheffer, A.C. Shotter, M. Trinczek, and P. Walden
*TRIUMF, 4004 Wesbrook Mall, Vancouver, BC, V6T 2A3, Canada*

H. Savajols, T. Roger, M. Caamano, W. Mittig,‡ and P. Roussel-Chomaz
*GANIL, Bd Henri Becquerel, BP 55027, 14076 Caen Cedex 05, France*

R. Kanungo and A. Gallant
*Saint Mary's University, 923 Robie St., Halifax, Nova Scotia B3H 3C3, Canada*

M. Notani and G. Savard
*ANL, 9700 S. Cass Ave., Argonne, Illinois 60439, USA*

I. J. Thompson
*LLNL, L-414, P.O. Box 808, Livermore, California 94551, USA*
(Received 22 January 2008; published 14 May 2008)

# Calculation of absolute two-nucleon transfer cross section by finite-range DWBA calculation

## simultaneous and successive contributions

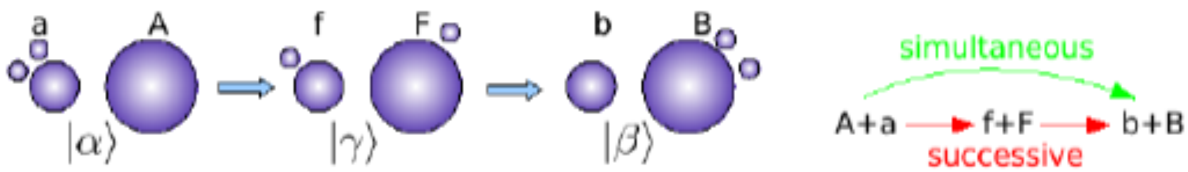


the initial and final channel wave functions are

$$|\alpha\rangle = \phi_a(\xi_b, \mathbf{r}_1, \mathbf{r}_2)\phi_A(\xi_A)\chi_{aA}(\mathbf{r}_{aA})$$
$$|\beta\rangle = \phi_b(\xi_b)\phi_B(\xi_A, \mathbf{r}_1, \mathbf{r}_2)\chi_{bB}(\mathbf{r}_{bB})$$

very schematically, the first order (*simultaneous*) contribution is

$$T^{(1)} = \langle\beta|V|\alpha\rangle,$$

while the second order contribution can be separated in a *successive* and a *non-orthogonality* term

$$T^{(2)} = T^{(2)}_{succ} + T^{(2)}_{NO}$$
$$= \sum_{\gamma}\langle\beta|V|\gamma\rangle G\langle\gamma|V|\alpha\rangle - \sum_{\gamma}\langle\beta|\gamma\rangle\langle\gamma|V|\alpha\rangle.$$


B.F. Bayman and J. Chen, Phys. Rev. C 26 (1982) 150
M. Igarashi, K. Kubo and K. Yagi, Phys. Rep. 199 (1991) 1
G. Potel et al., arXiv: 0906.4298

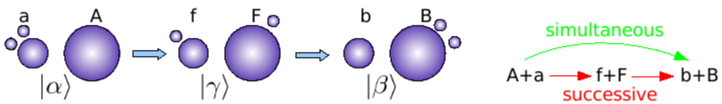


**Simultaneous transfer**

$$T^{(1)}(j_i, j_f) = 2\sum_{\sigma_1\sigma_2}\int d\mathbf{r}_{fF}\, d\mathbf{r}_{b1}\, d\mathbf{r}_{A2} [\Psi^{j_f}(\mathbf{r}_{A1},\sigma_1)\Psi^{j_f}(\mathbf{r}_{A2},\sigma_2)]_0^{0*}\chi_{bB}^{(-)*}(\mathbf{r}_{bl}$$
$$\times\, v(\mathbf{r}_{b1})[\Psi^{j_i}(\mathbf{r}_{b1},\sigma_1)\Psi^{j_i}(\mathbf{r}_{b2},\sigma_2)]_0^0\chi_{aA}^{(+)}(\mathbf{r}_{aA})$$

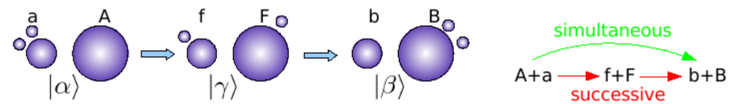


**Successive transfer**

$$T^{(2)}_{succ}(j_i, j_f) = 2\sum_{K,M}\sum_{\substack{\sigma_1\sigma_2\\ \sigma_1'\sigma_2'}}\int d\mathbf{r}_{fF}\, d\mathbf{r}_{b1}\, d\mathbf{r}_{A2}[\Psi^{j_f}(\mathbf{r}_{A1},\sigma_1)\Psi^{j_f}(\mathbf{r}_{A2},\sigma_2)]_0^{0*}$$
$$\times\, \chi_{bB}^{(-)*}(\mathbf{r}_{bB})v(\mathbf{r}_{b1})[\Psi^{j_f}(\mathbf{r}_{A2},\sigma_2)\Psi^{j_i}(\mathbf{r}_{b1},\sigma_1)]_M^K$$
$$\times \int d\mathbf{r}'_{fF}\, d\mathbf{r}'_{b1}\, d\mathbf{r}'_{A2}\, G(\mathbf{r}_{fF},\mathbf{r}'_{fF})[\Psi^{j_f}(\mathbf{r}'_{A2},\sigma'_2)\Psi^{j_i}(\mathbf{r}'_{b1},\sigma'_1)]_M^K$$
$$\times\, \frac{2\mu_{fF}}{\hbar^2} v(\mathbf{r}'_{f2})[\Psi^{j_i}(\mathbf{r}'_{A2},\sigma'_2)\Psi^{j_i}(\mathbf{r}'_{b1},\sigma'_1)]_0^0\chi_{aA}^{(+)}(\mathbf{r}'_{aA})$$

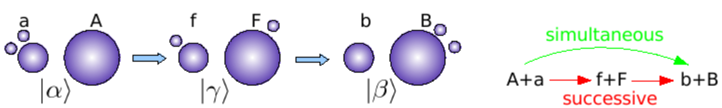


**Non–orthogonality term**

$$T^{(2)}_{NO}(j_i, j_f) = 2\sum_{K,M}\sum_{\substack{\sigma_1\sigma_2\\ \sigma_1'\sigma_2'}}\int d\mathbf{r}_{fF}\, d\mathbf{r}_{b1}\, d\mathbf{r}_{A2}[\Psi^{j_f}(\mathbf{r}_{A1},\sigma_1)\Psi^{j_f}(\mathbf{r}_{A2},\sigma_2)]_0^{0*}$$
$$\times\, \chi_{bB}^{(-)*}(\mathbf{r}_{bB})v(\mathbf{r}_{b1})[\Psi^{j_f}(\mathbf{r}_{A2},\sigma_2)\Psi^{j_i}(\mathbf{r}_{b1},\sigma_1)]_M^K$$
$$\times \int d\mathbf{r}'_{b1}\, d\mathbf{r}'_{A2}[\Psi^{j_f}(\mathbf{r}'_{A2},\sigma'_2)\Psi^{j_i}(\mathbf{r}'_{b1},\sigma'_1)]_M^K$$
$$\times\, [\Psi^{j_i}(\mathbf{r}'_{A2},\sigma'_2)\Psi^{j_i}(\mathbf{r}'_{b1},\sigma'_1)]_0^0\chi_{aA}^{(+)}(\mathbf{r}'_{aA})$$

$$T^{(1)}(j_i, j_f) = 2\sum_{\sigma_1\sigma_2}\int d\mathbf{r}_{fF}d\mathbf{r}_{b1}d\mathbf{r}_{A2}[\Psi^{j_f}(\mathbf{r}_{A1},\sigma_1)\Psi^{j_f}(\mathbf{r}_{A2},\sigma_2)]_0^{0*}\chi_{bB}^{(-)*}(\mathbf{r}_{bB})$$
$$\times\, v(\mathbf{r}_{b1})[\Psi^{j_i}(\mathbf{r}_{b1},\sigma_1)\Psi^{j_i}(\mathbf{r}_{b2},\sigma_2)]_0^{0}\chi_{aA}^{(+)}(\mathbf{r}_{aA}),$$

Simultaneous

$$T^{(2)}_{succ}(j_i, j_f) = 2\sum_{K,M}\sum_{\substack{\sigma_1\sigma_2\\ \sigma_1'\sigma_2'}}\int d\mathbf{r}_{fF}d\mathbf{r}_{b1}d\mathbf{r}_{A2}[\Psi^{j_f}(\mathbf{r}_{A1},\sigma_1)\Psi^{j_f}(\mathbf{r}_{A2},\sigma_2)]_0^{0*}$$
$$\times\,\chi_{bB}^{(-)*}(\mathbf{r}_{bB})v(\mathbf{r}_{b1})[\Psi^{j_f}(\mathbf{r}_{A2},\sigma_2)\Psi^{j_i}(\mathbf{r}_{b1},\sigma_1)]_M^K$$
$$\times\int d\mathbf{r}'_{fF}d\mathbf{r}'_{b1}d\mathbf{r}'_{A2}G(\mathbf{r}_{fF},\mathbf{r}'_{fF})[\Psi^{j_f}(\mathbf{r}'_{A2},\sigma_2')\Psi^{j_i}(\mathbf{r}'_{b1},\sigma_1')]_M^K$$
$$\times\,\frac{2\mu_{fF}}{\hbar^2}v(\mathbf{r}'_{f2})[\Psi^{j_i}(\mathbf{r}'_{A2},\sigma_2')\Psi^{j_i}(\mathbf{r}'_{b1},\sigma_1')]_0^0\chi_{aA}^{(+)}(\mathbf{r}'_{aA}),$$

Successive

$$T^{(2)}_{NO}(j_i, j_f) = 2\sum_{K,M}\sum_{\substack{\sigma_1\sigma_2\\ \sigma_1'\sigma_2'}}\int d\mathbf{r}_{fF}d\mathbf{r}_{b1}d\mathbf{r}_{A2}[\Psi^{j_f}(\mathbf{r}_{A1},\sigma_1)\Psi^{j_f}(\mathbf{r}_{A2},\sigma_2)]_0^{0*}$$
$$\times\,\chi_{bB}^{(-)*}(\mathbf{r}_{bB})v(\mathbf{r}_{b1})[\Psi^{j_f}(\mathbf{r}_{A2},\sigma_2)\Psi^{j_i}(\mathbf{r}_{b1},\sigma_1)]_M^K$$
$$\times\int d\mathbf{r}'_{b1}d\mathbf{r}'_{A2}[\Psi^{j_f}(\mathbf{r}'_{A2},\sigma_2')\Psi^{j_i}(\mathbf{r}'_{b1},\sigma_1')]_M^K$$
$$\times\,[\Psi^{j_i}(\mathbf{r}'_{A2},\sigma_2')\Psi^{j_i}(\mathbf{r}'_{b1},\sigma_1')]_0^0\chi_{aA}^{(+)}(\mathbf{r}'_{aA}).$$

Non orthogona

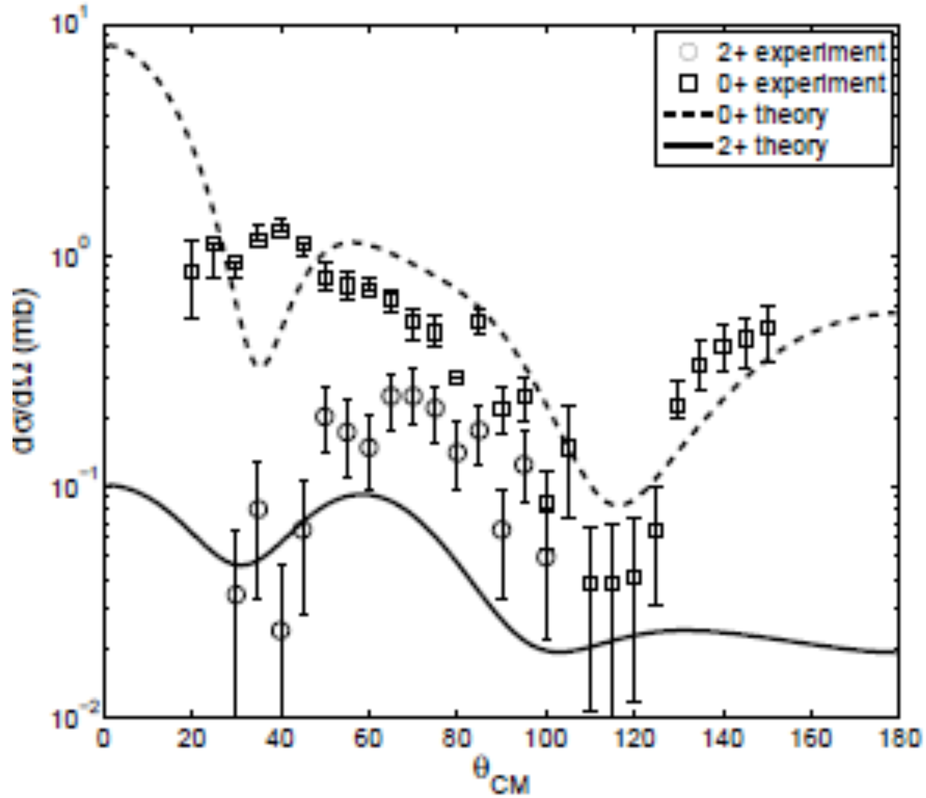


| | $\sigma(^{11}\mathrm{Li(gs)} \rightarrow {}^{9}\mathrm{Li\ (i)})$ (mb) | | |
|---|---|---|---|
| i | $\Delta L$ | Theory | Experiment |
| gs $(3/2^-)$ | 0 | 6.1 | 5.7 ± 0.9 |
| 2.69 MeV $(1/2^-)$ | 2 | 0.5 | 1.0 ± 0.36 |

G. Potel et al., PRl 105 (2010) 172502

# Channels $c$ leading to the first $1/2^-$ excited state of $^9$Li

$c = 1$: Transfer of the two halo neutrons

$c = 2$: Transfer of a $p_{1/2}$ halo neutron and a $p_{3/2}$ core neutron

$c = 3$: Transfer to the ground state + inelastic excitation

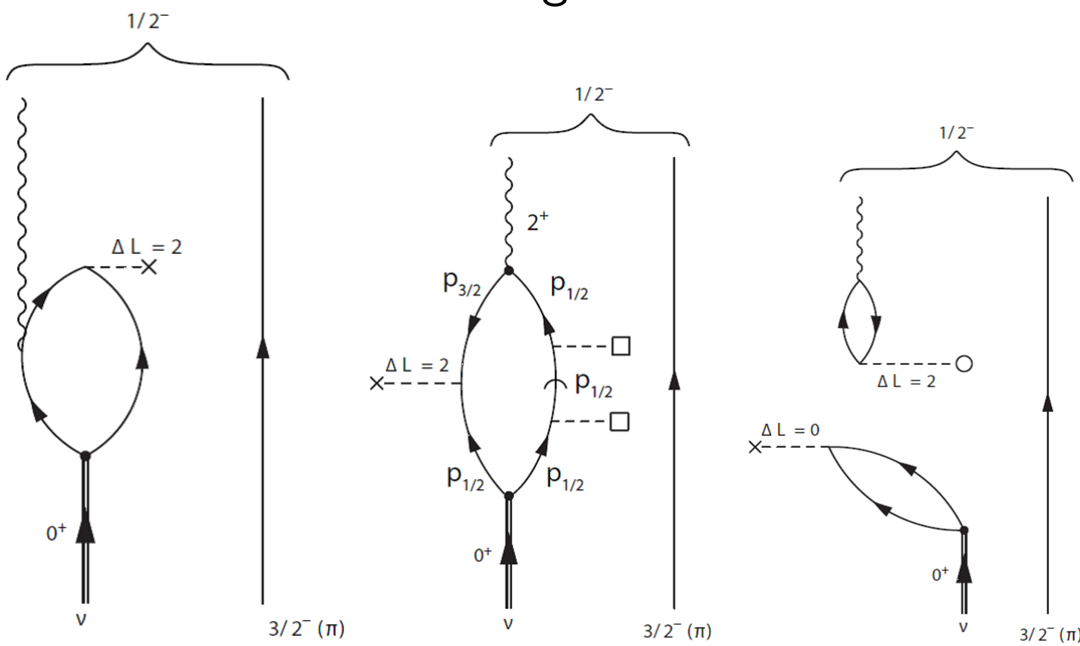


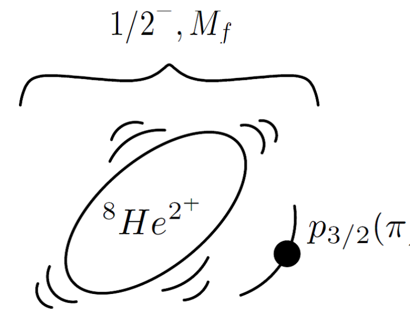


$P^{(1)} = 1.3 \times 10^{-3}$

$P^{(2)} = 4.6 \times 10^{-5}$

$P^{(3)} = 2.6 \times 10^{-6}$

$\sigma_c = \frac{\pi}{k^2} \sum_l (2l+1)|S_l^{(c)}|^2$, $P^{(c)} = \sum_l |S_l^{(c)}|^2$ $(c = 1, 2, 3)$.

Small probabilities $\Rightarrow$ use of second order perturbation theory.

$^{122}Sn(p,t)^{120}Sn \quad E_{lab} = 26\ MeV$

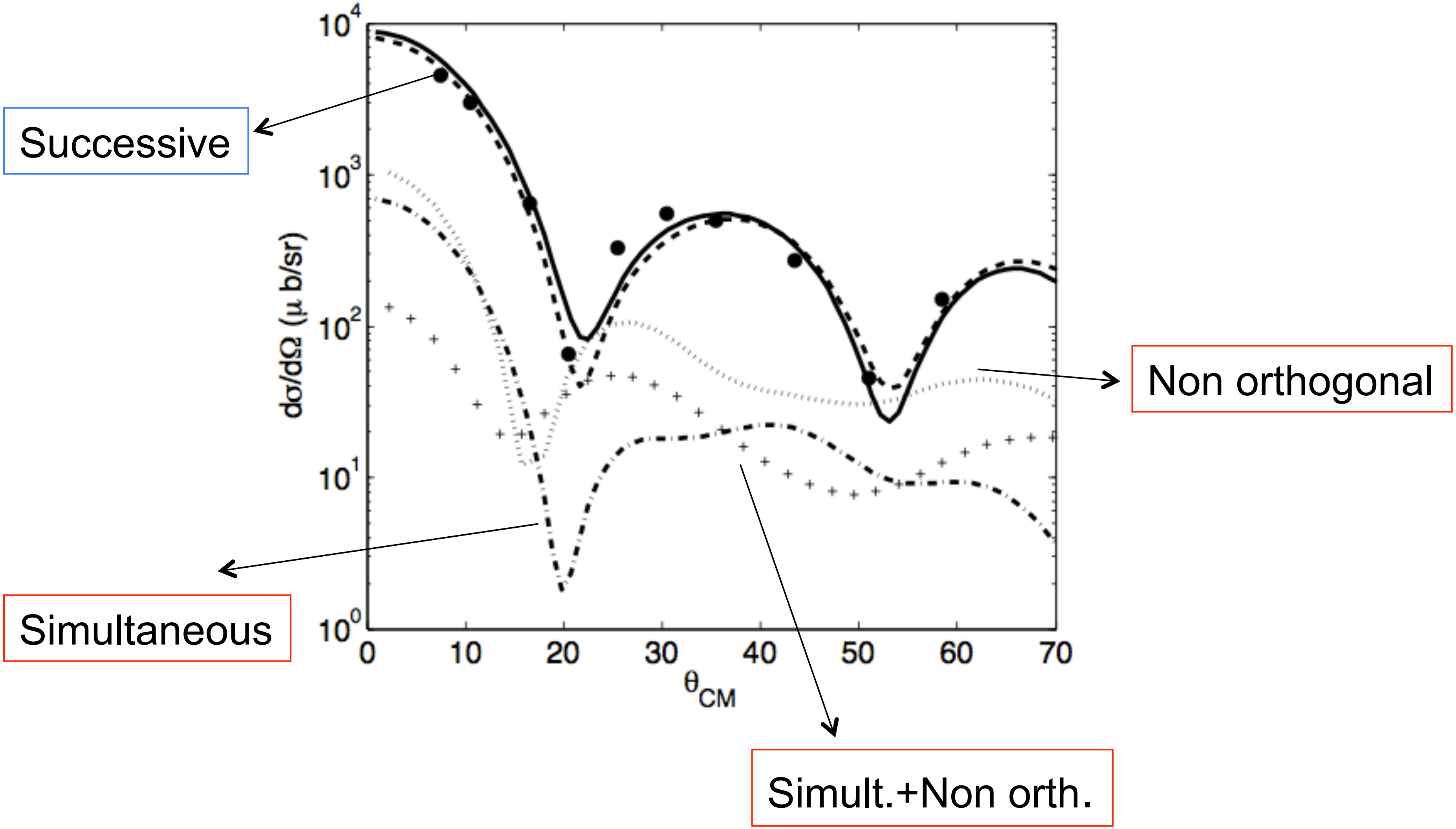

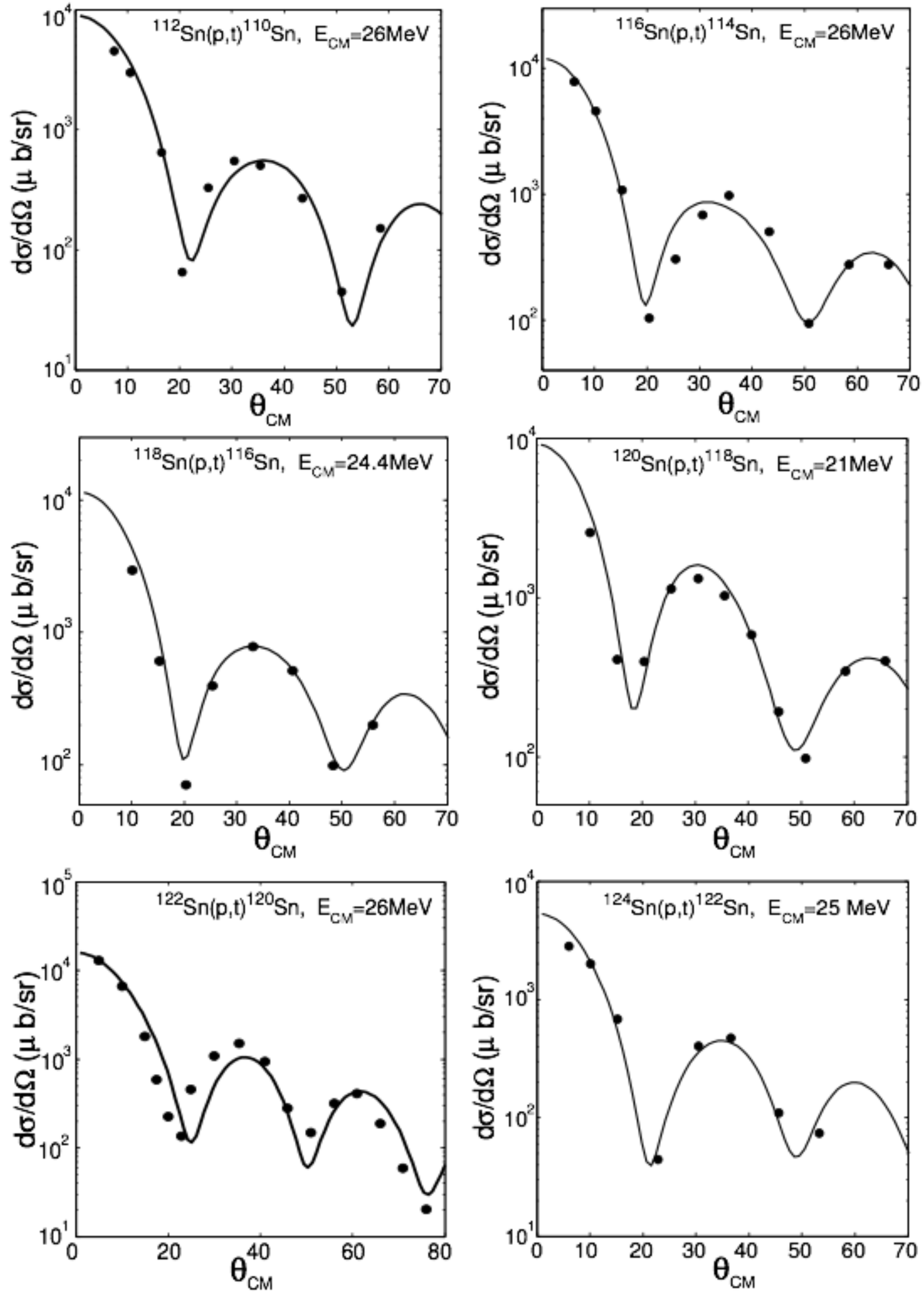


G. Potel et al., nucl-th/1105.6250

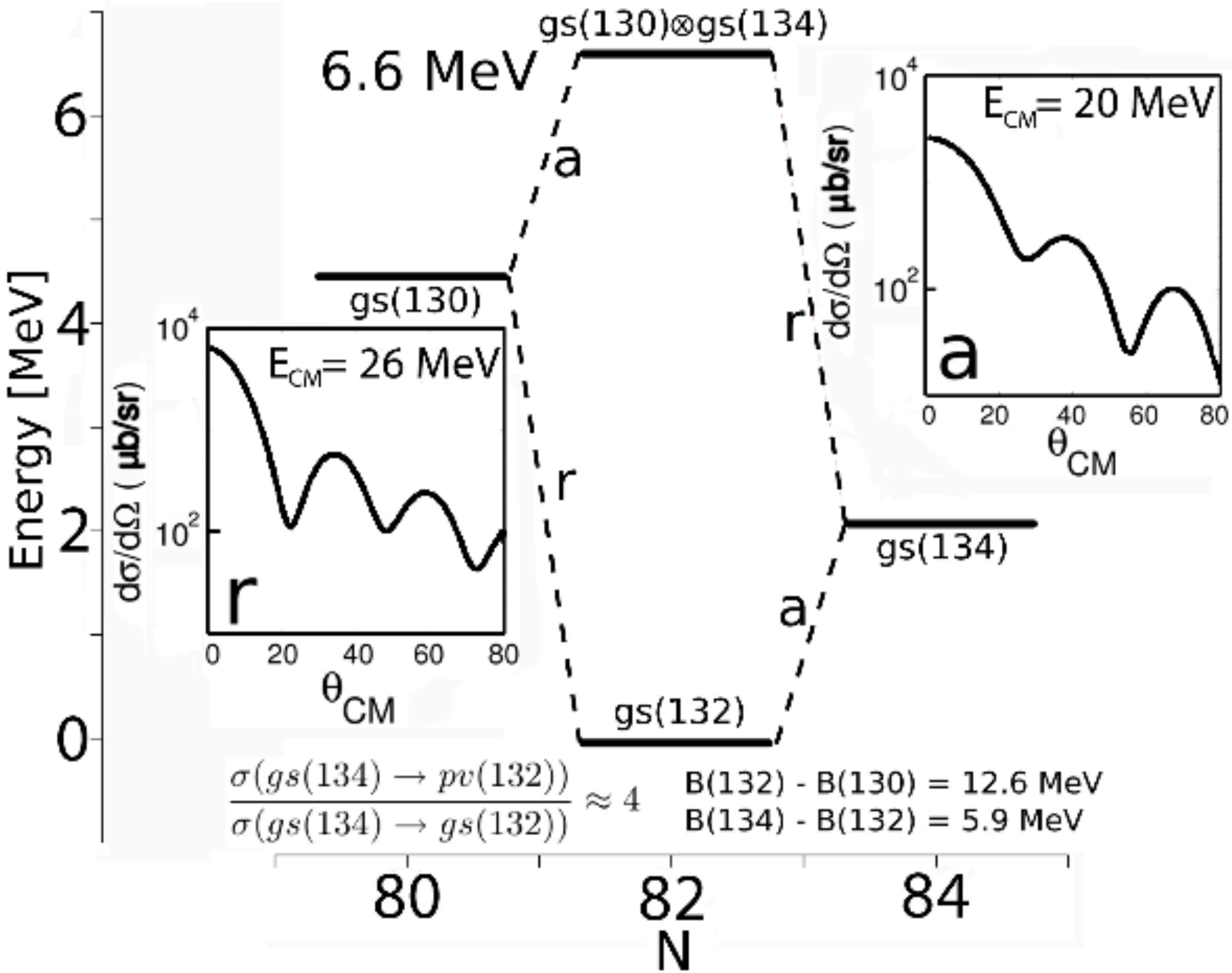
gs(130)⊗gs(134)
6.6 MeV
Energy [MeV]
gs(130)
gs(132)
gs(134)
a
r
r
a
E_CM= 26 MeV
E_CM= 20 MeV
dσ/dΩ ( μb/sr)
θ_CM
$\frac{\sigma(gs(134) \to pv(132))}{\sigma(gs(134) \to gs(132))} \approx 4$
B(132) - B(130) = 12.6 MeV
B(134) - B(132) = 5.9 MeV
N

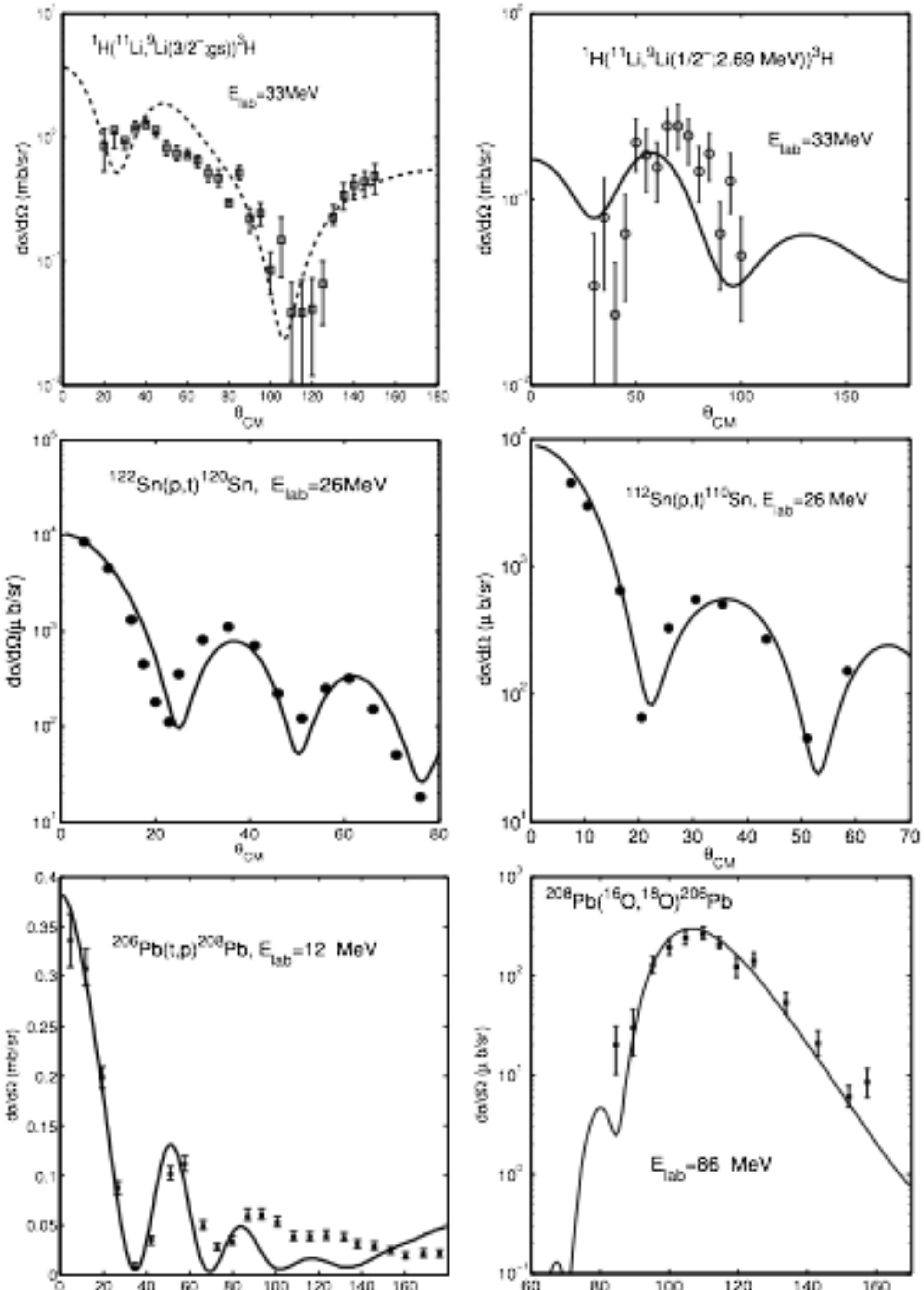


A recent analysis of various two-neutron transfer reactions Based on second order DWBA reproduces absolute cross sections

G. Potel et al., nucl_th/ 0906.4298

## summary and conclusions

- A recent two–neutron transfer experiment ($^{1}H(^{11}Li,^{9}Li)^{3}H$, Tanihata *et al.*, 2008) provided new insight in the structure of $^{11}Li$.
- We show that the differential cross section is quantitatively consistent with the *s*–*p* mixing in the ground state of $^{11}Li$ already predicted (see e.g. Barranco *et al.* 2001).

- We found hat the differential cross section for the excitation of the first $1/2^{-}$ (2.69 MeV) provides evidence of phonon–mediated pairing between the two halo neutrons of $^{11}Li$.

# Setting these findings in a broader context – pairing in heavy nuclei

Various effective forces in the pairing
channel have been proposed, with different features (finite/zero range, density dependence…)
Unfortunately it is difficult to discriminate among them comparing with available data.

We want to follow a different strategy:

- Start from an Hartree-Fock calculation with a 'reasonable' interaction. Then solve the pairing problem with a bare interaction in the $^1S_0$ channel. And finally add correlations beyond mean field.

We know that these correlations strongly renormalize the density of single-particle levels (effective mass) and their occupation factors (fragmentation), and we expect that they can have a large effect on pairing properties.

# Going beyond the quasi-particle approximation

J. Terasaki et al., Nucl.Phys. **A697**(2002)126

by extending the Dyson equation…

$$G_{\mu}^{-1}=(G_{\mu}^{o})^{-1}-\Sigma_{\mu}(\omega)$$

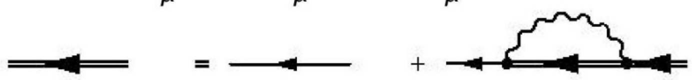

$$\Sigma_{\mu}(\omega)=\int_{-\infty}^{+\infty}\frac{d\omega'}{2\pi}\sum_{\mu'}\frac{1}{\hbar}G_{\mu'}(\omega')\sum_{\alpha}\frac{1}{\hbar}D_{\alpha}^{o}(\omega-\omega')*V_{\mu\mu',\alpha}^{2}$$

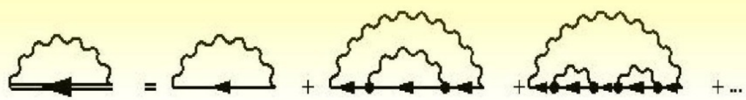

to the case of superfluid nuclei (Nambu-Gor’kov), it is possible to consider both

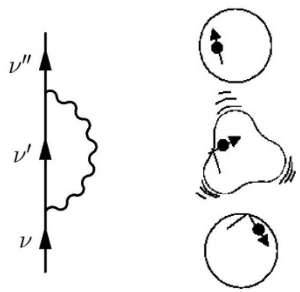


and

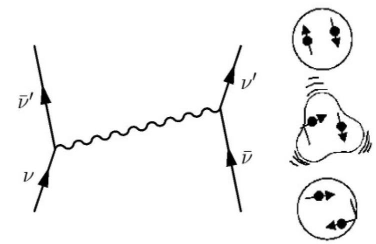

# Renormalization of quasiparticles

120Sn

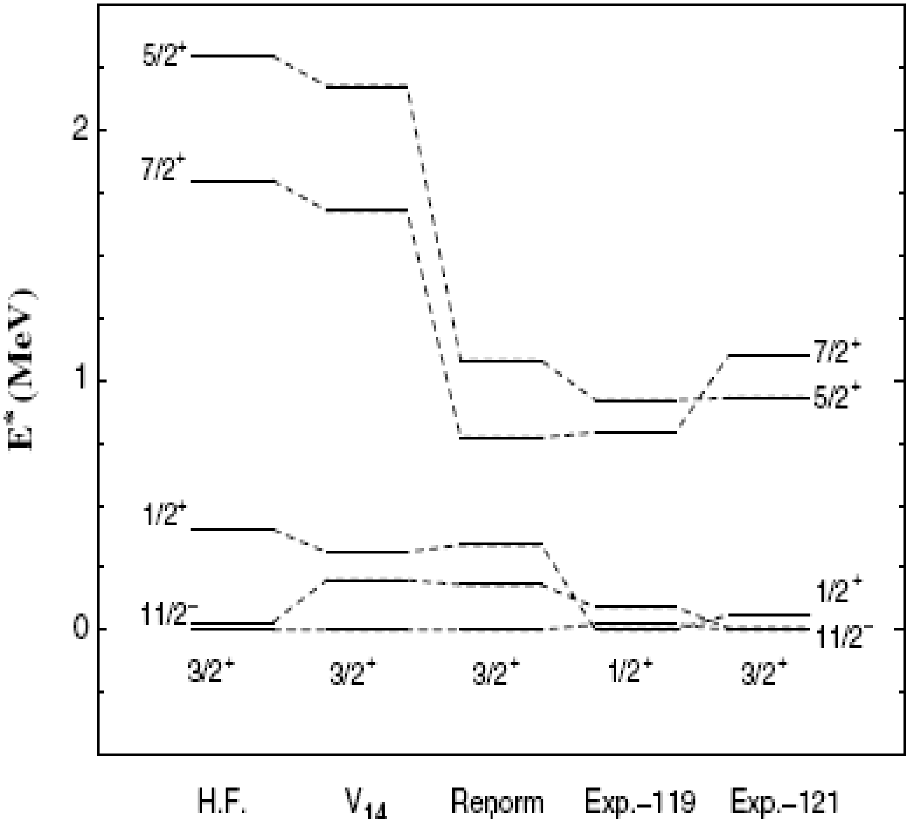


Argonne

Argonne + induced interaction

# $h_{11/2}$

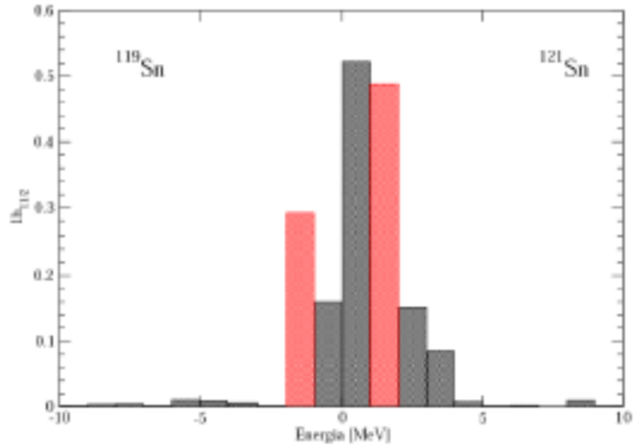


SII

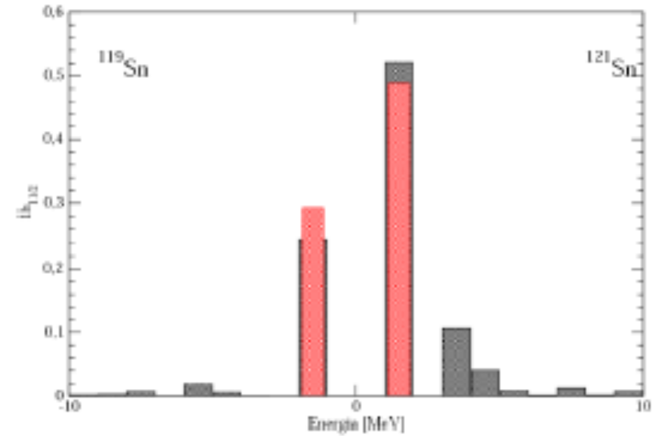


SLy4

Exp.

Th.

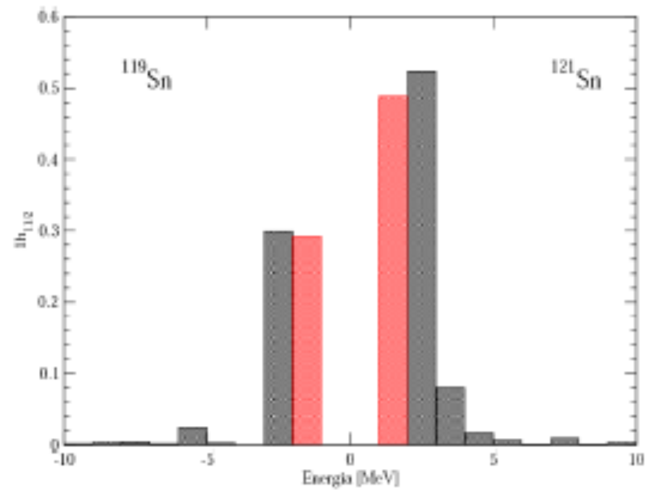


SGII

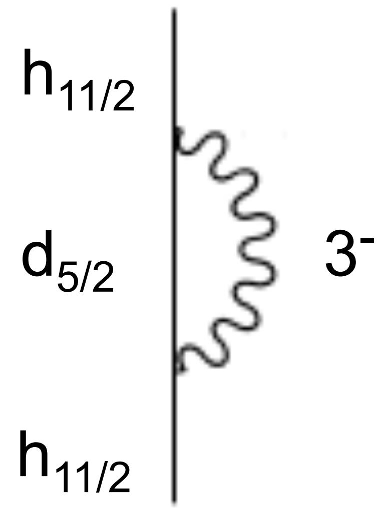

Semiclassical diagonal pairing matrix elements (120Sn)

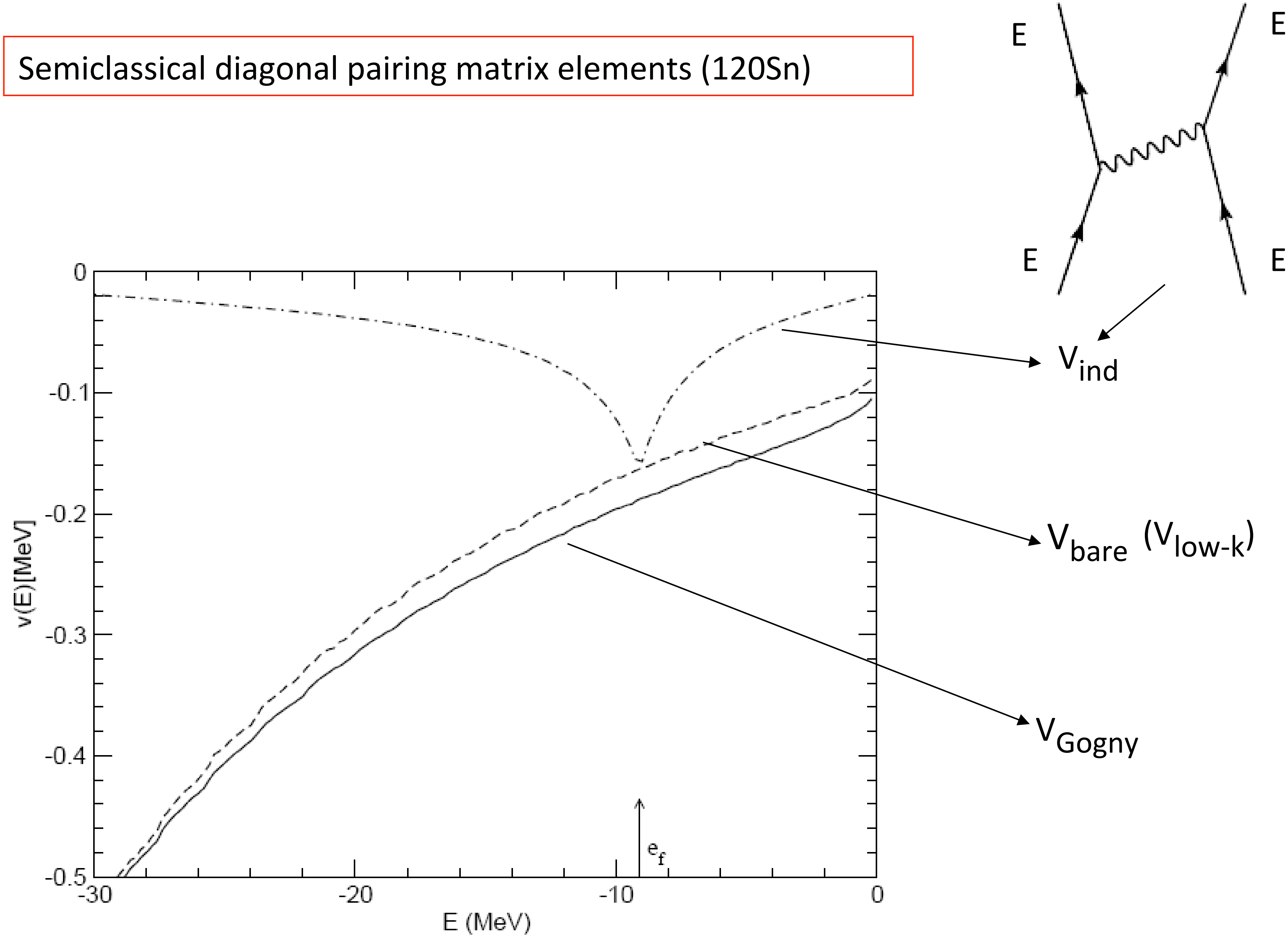


F. Barranco et al., Phys. Rev. 72(2005)054314

# Renormalized pairing gaps

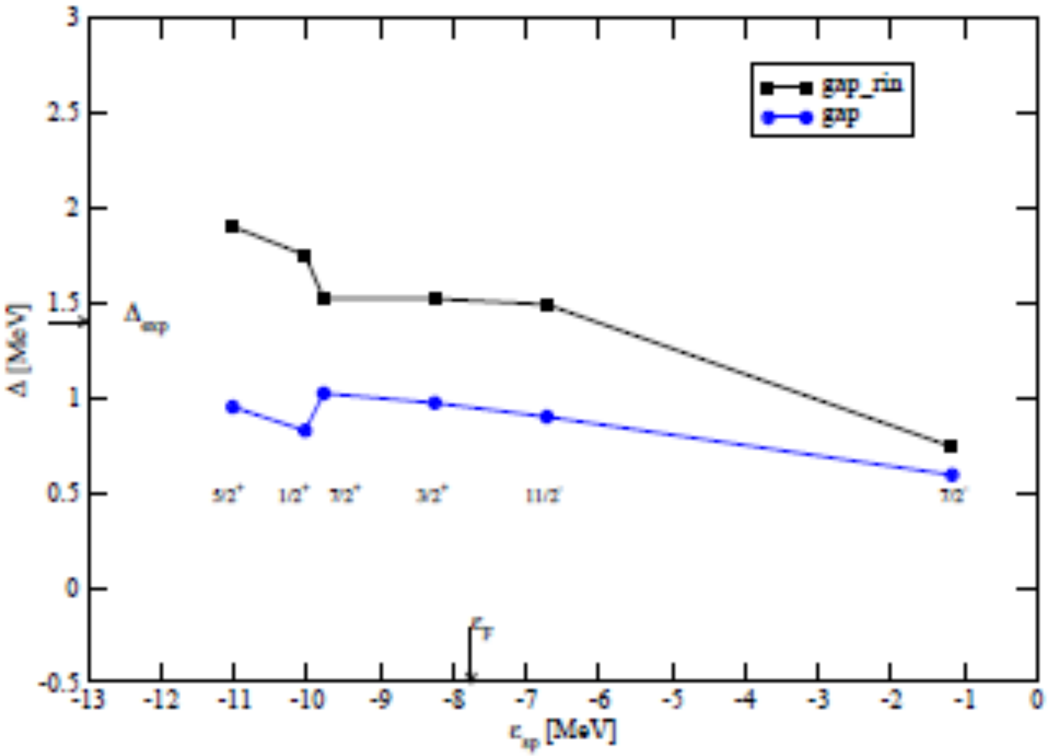

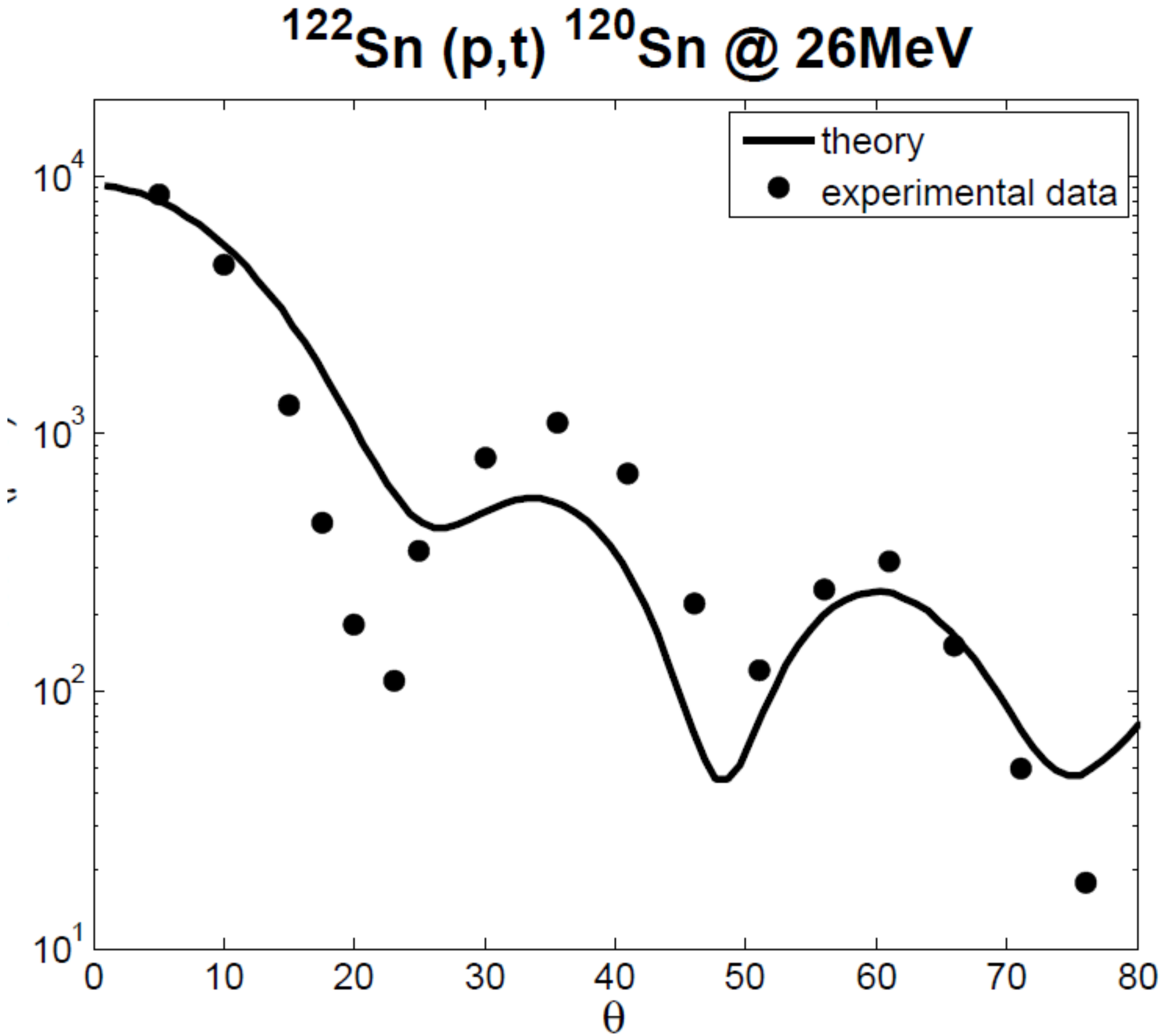

122Sn (p,t) 120Sn @ 26MeV
theory
experimental data
10^4
10^3
10^2
10^1
0
10
20
30
40
50
60
70
80
θ

# Local approximation

The pairing gap associated with the bare interaction  is surface peaked;
the induced interaction reinforces this feature

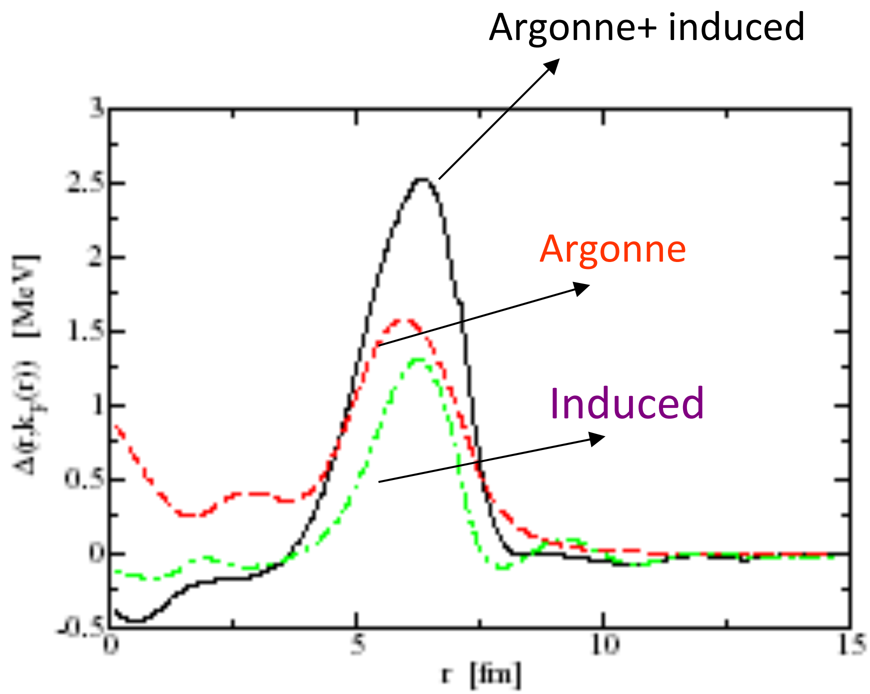


Microscopic justification of surface peaked, density-dependent pairing force

A. Pastore et al., Phys. Rev. C78 (2008) 024315

Mean field calculation with Vlow-k pairing force:
3-body force reduces the pairing gaps

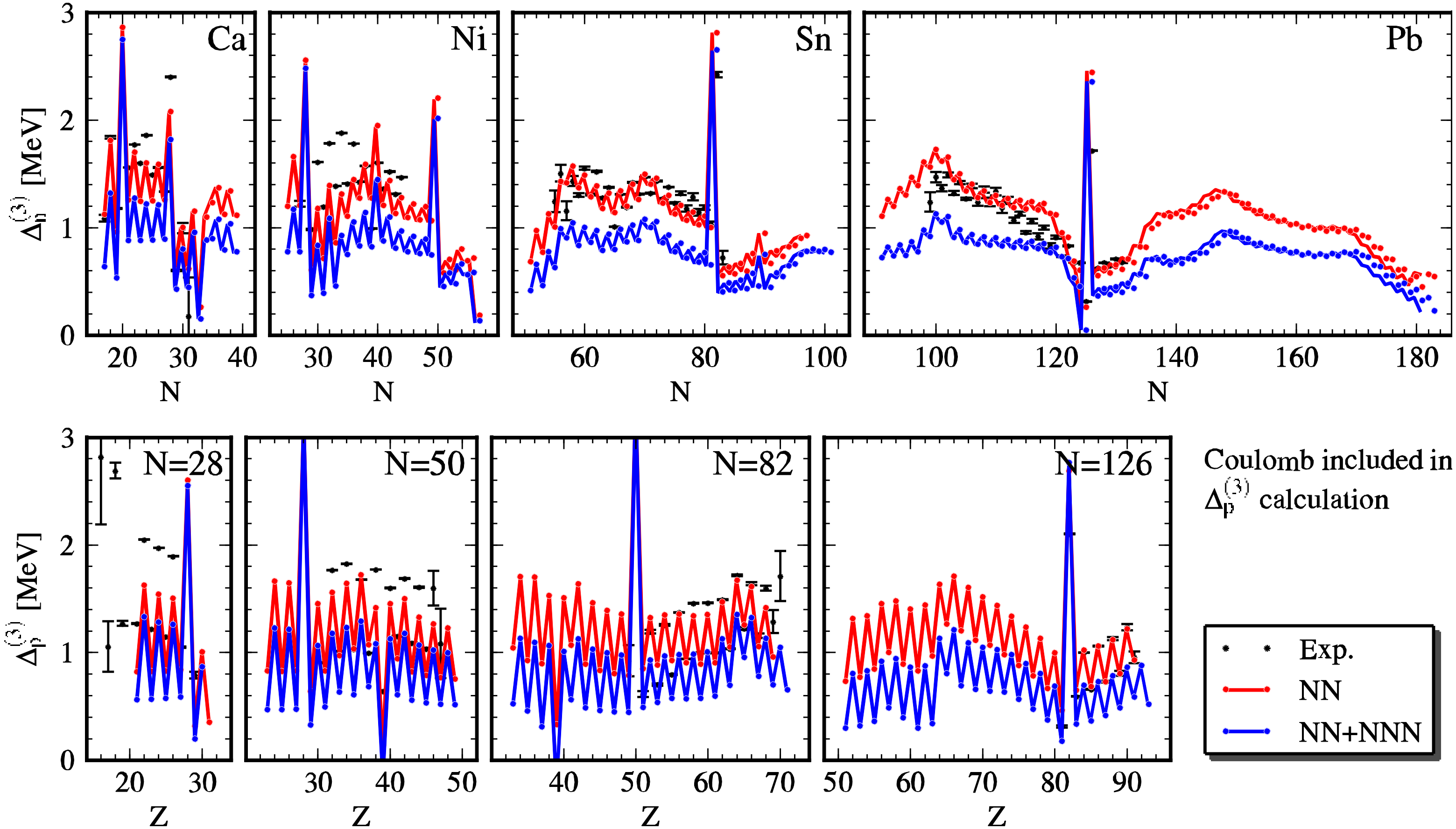


T. Duguet, T. Lesinski, A.Schwenk, in preparation

According to a dynamical model of the halo nucleus 11Li,
a key role is played by the coupling of the valence nucleons
with the vibrations of the system.
The structure model has been tested with a detailed reaction
calculation, comparing with data obtained in a recent (t,p) experiment.
Theoretical and experimental cross section are in reasonable agreement.

Vlow-k with SLy5 mean field

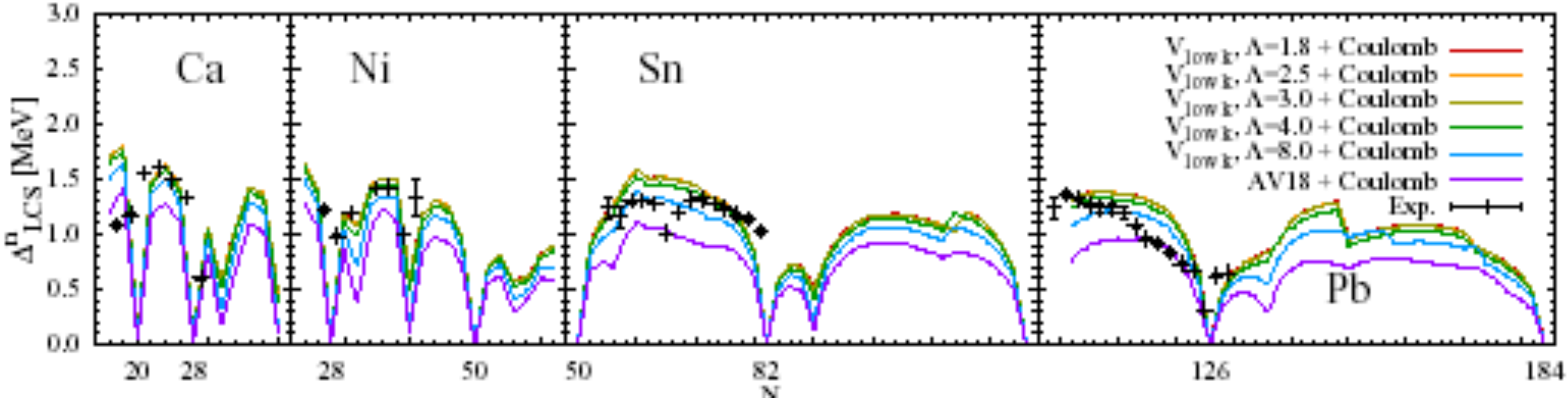


T. Duguet et al., arXiv:0809.2895 and Catania Workshop

ELSEVIER

Nuclear Physics A649 (1999) 45c

NUCLEAR PHYSICS A

# Why are nuclei described by independent particle motion ?

B.R. Mottelson[a*]

[a]The Niels Bohr Institute and NORDITA, Blegdamsvej 17, DK-2100 Copenhagen Ø, Denmark

| Constituents | M | $V_0$ [eV] | a [cm] | $\Lambda$ | T=0 matter |
|---|---|---|---|---|---|
| $^3$He | 3 | $9{\cdot}10^{-4}$ | $2.9{\cdot}10^{-8}$ | 0.21 | liquid |
| $^4$He | 4 | $9{\cdot}10^{-4}$ | $2.9{\cdot}10^{-8}$ | 0.16 | liquid |
| $H_2$ | 2 | $3{\cdot}10^{-3}$ | $3.3{\cdot}10^{-8}$ | 0.07 | solid |
| Ne | 20 | $3{\cdot}10^{-3}$ | $3.1{\cdot}10^{-8}$ | 0.007 | solid |
| nuclei | 1 | $1{\cdot}10^{8}$ | $9{\cdot}10^{-14}$ | 0.4 | liquid |

Table 1
The "quantality" parameter $\Lambda = \hbar^2/Ma^2V_0$ measures the strength of the two-body attraction, $V_0$, expressed in units of the quantal kinetic energy associated with a localization of a constituent particle of mass M within the distance a corresponding to the radius of the force at maximum attraction. For small $\Lambda$ the quantal effect is small and the ground state of the many body system will be, as in classical mechanics, a configuration in which each particle finds a static optimal position with respect to its nearest neighbors. If $\Lambda$ is big enough the ground state may be a quantum liquid in which the individual particles are delocalized and the low-energy excitations (quasi-particles) have infinite mean free path. A parameter related to $\Lambda$ was first used by de Boer in the analysis of quantal constants of the noble gas solids.

TAB. 4.2 – *Paramètres des potentiels optiques globaux utilisés pour la voie $^{11}Li+p$. à 4.3A MeV*

| | V (MeV) | $r_v$ (fm) | $a_v$ (fm) | $W_d$ (MeV) | $r_d$ (fm) | $a_d$ (fm) | $V_{so}$ (MeV) | $r_{so}$ (fm) | $a_{so}$ (fm) |
|---|---|---|---|---|---|---|---|---|---|
| CH89 | 58.1 | 1.15 | 0.69 | 12.9 | 1.14 | 0.69 | 5.9 | 0.80 | 0.63 |
| B&G | 64.0 | 1.17 | 0.75 | 16.2 | 1.32 | 0.83 | 6.2 | 1.01 | 0.75 |
| Perey | 63.7 | 1.25 | 0.65 | 13.5 | 1.25 | 0.47 | 7.5 | 1.25 | 0.47 |

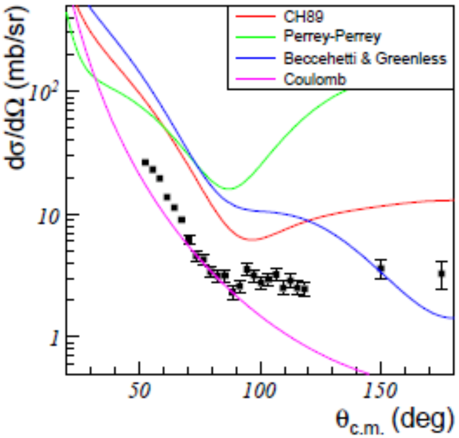


FIG. 4.8 – *Comparaison entre les données expérimentales de diffusion élastique et les calculs effectués avec des potentiels optiques globaux. Les deux derniers points aux angles arrière proviennent des données en cible épaisse.*

T. Roger, Ph.D. Thesis (2009)

An opposite view

VOLUME 78, NUMBER 14 PHYSICAL REVIEW LETTERS 7 APRIL 1997

## Suppression of Core Polarization in Halo Nuclei

T. T. S. Kuo,[1] F. Krmpotić,[2] and Y. Tzeng[3]
[1]Department of Physics, SUNY-Stony Brook, Stony Brook, New York 11794
[2]Departamento de Fisica, Facultad de Ciencias Exactas, Universidad Nacional de La Plata, C. C. 67, 1900 La Plata, Argentina
[3]Institute of Physics, Academia Sinica, Nankang, Taipei, Taiwan
(Received 18 June 1996; revised manuscript received 8 October 1996)

Halo nuclei are studied using a $G$-matrix interaction derived from the Paris and Bonn potentials and employing a two-frequency shell model approach. It is found that the core-polarization effect is dramatically suppressed in such nuclei. Consequently, the effective interaction for halo nucleons is almost entirely given by the bare $G$ matrix alone, which presently can be evaluated with a high degree of accuracy. The experimental pairing energies between the two halo neutrons in $^6$He and $^{11}$Li nuclei are satisfactorily reproduced by our calculation. It is suggested that the fundamental nucleon-nucleon interaction can be probed in a clearer and more direct way in halo nuclei than in ordinary nuclei. [S0031-9007(97)02891-3]

# Going beyond mean field: medium polarization effects

Self-energy

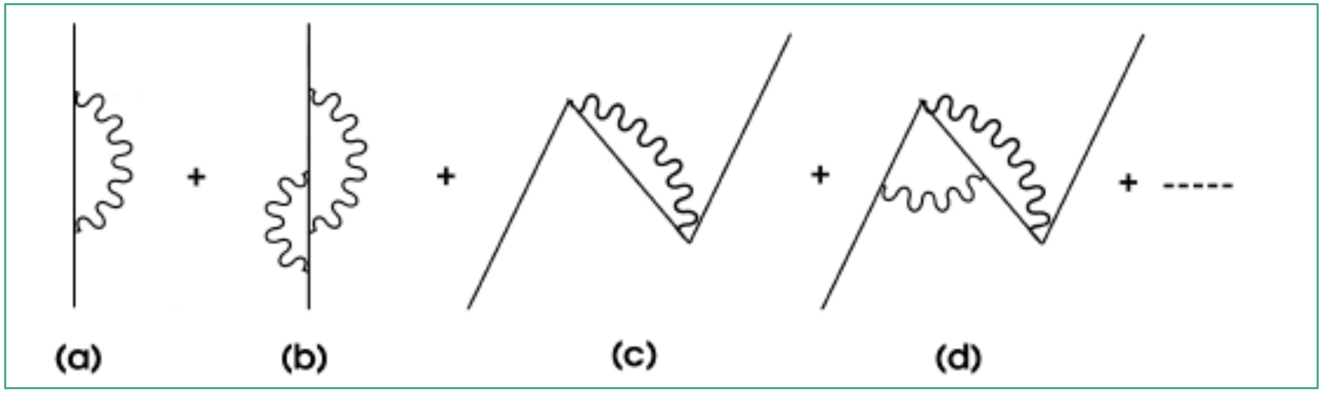


Induced interaction (screening)

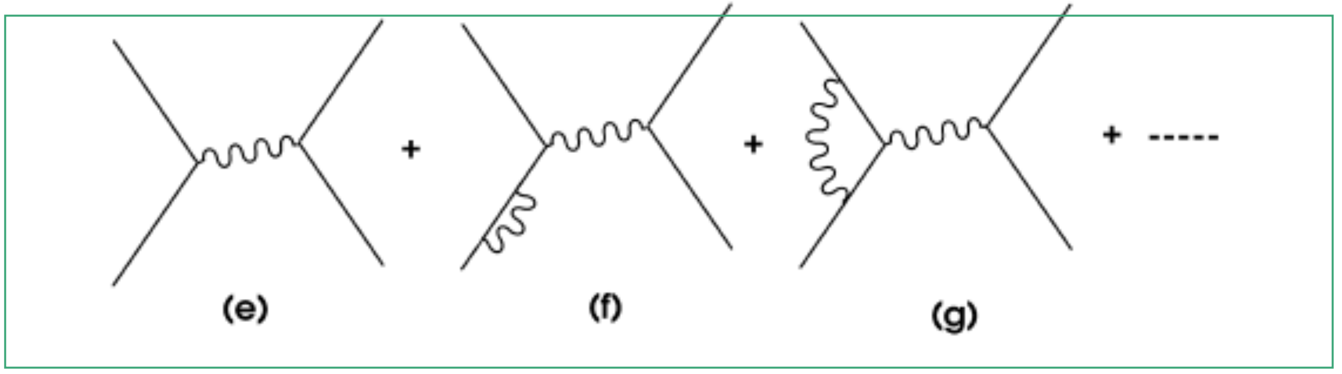

C. Mahaux et al., Dynamics of the shell model

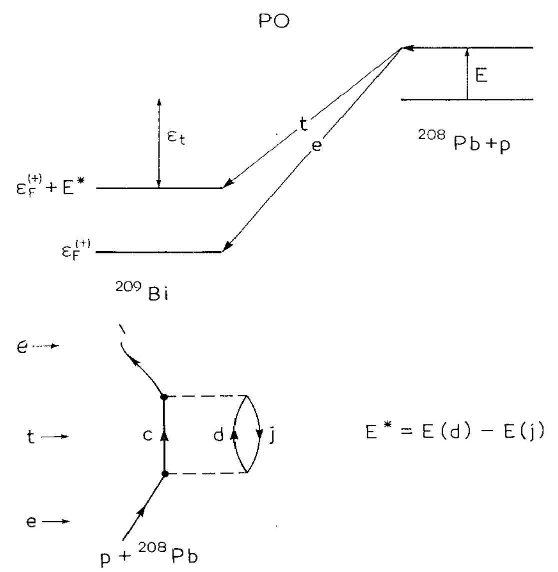


C. Mahaux et al., Dynamics of the shell model

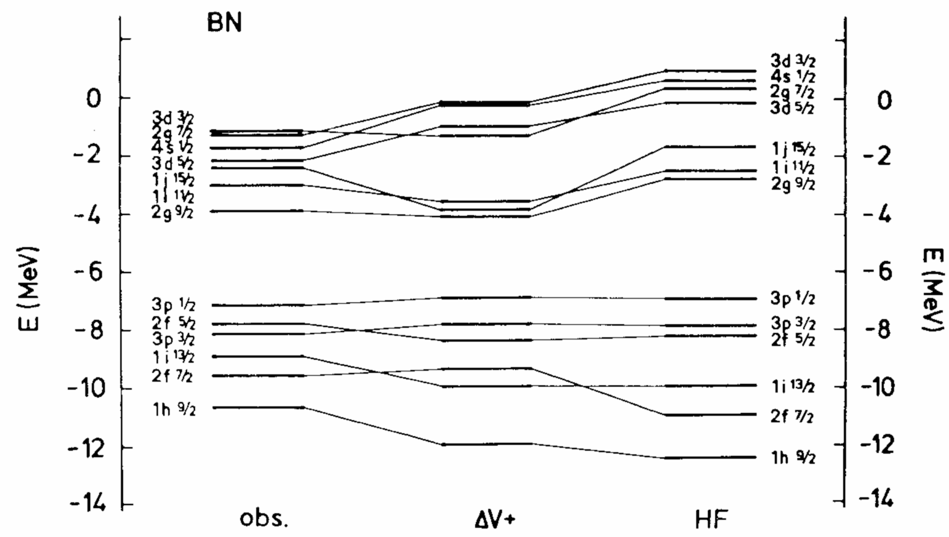


# Coupling of vibrations to single-particle motion

# Effective mass $m_\omega$

# Increased level density at the Fermi energy

# Self-energy and effective mass

$$m_\omega \approx \left(1 + \frac{N(0)V^2}{\hbar\omega_\lambda}\right)m$$

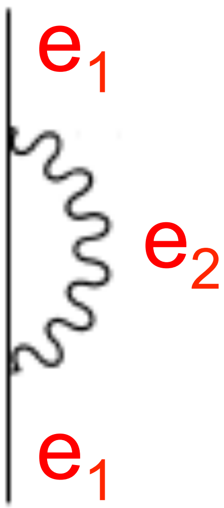


$$= \frac{V^2}{e_1 - (e_2 + \hbar\omega_\lambda)} \approx -\frac{V^2}{\hbar\omega_\lambda}$$

$$m_\omega \approx 1.5m$$

$$\hbar\omega_\lambda \approx 2\text{MeV}$$

$$\text{N}(0) \approx 3\ \text{MeV}^{-1}$$

$$\Longrightarrow$$

$$V^2 \approx 0.3\ \text{MeV}^2$$

# Pairing from exchange of vibrations (induced interaction)

Two time orderings

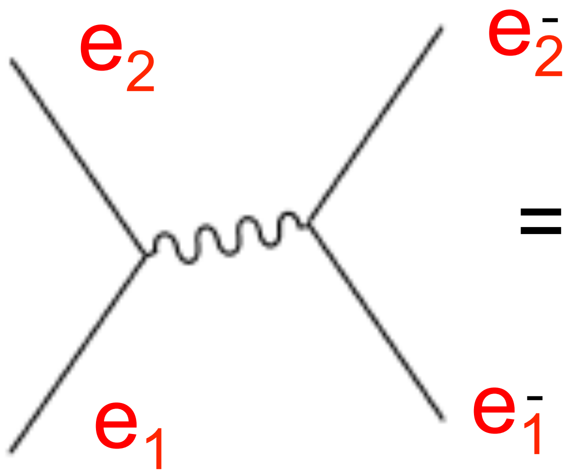


$$= \frac{V^2}{2e_1 - (e_1 + e_2 + \hbar\omega_\lambda)} =$$

$$\frac{V^2}{e_1 - (e_2 + \hbar\omega_\lambda)} \approx -\frac{V^2}{\hbar\omega_\lambda}$$

$$V_{ind} = -\frac{2V^2}{\hbar\omega_\lambda} \approx \text{- 0.3 MeV}$$

Pairing field in momentum space

$$\Delta(\vec{R}_{CM},\vec{k}) \quad = \quad \frac{1}{(2\pi)^3}\int d^3r_{12}\, e^{i\vec{k}\bullet\vec{r}_{12}}\,\Delta(\vec{R}_{CM},\vec{r}_{12})$$

Gogny

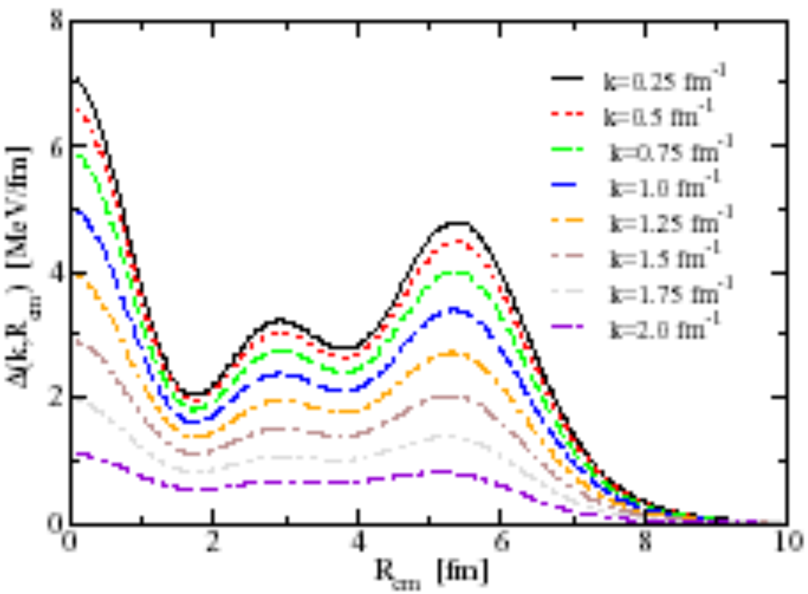


Argonne

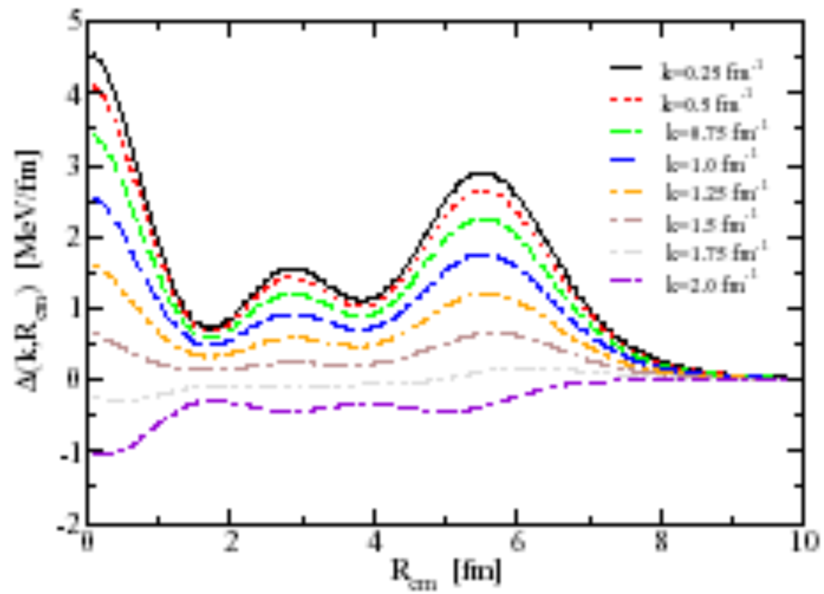

# Density Dependent Delta Interaction

We give a description in terms of density dependent delta force of our local approximation:

$$v(\vec{r}_1, \vec{r}_2) = v_0 \left[ 1 - \eta \left( \frac{\rho\left(\frac{\vec{r}_1+\vec{r}_2}{2}\right)}{\rho_0} \right)^{\alpha} \right] \delta(\vec{r}_1 - \vec{r}_2)$$

We fix the parameter $v_0 = -458.4$ MeVfm $^3$ and consequently the cut-off in single-particle energy spectrum $\epsilon_{cut} = 60$ MeV.

M.Matsuo, Phys. Rev. C 73 (2006), 044309

We use the following procedure:

1. I take trial values for $\alpha$ and $\eta$,and I use them to solve HFB equations self-consistently, so I obtain the anomalous density, $\Phi(\vec{r}_1, \vec{r}_2)$
2. I fit $\Delta_{loc}(r)$, obtained with the semiclassical approximation, with the least square method with the function $v(\vec{r}_1, \vec{r}_2) \cdot \Phi(\vec{r}_1, \vec{r}_2)$, and I obtain two new values of the constants $\alpha$ and $\eta$.
3. I insert the new values of $\alpha, \eta$ in the HFB equations and I recalculate the anomalous density $\Phi(\vec{r}_1, \vec{r}_2)$
4. I repeat all this procedure until the values of $\alpha, \eta$ I obtained from the fitting-procedure are close to the ones I used in the previous step to calculate $\Phi(\vec{r}_1, \vec{r}_2)$; the tolerance is $|\alpha_{fit} - \alpha_{previous}| < 0.05$ and $|\eta_{fit} - \eta_{previous}| < 0.05$

# Local approximation

| Interaction | $\alpha$ | $\eta$ |
|---|---|---|
| Argonne $v18$ plus Induced | 1.2 | 1.0 |
| Gogny D1 | 0.55 | 0.62 |
| Argonne $v18$ | 0.66 | 0.84 |
| Induced | 0.85 | 1 |

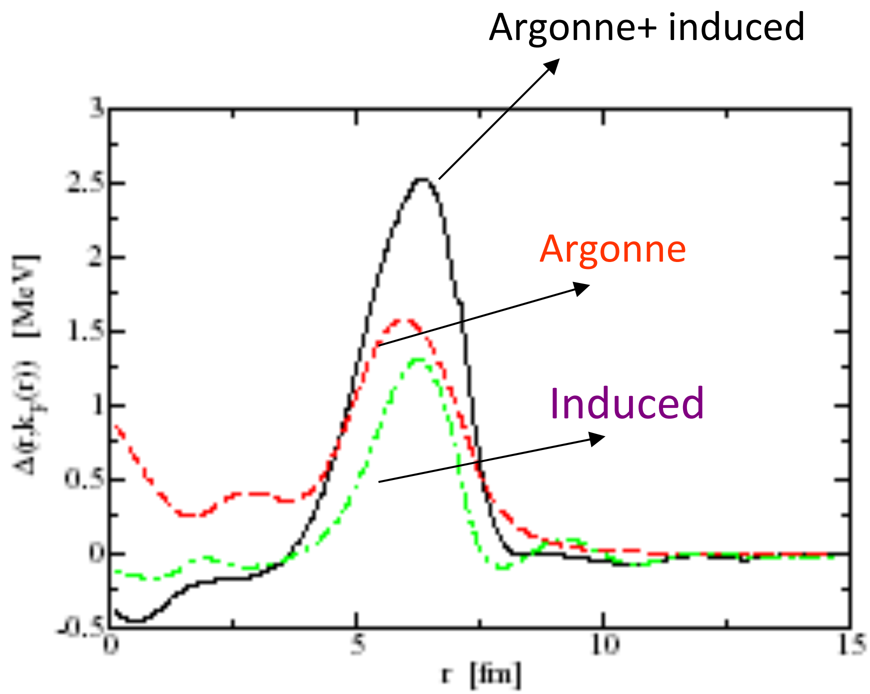


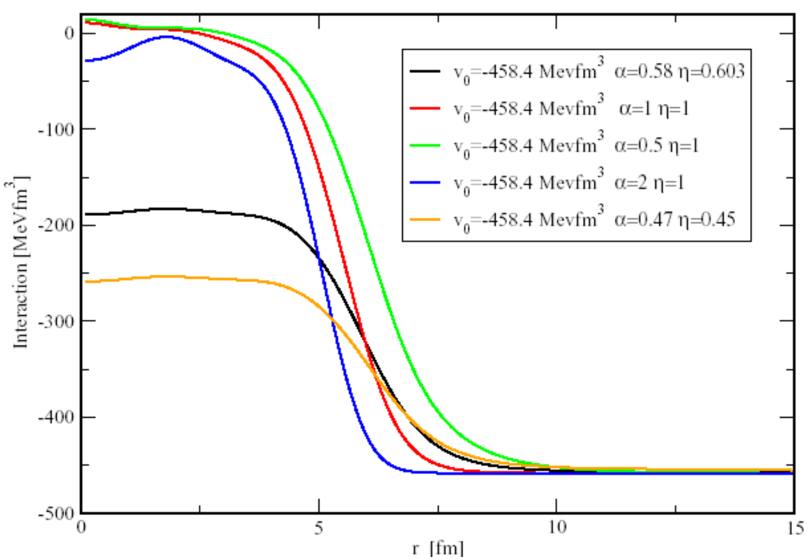

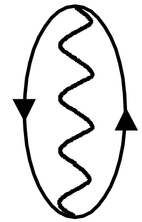

( a )

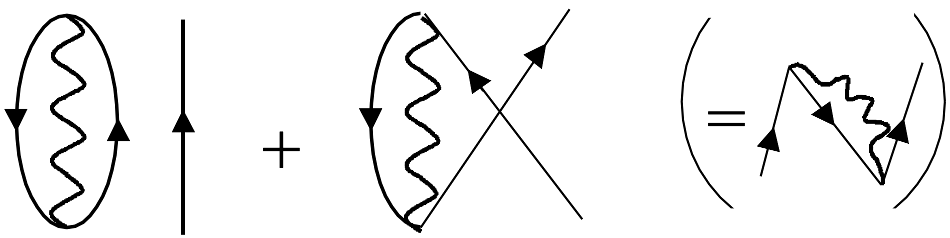

( b ) ( c ) ( d )

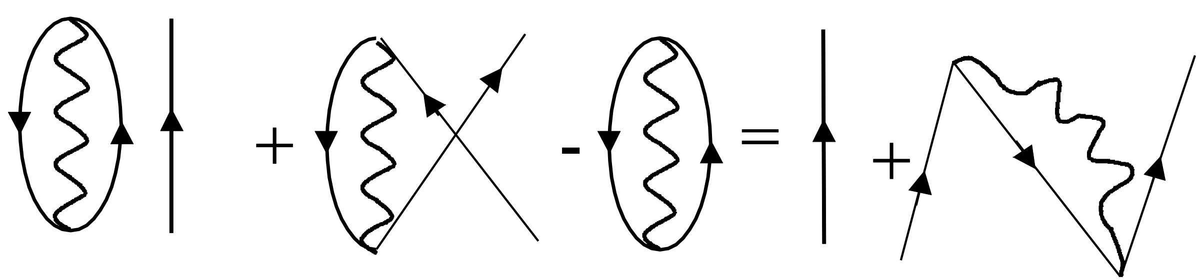

( e )

$$|\tilde{0}\rangle = |0\rangle + 0.7|(ps)_{1^-} \otimes 1^-; 0\rangle + 0.1|(sd)_{2^+} \otimes 2^+; 0\rangle \tag{1}$$

where

$$|0\rangle = 0.45|s^2_{1/2}(0)\rangle + 0.55|p^2_{1/2}(0)\rangle + 0.04|d^2_{5/2}(0)\rangle \tag{2}$$

From this wavefunction, but even more directly from the diagrams displayed in Figs. 1 (b) and 1 (c) (see also Brink and Broglia (2005) Fig. 11.6), it is easy to understand how the virtual propagation of collective vibrations (in the present case $1^-$ and $2^+$ states) between Cooper pair partners can be forced to become a real process: by transferring one or two units of angular momentum in a two–neutron pick–up process (Figs. 1 (e) and 1 (f)). In particular, the correlation mechanism of Figs. 1 (b) and 1 (c) predicts the possibility of a direct excitation of the quadrupole multiplet of $^9$Li, in a two–particle pick–up process.

With the help of the wavefunction (1), a simple estimate of the expected ratio for populating the $^9$Li ground ($3/2^-$) and first excited (2.69 MeV; $1/2^-$) states (see Figs. 1(d) and (e), (f) respectively) can be made, namely,

$$R_1 = \frac{0.01}{0.20 + 0.30 + 0.0002} \approx 0.02\ . \tag{3}$$

That is,one expects the ratio $\sigma$ ($^{11}$Li $\to$ $^9$Li(2.69 MeV))/$\sigma$ ($^{11}$Li $\to$ $^9$Li(gs)) to amount to a few percent.

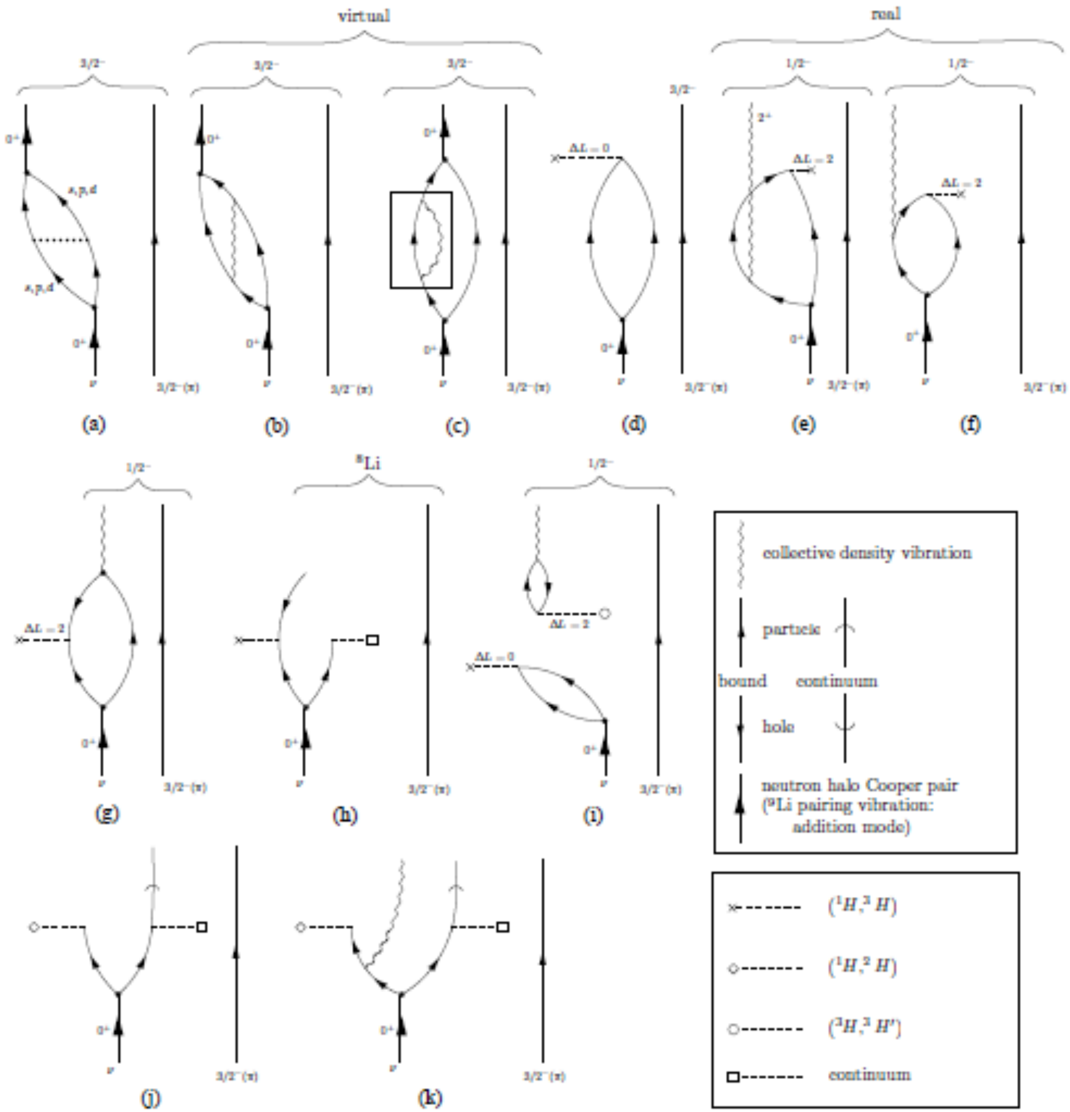
virtual
real
3/2⁻
1/2⁻
0⁺
2⁺
s, p, d
ΔL = 0
ΔL = 2
ν
3/2⁻(π)
(a)
(b)
(c)
(d)
(e)
(f)
(g)
(h)
(i)
(j)
(k)
⁸Li
collective density vibration
particle
bound
continuum
hole
neutron halo Cooper pair
(⁹Li pairing vibration:
addition mode)
(¹H,³H)
(¹H,²H)
(³H,³H′)
continuum

# Bare (Argonne) gaps

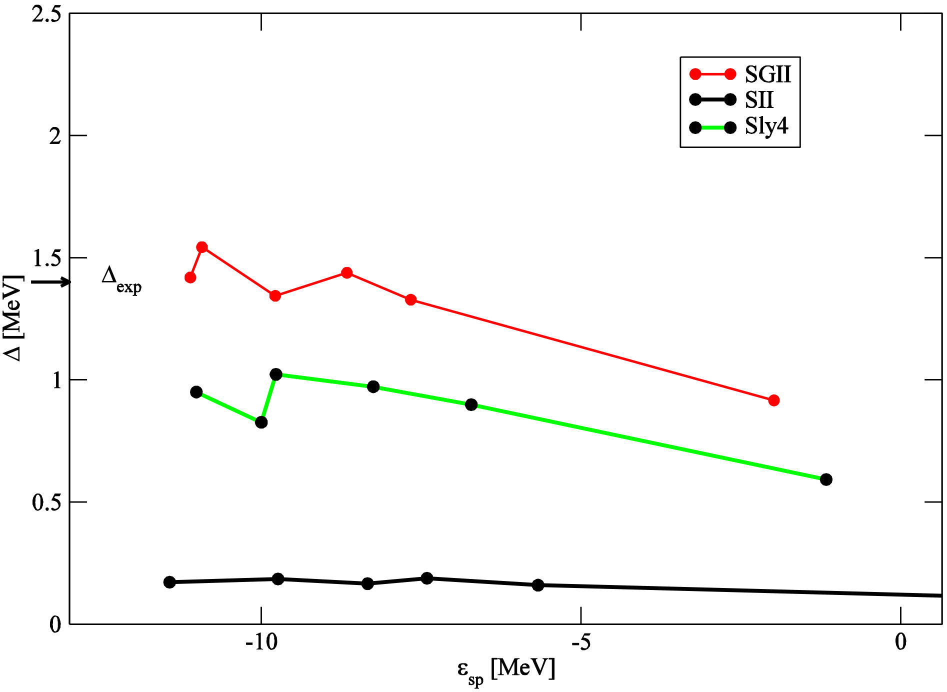


# Renormalized gaps

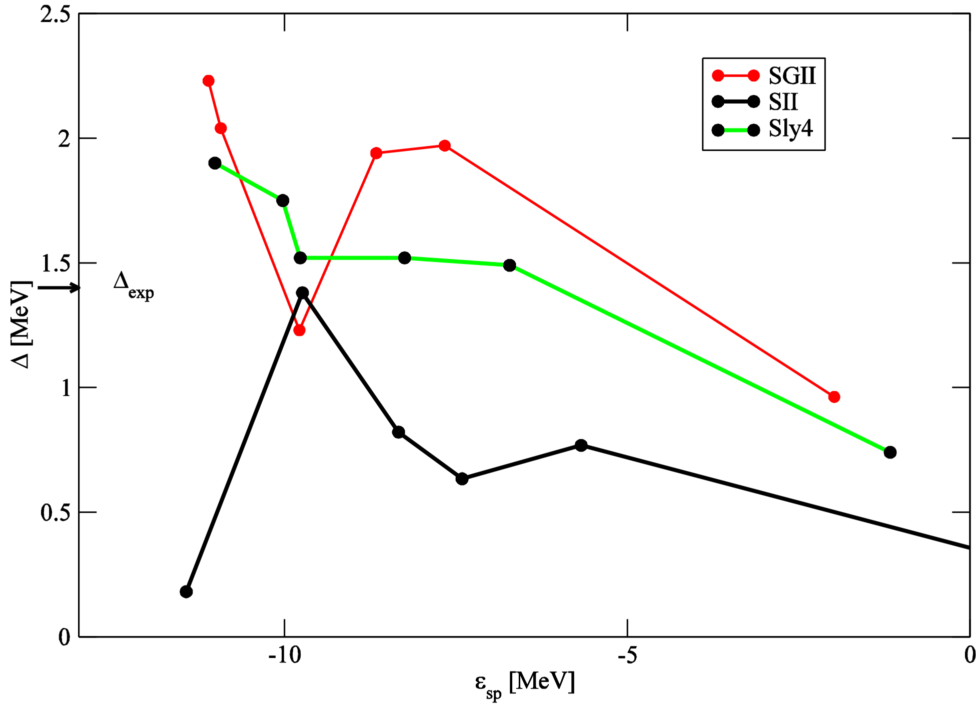


# Effective masses

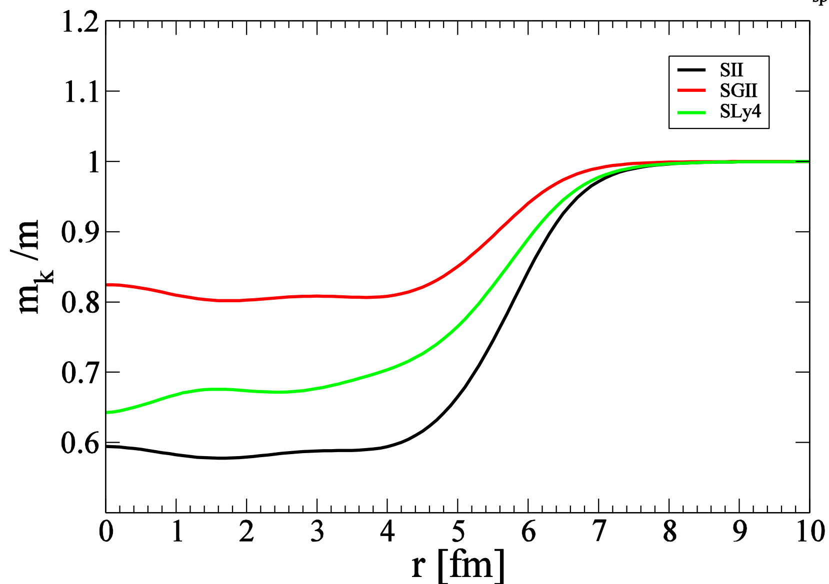

It could furthermore be argued that the observation of the 2.69 MeV(1/2$^-$) first excited $^9$Li final state is the result of a two–step process (see Fig. 1(h)): two–particle transfer to

## ssion of the transfer amplitude

$$)) = P_{2n}(^{11}\mathrm{Li(gs)} \to ^{9} \mathrm{Li(gs)}) \quad (4)$$

$$\frac{\mathrm{Li(gs)} \to ^{9} \mathrm{Li(gs)})}{\sigma_{el}}, \quad (5)$$

$$j_i, j_f) = 2 \sum_{\sigma_1 \sigma_2} \int d\mathbf{r}_{fF}\, d\mathbf{r}_{b1}\, d\mathbf{r}_{A2} [\Psi^{j_f}(\mathbf{r}_{A1}, \sigma_1) \Psi^{j_f}(\mathbf{r}_{A2}, \sigma_2)]^{0*}_0 \chi^{(-)*}_{bB}(\mathbf{r}_{bB})$$

$$\times v(\mathbf{r}_{b1}) [\Psi^{j_i}(\mathbf{r}_{b1}, \sigma_1) \Psi^{j_i}(\mathbf{r}_{b2}, \sigma_2)]^0_0 \chi^{(+)}_{aA}(\mathbf{r}_{aA})$$

while $\sigma_{inel}(^9\mathrm{Li}(1/2^-; \Delta L = 2))$ is
rocess $^3$H+ $^9$Li→ $^3$H+ $^9$Li(1/2$^-$)
particle transfer and elastic cross
tains $P_{2n} \approx 2 \times 10^{-2}$. Thus

$$\approx 7 \times 10^{-2} \beta_2^2 \,\mathrm{mb}, \quad (6)$$

with the lowest state of $^9$Li while
ficient. Thus,

$$\beta_2^2 \,\mathrm{mb}. \quad (7)$$

In keeping with the fact that $0.5 \leq \beta \leq 0.8$, $10^{-2} \leq R_2 \leq 10^{-1}$. This can be

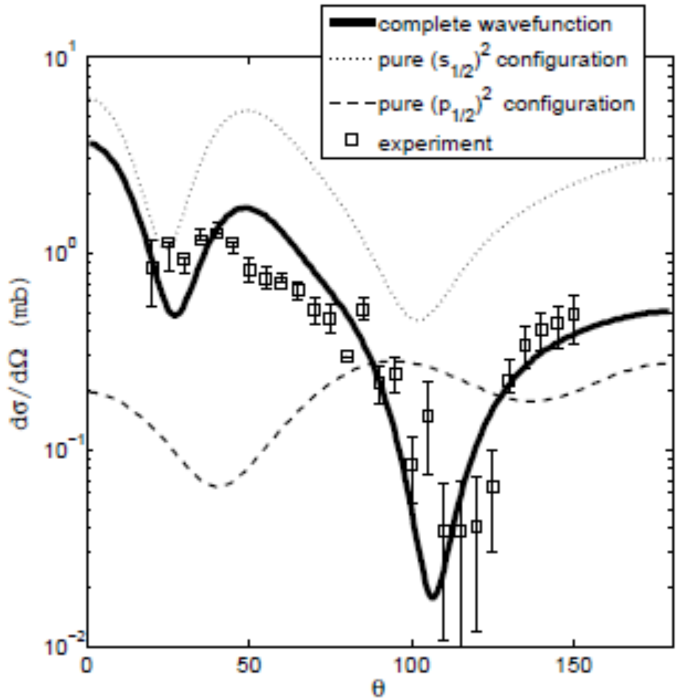


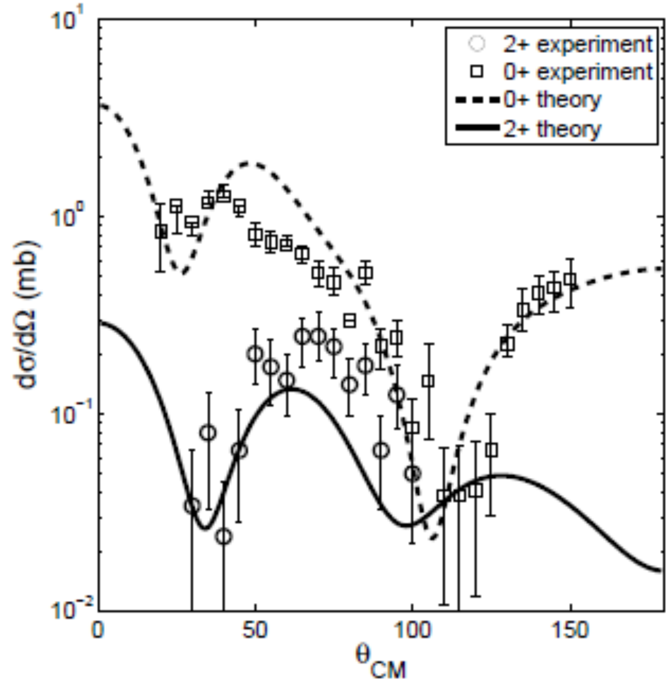


| | $\sigma(^{11}\mathrm{Li(gs)} \to {}^{9}\mathrm{Li\ (i)})$ (mb) | | |
|---|---|---|---|
| i | $\Delta L$ | Theory | Experiment |
| gs $(3/2^-)$ | 0 | 6.1 | $5.7 \pm 0.9$ |
| 2.69 MeV $(1/2^-)$ | 2 | 0.5 | $1.0 \pm 0.36$ |

It could furthermore be argued that the observation of the 2.69 MeV($1/2^-$) first excited $^9$Li final state is the result of a two–step process (see Fig. 1(i)): two–particle transfer to the ground state of $^9$Li and Final State (inelastic scattering) Interaction (FSI) between the outgoing triton and $^9$Li in its ground state, resulting in the inelastic excitation of the $1/2^-$ state. A simple estimate rules out such a scenario. In fact, one can write the cross section associated with the two step process as

$$(\sigma^{1/2^-})_{FSI} = \sigma(^{11}\mathrm{Li(gs)} \rightarrow^9 \mathrm{Li(gs)} \rightarrow^9 \mathrm{Li}(1/2^-)) = P_{2n}(^{11}\mathrm{Li(gs)} \rightarrow^9 \mathrm{Li(gs)}) \times \sigma_{inel}(^9\mathrm{Li}(1/2^-;\Delta L = 2)). \tag{4}$$

The quantity

$$P_{2n}(^{11}\mathrm{Li(gs)} \rightarrow^9 \mathrm{Li(gs)}) = \frac{\sigma_{2n}(^{11}\mathrm{Li(gs)} \rightarrow^9 \mathrm{Li(gs)})}{\sigma_{el}}, \tag{5}$$

is the probability of populating the final channel, while $\sigma_{inel}(^9\mathrm{Li}(1/2^-;\Delta L = 2))$ is the inelastic cross section associated with the process $^3$H+ $^9$Li→ $^3$H+ $^9$Li($1/2^-$) (see Fig.4). Making use of the calculated two–particle transfer and elastic cross section $\sigma_{2n}$ and $\sigma_{el}$ respectively (Table 2) one obtains $P_{2n} \approx 2 \times 10^{-2}$. Thus

$$(\sigma^{1/2^-})_{FSI} \approx P_{2n} \times \beta^2 \times 35\mathrm{mb}/10 \approx 7 \times 10^{-2}\beta_2^2\,\mathrm{mb}, \tag{6}$$

where $\beta_2^2$ is the deformation parameter associated with the lowest state of $^9$Li while the factor 1/10 is the square of a recoupling coefficient. Thus,

$$R_2 = \frac{(\sigma^{1/2^-})_{FSI}}{\sigma_{2n}^{1/2^-}} \approx 10^{-1}\beta_2^2\,\mathrm{mb}. \tag{7}$$

In keeping with the fact that $0.3 \leq \beta \leq 0.8$, $10^{-2} \leq R_2 \leq 10^{-1}$. This can be considered an upper limit of the ratio $R_2$, in keeping with the fact that the final state interaction starts essentially only around the distance of closest approach, while the above estimates assume they take place over the whole trajectory of relative motion. Before ending this Section, let us return to the first subject discussed in it,

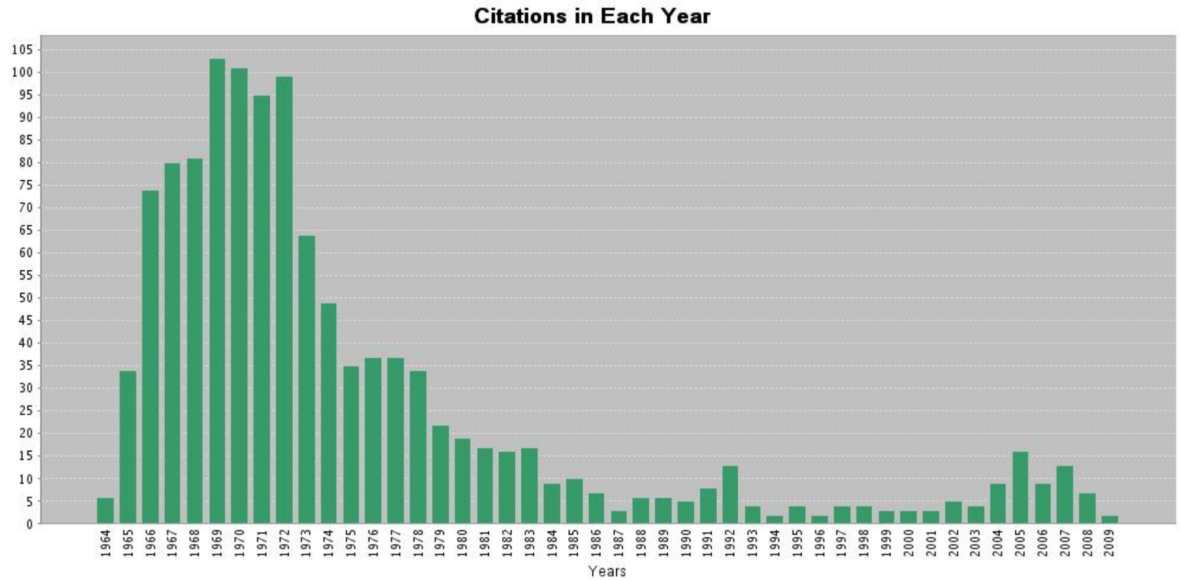


(t,p) transfer experimen
citations

the initial and final channel wave functions are

$$
\begin{aligned}
|\alpha\rangle &= \phi_a(\xi_b, \mathbf{r}_1, \mathbf{r}_2)\phi_A(\xi_A)\chi_{aA}(\mathbf{r}_{aA}) \\
|\beta\rangle &= \phi_b(\xi_b)\phi_B(\xi_A, \mathbf{r}_1, \mathbf{r}_2)\chi_{bB}(\mathbf{r}_{bB})
\end{aligned}
$$

very schematically, the first order (*simultaneous*) contribution is

$$T^{(1)} = \langle\beta|V|\alpha\rangle,$$

while the second order contribution can be separated in a *successive* and a *non-orthogonality* term

$$
\begin{aligned}
T^{(2)} &= T^{(2)}_{succ} + T^{(2)}_{NO} \\
&= \sum_{\gamma}\langle\beta|V|\gamma\rangle G\langle\gamma|V|\alpha\rangle - \sum_{\gamma}\langle\beta|\gamma\rangle\langle\gamma|V|\alpha\rangle.
\end{aligned}
$$

2n transfer theory:
2nd order DWBA

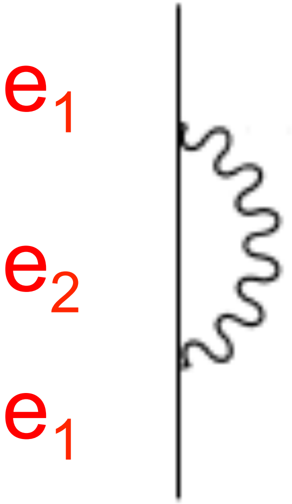


$$= \frac{V^2}{e_1 - (e_2 + \hbar\omega_\lambda)} \approx -\frac{V^2}{\hbar\omega_\lambda}$$

$$m_\omega \approx \left(1 + \frac{2N(0)V^2}{\hbar\omega_\lambda}\right) m$$

$$m_\omega \approx 1.5m$$
$$\hbar\omega_\lambda \approx 1\text{MeV}$$
$$N(0) \approx 3\text{MeV}^{-1}$$

$$\rightarrow \quad V^2 \approx 0.1 \quad \text{MeV}^2$$

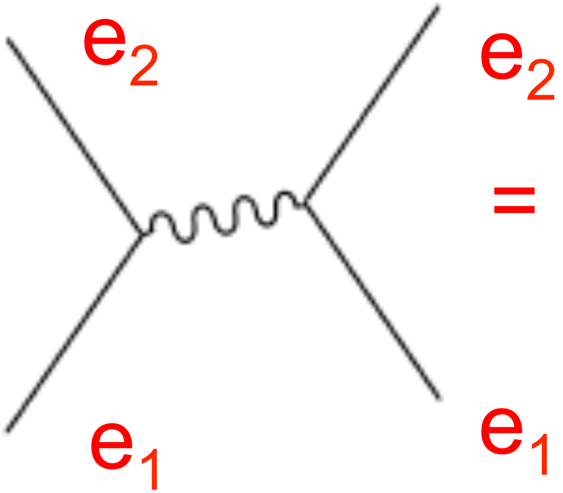


$$= \frac{V^2}{2e_1 - (e_1 + e_2 + \hbar\omega_\lambda)} = \frac{V^2}{e_1 - (e_2 + \hbar\omega_\lambda)} \approx -\frac{V^2}{\hbar\omega_\lambda}$$

$$V_{ind} \approx -0.2\text{MeV}$$

A more phenomenological approach: particle-vibration matrix ele
from properties of experimental surface vibrations

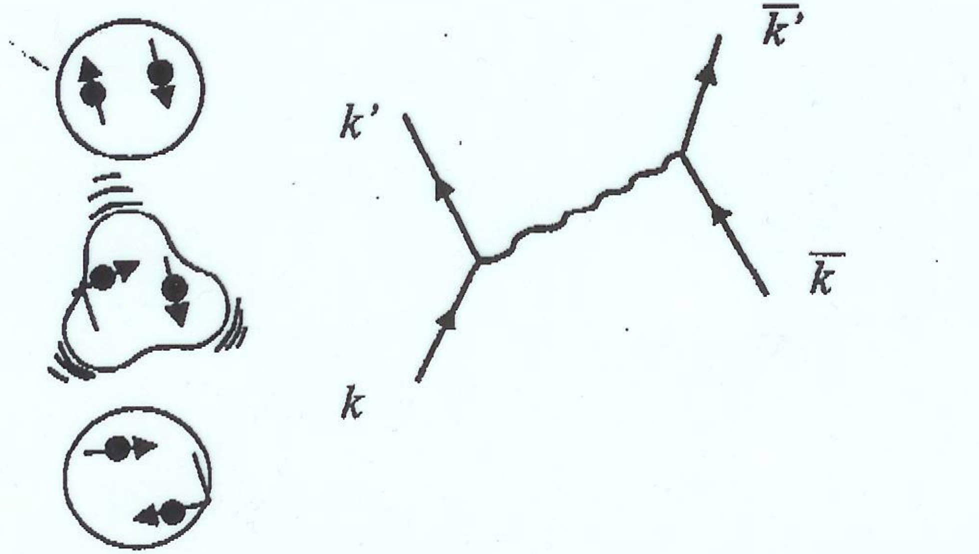


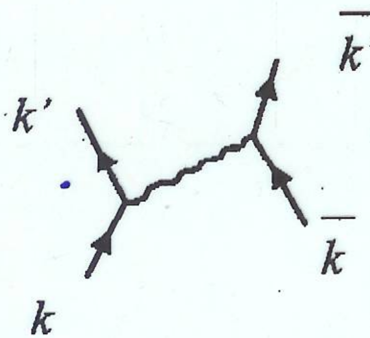


$$= \sum_{\lambda} \frac{2\beta_\lambda^2}{(2\lambda+1)} \frac{\left| \left\langle k \left\| R_0 \frac{\partial U}{\partial r} Y_\lambda \right\| k' \right\rangle \right|^2}{\sqrt{2j_k+1}\sqrt{2j_{k'}+1}} * \frac{1}{E_0 - \left( |\varepsilon_k - \varepsilon_F| + |\varepsilon_{k'} - \varepsilon_F| + \hbar\omega_\lambda \right)}$$

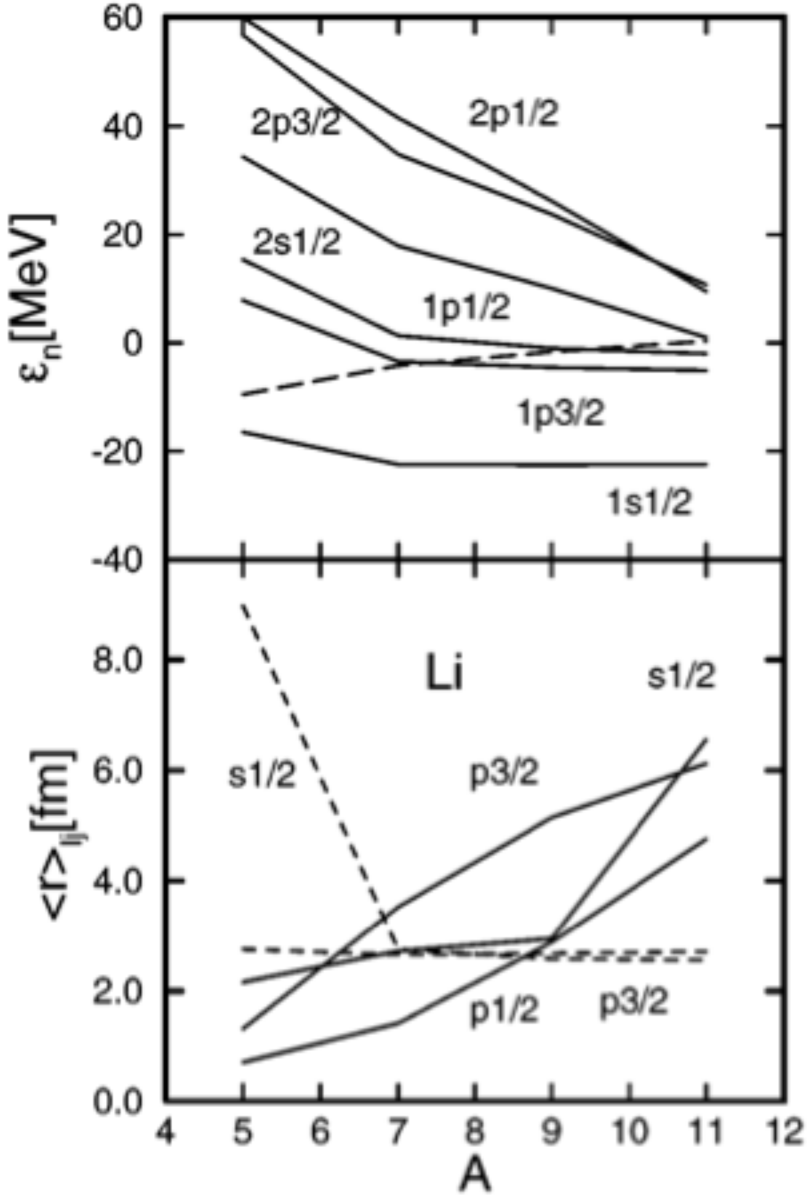


J. Meng and P. Ring, PRL 77(1998)3963

# $^{12}$Be

**Fermionic degrees of freedom:**

• two particle states coupled to zero angular momentum on s1/2, p1/2, d5/2 Woods-Saxon levels up to 150 MeV

**Bosonic degrees of freedom:**

•1-, 2+ and 3- QRPA solutions up to 50 MeV, associated to a multipole-multipole separable interaction with coupling constant tuned to reproduce E(1-)=2.7 MeV and B(E1)=0.052 e$^2$fm$^2$ E(2+)=2.1 MeV and 0.6<$\beta_2$<0.7

Spectroscopic factors: overlap between $^{11}$Be and $^{12}$Be

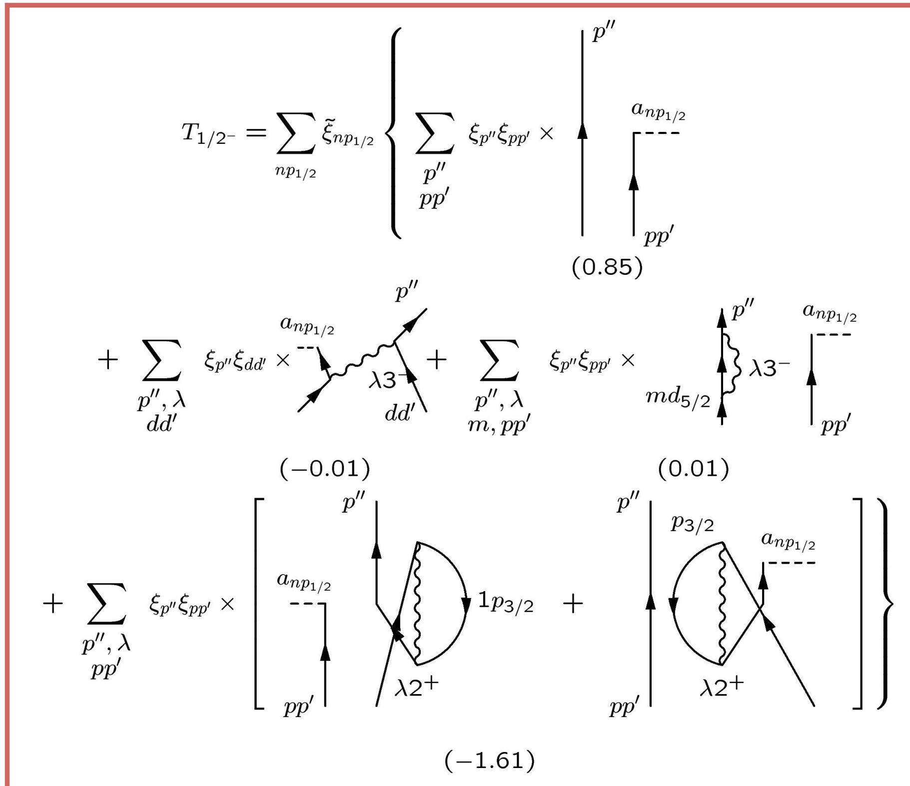

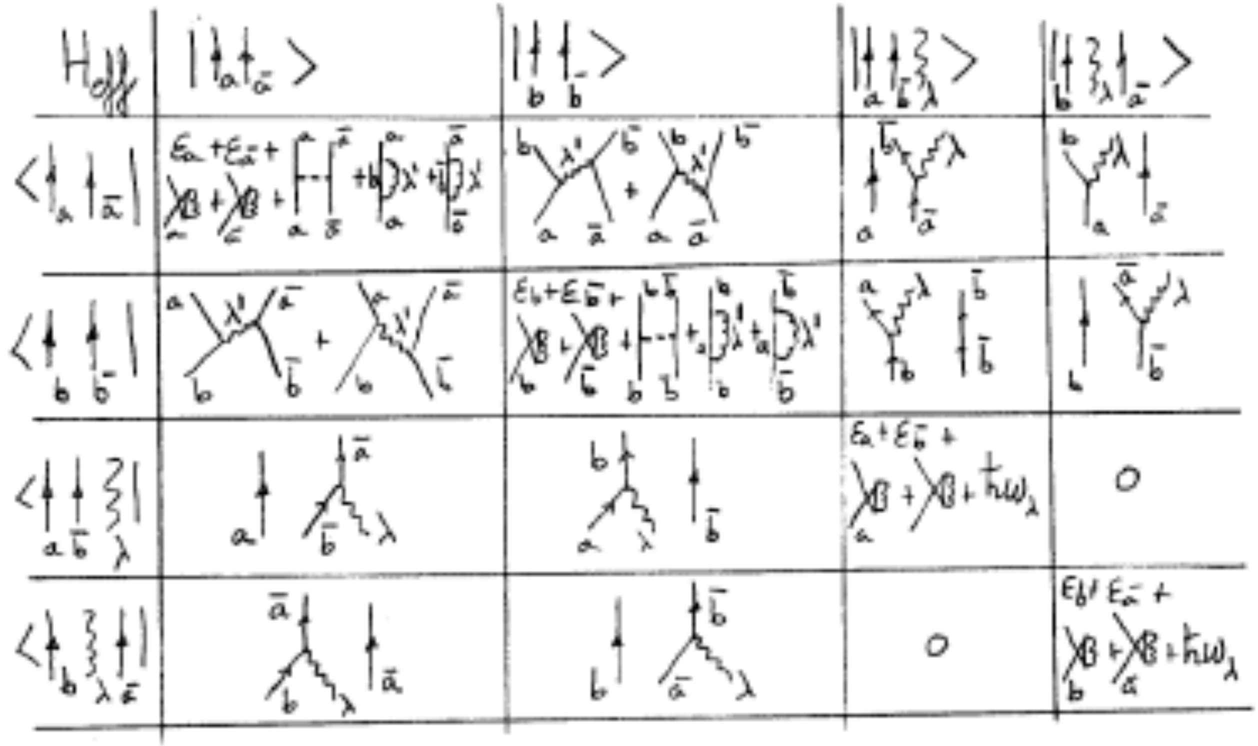
Heff
0
0

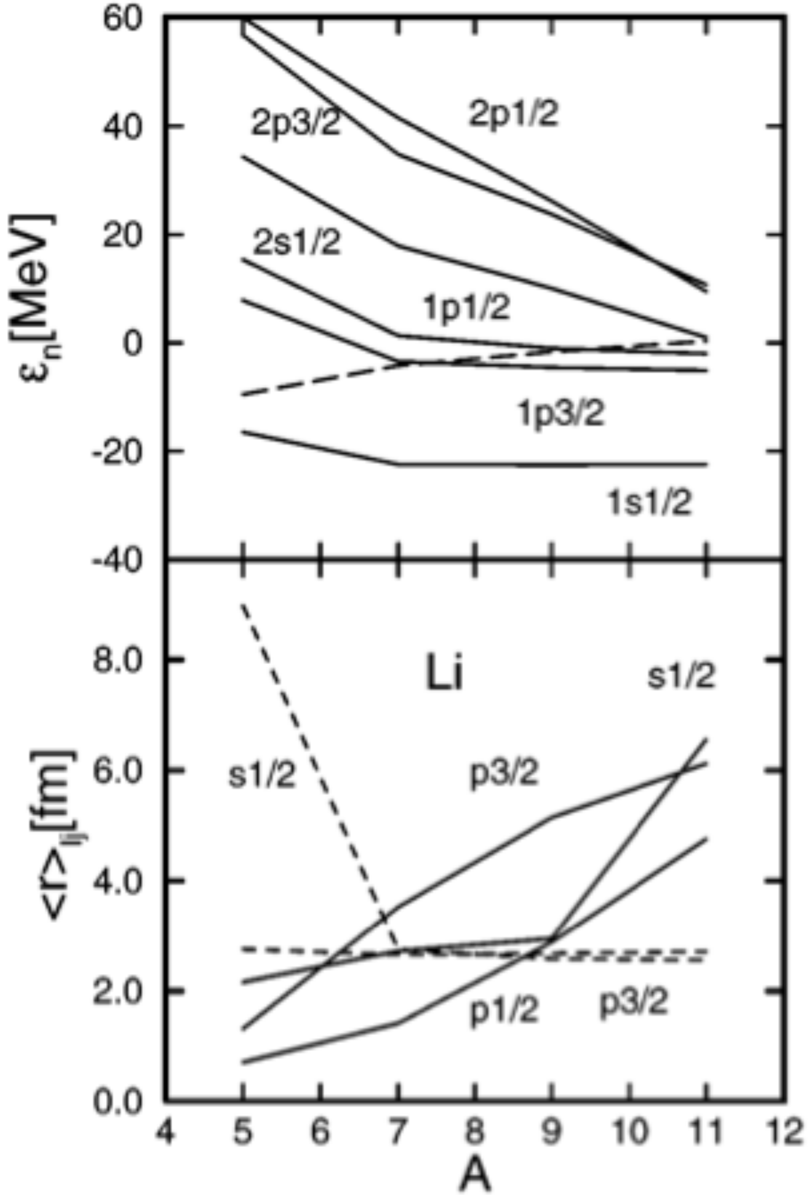


J. Meng and P. Ring, PRL 77(1998)3963

# Comparison with the model by Bertsch and Esbensen

OUR MODEL

Ann. Phys.209(1991)327
PRC56(1997)3054

**Single-particle potential**

Standard Bohr-Mottelson

Depth adjusted to experimental $p_{1/2}$ single particle energy

**2-body interaction**

Bare Argonne interaction+ particle-vibration coupling with phenomenological parameters (low-lying vibrations)

Strength fitted to $S_{2n}$ in $^{12}$Be

$$v_{\rm eff}(\mathbf{r}_1, \mathbf{r}_2) = \delta(\mathbf{r}_1 - \mathbf{r}_2)\left(v_0 + v_\rho\left(\frac{\rho_c((\mathbf{r}_1 + \mathbf{r}_2)/2)}{\rho_0}\right)^P\right).$$

**Results**

Good reproduction of binding energies in $^{12}$Be and $^{11}$Li
50% $(s_{1/2})^2$

Good reproduction of binding energy
Low $(s_{1/2})^2$ admixture unless two different s.p. potentials are used

A + [b+n1+n2] -> [A+ n1 +n2] + b

(a)

$n_1$ b

$n_2$

A

(b)

$n_1$ b

A $n_2$

$$T^{(1)}(j_i, j_f) = 2 \sum_{\sigma_1 \sigma_2} \int d\mathbf{r}_{fF} d\mathbf{r}_{b1} d\mathbf{r}_{A2} [\Psi^{j_f}(\mathbf{r}_{A1}, \sigma_1) \Psi^{j_f}(\mathbf{r}_{A2}, \sigma_2)]_0^{0*} \chi_{bB}^{(-)*}(\mathbf{r}_{bB})$$
$$\times\, v(\mathbf{r}_{b1}) [\Psi^{j_i}(\mathbf{r}_{b1}, \sigma_1) \Psi^{j_i}(\mathbf{r}_{b2}, \sigma_2)]_0^0 \chi_{aA}^{(+)}(\mathbf{r}_{aA})$$

$$T^{(2)}_{succ}(j_i, j_f) = 2 \sum_{K,M} \sum_{\substack{\sigma_1 \sigma_2 \\ \sigma'_1 \sigma'_2}} \int d\mathbf{r}_{fF} d\mathbf{r}_{b1} d\mathbf{r}_{A2} [\Psi^{j_f}(\mathbf{r}_{A1}, \sigma_1) \Psi^{j_f}(\mathbf{r}_{A2}, \sigma_2)]_0^{0*}$$
$$\times\, \chi_{bB}^{(-)*}(\mathbf{r}_{bB}) v(\mathbf{r}_{b1}) [\Psi^{j_f}(\mathbf{r}_{A2}, \sigma_2) \Psi^{j_i}(\mathbf{r}_{b1}, \sigma_1)]_M^K$$
$$\times \int d\mathbf{r}'_{fF} d\mathbf{r}'_{b1} d\mathbf{r}'_{A2} G(\mathbf{r}_{fF}, \mathbf{r}'_{fF}) [\Psi^{j_f}(\mathbf{r}'_{A2}, \sigma'_2) \Psi^{j_i}(\mathbf{r}'_{b1}, \sigma'_1)]_M^K$$
$$\times\, \frac{2\mu_{fF}}{\hbar^2} v(\mathbf{r}'_{f2}) [\Psi^{j_i}(\mathbf{r}'_{A2}, \sigma'_2) \Psi^{j_i}(\mathbf{r}'_{b1}, \sigma'_1)]_0^0 \chi_{aA}^{(+)}(\mathbf{r}'_{aA})$$

$$
\begin{aligned}
T^{(2)}_{NO}(j_i, j_f) = 2 \sum_{K,M} \sum_{\substack{\sigma_1\sigma_2 \\ \sigma_1'\sigma_2'}} \int & d\mathbf{r}_{fF}\, d\mathbf{r}_{b1}\, d\mathbf{r}_{A2} [\Psi^{j_f}(\mathbf{r}_{A1}, \sigma_1)\Psi^{j_f}(\mathbf{r}_{A2}, \sigma_2)]^{0*}_{0} \\
& \times \chi^{(-)*}_{bB}(\mathbf{r}_{bB}) v(\mathbf{r}_{b1}) [\Psi^{j_f}(\mathbf{r}_{A2}, \sigma_2)\Psi^{j_i}(\mathbf{r}_{b1}, \sigma_1)]^{K}_{M} \\
& \times \int d\mathbf{r}'_{b1}\, d\mathbf{r}'_{A2} [\Psi^{j_f}(\mathbf{r}'_{A2}, \sigma'_2)\Psi^{j_i}(\mathbf{r}'_{b1}, \sigma'_1)]^{K}_{M} \\
& \times [\Psi^{j_i}(\mathbf{r}'_{A2}, \sigma'_2)\Psi^{j_i}(\mathbf{r}'_{b1}, \sigma'_1)]^{0}_{0} \chi^{(+)}_{aA}(\mathbf{r}'_{aA})
\end{aligned}
$$

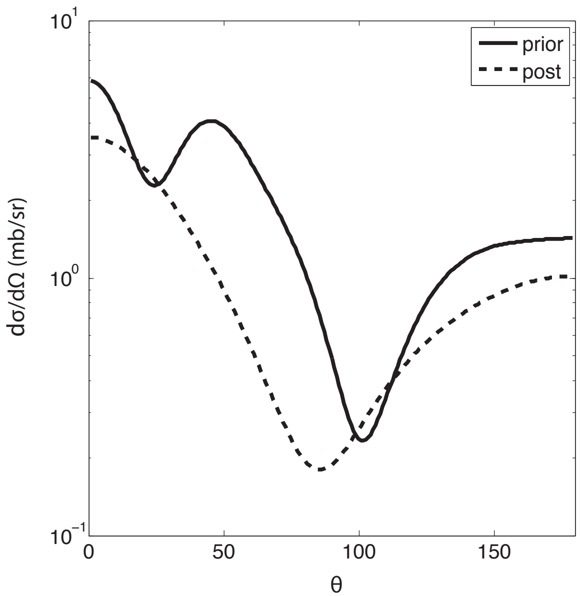
prior
post
dσ/dΩ (mb/sr)
θ

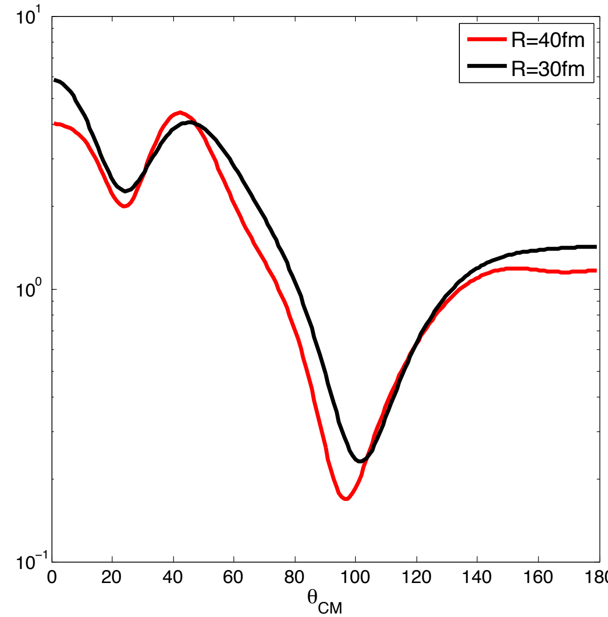
R=40fm
R=30fm
θ_CM

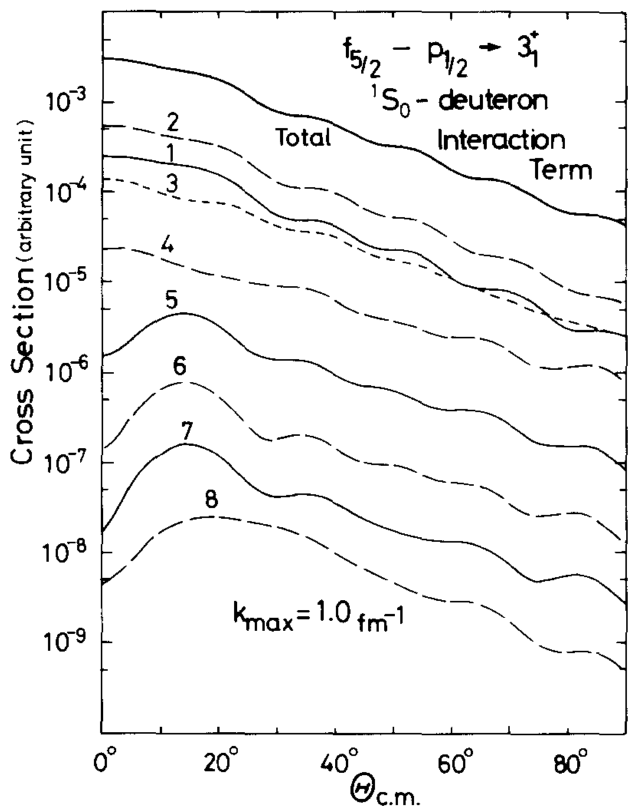


Open problems:
Inclusion of d* channels
Elastic scattering

M. Igarashi et al., Phys. Rep. 199 (1999) 1